Modeling Transformation from Myeloproliferative Neoplasms

by

Anna Sophia McKenney

A Dissertation

Presented to the Faculty of the Louis V. Gerstner, Jr.

Graduate School of Biomedical Sciences,

Memorial Sloan Kettering Cancer Center

in Partial Fulfillment of the Requirements for the Degree of

Doctor of Philosophy

New York, NY

July 2016

_____ _____

Ross L. Levine
Dissertation Mentor

Date

DEDICATION

To my mentors, my students, and most of all my loved ones

From whom I am always learning

ABSTRACT

Myeloproliferative neoplasms (MPN) can transform into Acute Myeloid Leukemia (AML) with short survival and no therapeutic options beyond supportive care. Studies of patients with post-MPN AML revealed hotspot mutations in IDH genes acquired at transformation. We characterized a mouse model that combined *Jak2*^{V617F} with *IDH1*^{R132H} and *Idh2*^{R140Q} that developed a lethal myeloproliferative neoplasm with preleukemic features, including acceleration of disease on transplant, a competitive advantage in the bone marrow niche and perturbed stem and progenitor compartments consistent with a hematopoietic differentiation block. Treatment of double-mutant mice with targeted inhibitors against JAK2 and IDH2 results in resolution of disease phenotype, normalization of stem and progenitor compartments, and reduction in disease burden in mice. RNA-Seq of hematopoietic stem and progenitor cells revealed a characteristic disease gene set, and treatment of sick mice normalized expression of these genes. *Ex vivo* treatment of human MPN and post-MPN AML *JAK2*^{mut} *IDH2*^{mut} tissues *ex vivo* showed a differentiation phenotype with AG221 treatment, consistent with current studies of the drug in *de novo* AMLs. Furthermore, this differentiation response was corroborated by a patient derived xenograft model developed from a *JAK2*^{mut} *IDH1*^{mut} patient treated with AGI-5198.

BIOGRAPHICAL SKETCH

Sophie was born on April 17, 1984 and grew up with her parents, Bruce and Halina, and her sister Chiara, in Selkirk, NY. She graduated from RCS Central High School two years before her peers and moved on to pursue a degree in Biomedical Engineering and Electronic Media at Rensselaer Polytechnic Institute (RPI.). There, she was an a cappella singer, teacher, and campus leader, and performed research that exposed her to intersections between engineering, science, and medicine: the lab of Mr. George Edick at RPI, the Cleveland Clinic Foundation with Dr. K. Jane Grande-Allen, and the NIH with Dr. Philip Anfinrud.

She joined Dr. Michael Rout's Laboratory of Cellular and Structural Biology at The Rockefeller University to help Dr. Jaclyn Novatt elucidate the biophysical role of unstructured proteins in the nuclear pore, while she completed pre-medical coursework and taught test preparation classes. Sophie subsequently seized a rare opportunity to teach high school physics, chemistry and math in Mexico. Returning from abroad, she earned her Masters in Public Health at the Johns Hopkins Bloomberg School of Public Health, focusing on the design of diagnostic devices for low resource settings.

She began the Tri-Institutional MD-PhD program eager to use translational research and population data to improve patients' lives, and soon came to the Laboratory of Ross Levine in the Gerstner Sloan Kettering Graduate School. In addition to this research, she has been very active in global health issues and has been a student leader in administration. She married her medical school sweetheart, Dr. Adam Faye, in May, 2016.

ACKNOWLEDGMENTS

First, to my mentor, Dr. Ross Levine -- for your support, kindness, and flexible approach in working with me on this project. In addition to your scientific mentorship, your charisma, energy, and enthusiasm are an inspiration to me.

To the Levine Lab -- over the years, you have taught me so much about science, teamwork, and independence. Special thanks to Dr. Olga Guryanova and Dr. Elodie Pronier, who took the initiative to mentor me through many technical and theoretical challenges.

To the members of my committee, Dr. Armstrong, Dr. Chi, and Dr. Guzman. – even in a hurricane, you each gave such wonderful attention to each development in this project, and I have appreciated your constructive feedback each step of the way.

To the Gerstner Sloan Kettering Graduate School – for taking me on as your first MD-PhD student. Every step from the first rotation to the formatting of my thesis, Dean Ken Marians, Ms. Linda Burnley, Ms. Iwona Abramek, Ms. Maria Torres, and Mr. Ivan Genera were all helpful and kind.

To the Tri-Institutional MD-PhD program, including Dr. Olaf Andersen and Mrs. Ruthie Gotian -- who have been available at every turn with support and solutions to problems logistical and personal alike.

To my classmates in the MD-PhD program – your support, your examples, and your commiseration have been a beacon for me through this entire experience.

To my inlaws, Gayle and Ronald Faye -- your presence and constant support has made all the difference as we have pursued our rigorous careers.

To my Mom and Dad and Sister, Chiara-- You have taught me and inspired me, each in your own way, to be independent and work toward my goals, despite any obstacles that may arise, with enthusiasm and persistence.

Finally, to my loving husband, Adam. Your dedication to your goals and values inspires mine, and you are always an encouraging voice and shoulder to cry on.

TABLE OF CONTENTS

LIST OF TABLES

LIST OF FIGURES

LIST OF ABBREVIATIONS

5hmC	5-hydroxymethyl cytosine
5mC	5-methyl cytosine
AML	Acute Myeloid Leukemia
BMT	Bone Marrow Transplant
CN-AML	Cytogenetically Normal AML
EPO	Erythropoietin
ET	Essential Thrombocythemia
FACS	Fluorescence Activated Cell Sorting
FH	Fumarate Hydratase
GM-CSF	Granulocyte Macrophage Colony Stimulating Factor
GSEA	Gene Set Enrichment Analysis
HIF	Hypoxia Inducible Factor
MF	Myelofibrosis
MPN	Myeloproliferative Neoplasm
P4H	Prolyl-4-Hydroxylase
PDX	Patient Derived Xenograft
PV	Polycythemia Vera
RAT	Retroviral Adoptive Transfer
SDH	Succinate Dehydrogenase
TET	Ten-Eleven Translocationi
TPO	Thrombopoietin
VHL	Von Hippel Lindau

Chapter 1 : INTRODUCTION

MYELOPROLIFERATIVE NEOPLASMS AND PROGRESSION TO ACUTE MYELOID LEUKEMIA

Myeloproliferative neoplasms (MPN) are hematopoietic disorders characterized by the clonal proliferation of mature myeloid elements (**Figure 1.1**). The most common MPNs are polycythemia vera (PV), essential thrombocythemia (ET) and primary myelofibrosis (PMF), and these diseases manifest clinically as an excess of red blood cells (PV), platelets (ET), or white blood cells (PMF), respectively. Despite administration of standard therapies, many develop progressive bone marrow failure and/or transform to acute myeloid leukemia (AML). The only curative therapy for MPN patients is allogeneic stem cell transplantation, which cannot be offered to most patients, given their advanced age. There is therefore a pressing need for novel therapies for MPN patients.

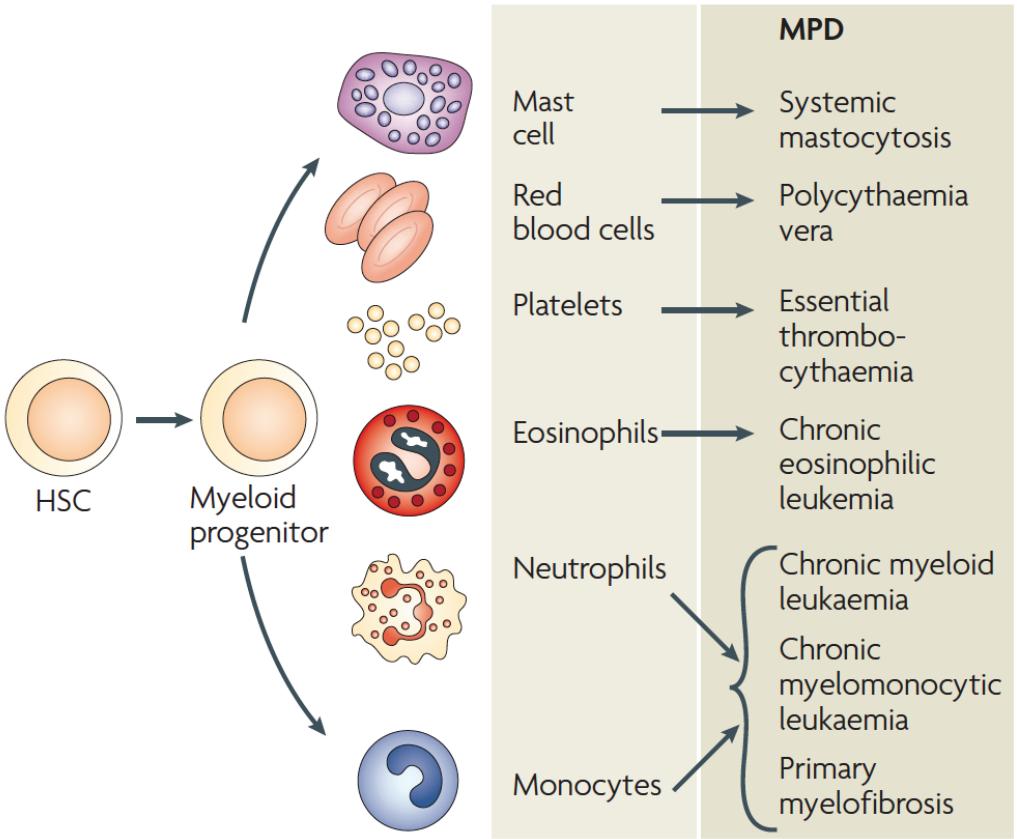

Figure 1.1: Classification of MPNs
Reprinted by permission from Macmillan Publishers Ltd: Nature Reviews Cancer, 7(9), 673-83, copyright 2007."

The somatic constitutively activating *JAK2*^{V617F} mutation[1,2] is observed in 81-99% of PV patients, 41-72% of ET patients, and 39-57% of PMF patients.[3,4] After this discovery, investigators identified somatic activating mutations in exon 12 of JAK2 in *JAK2*^{V617F} -negative patients.[5] Similarly, somatic MPL mutations (e.g.: *MPL*^{W515L}), which activate the TPO receptor, are found in approximately 8% of ET patients and 10-15% of PMF patients.[6-9] More recently, up to two thirds of MPN patients without mutations in the *JAK2* or *MPL* genes were found to have activating mutations in *CALR*.[10,11] *CALR* mutant overexpressing cells are reported to have a similar phenotype to *JAK2* and *MPL*-mutant overexpression, including induction of cytokine independence in Ba/F3 cells and activation of STAT5.[11] Together, these studies indicate that these oncogenic JAK-STAT pathway mutations are a pathogenetic feature of chronic MPN.

Transformation to AML from MPN is the most feared complication of MPN, and post-MPN AML is associated with a dismal prognosis. Several studies examining patients undergoing leukemic transformation from MF, PV, and ET, have observed median survival times ranging from 2.6 months to 4.6 months,[12-14] with no clear prognostic distinction for any given MPN.[15] Advanced age (>60 years,) disease-specific burden measures (e.g.: thrombocytosis and anemia in ET), and exposure to certain therapies including erythropoiesis-inducing and cytoreductive agents are associated with an increased risk of leukemic transformation. In contrast, leukemic progression has not been found to correlate with *JAK2*^{V617F} mutational status or exposure to cytotoxic drugs or hydroxyurea; however, *JAK2* mutant allele burden remains controversial in MPN.[14,16-24]

Importantly, no therapy has been demonstrated to improve outcome for post-MPN AML patients in comparison to supportive care.[12-14] In patient outcome studies, all surviving patients were treated with allogeneic transplants.[12,14] These data indicate a powerful need for new models and improved therapeutic approaches in order to improve outcomes for patients with this aggressive malignancy.

GENOMICS OF POST-MPN AML

Although post-MPN AML has only recently been characterized as a distinct clinical entity, studies show that this disease has a different mutational spectrum than observed in *de novo* AMLs.[25,26](**Figure 1.2.A, B**) implying that there is a distinct pathogenesis of these two AML subtypes. *JAK2*^{V617F} mutations are relatively rare in *de novo* AML[27] and AML patients that do have *JAK2*^{V617F} mutations are more likely to have a history of an antecedent MPN[28,29]. Certain specific mutated alleles are commonly found in post-MPN AML in higher proportions than classically associated with de novo AML, including *TET2*, *ASXL1*,[30] *IDH1/2*,[31] *RUNX1*,[32] *SRSF2*,[33] *P53*,[34] *LNK*,[35] *CBL*,[36] and *IKZF1*.[37] Therapy-associated transformation may have chromosomal abnormalities such as −5/5q or −7/7q−.[38] SNP analysis has further confirmed commonly modified regions including chromosomes 8, 12, 17, and 21 (which contain *MYC*, *ETV6*, *TP53*, and *RUNX1*), and these studies have postulated novel candidate tumor suppressors on 7q (*SH2B2*, *CUTL1*), 19p (*PIN1*, *ICAM1*, and *CDC37*) and 21q (*ERG*.)[39] Conversely, the mutations that are usually common in de novo AML, such as *DNMT3A* and *FLT3*, are largely absent from post-MPN AML.[25] These genetic data suggest a unique route of transformation for post-MPN AML.

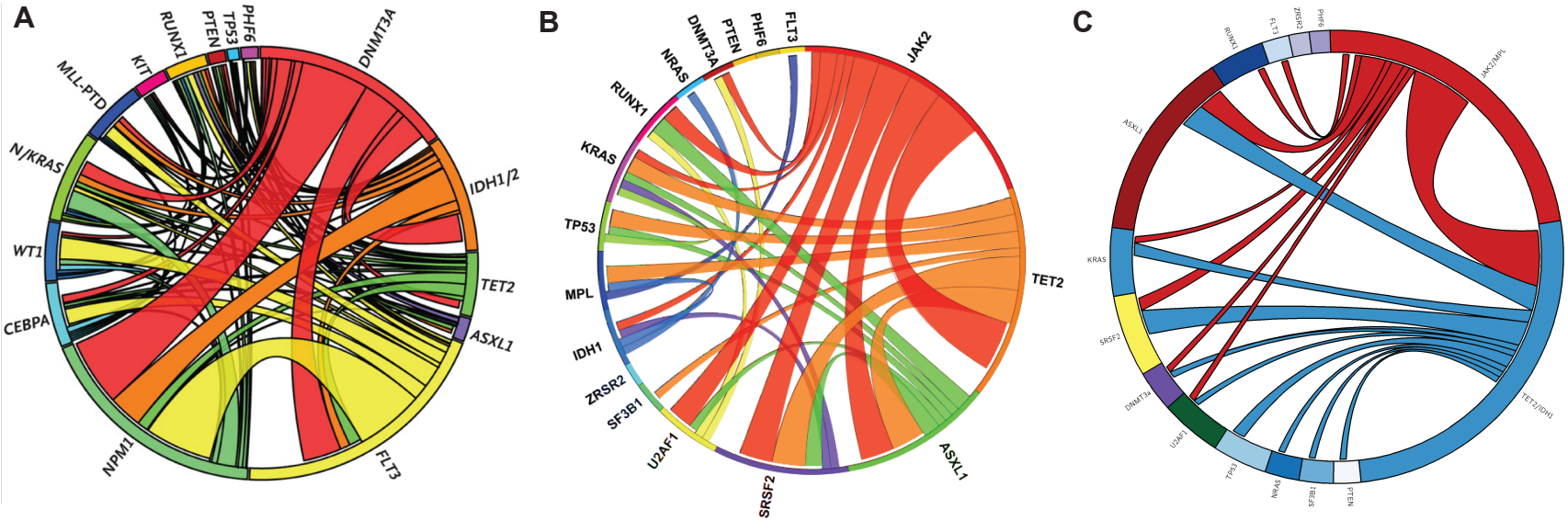

Figure 1.2: Post-MPN AML has a distinct mutational landscape from de novo AML

Circos plots representing mutational landscape of (A) de novo AML,[26] (B) Post-MPN AML, and (C) Post-MPN AML, isolating and combining JAK2/MPL mutant and IDH/TET2 mutant cases to reveal 20% overlap between these categories.[25]

Figure 1.2.A Reproduced with permission from N Engl J Med., 2012, 366(12), 1079-89, Copyright Massachusetts Medical Society.

Figure 1.2.B Adapted from Zhang SJ, Rampal R, Manshouri T, Patel J, Mensah N, Kayserian A, Hricik T, Heguy A, Hedvat C, Gönen M, Kantarjian H, Levine RL, Abdel-Wahab O, Verstovsek S. Genetic analysis of patients with leukemic transformation of myeloproliferative neoplasms shows recurrent SRSF2 mutations that are associated with adverse outcome. Blood. 2012 May 10;119(19):4480-5.

Post-MPN AML is characterized by a mutational spectrum distinct from chronic MPN or de novo AML; however, the sequence of events in leukemic transformation requires further evaluation. To this end, some studies have matched samples from both before and after leukemic transformation in individual patients, and they have demonstrated that genetic events beyond JAK-STAT activating mutations occur at transformation. One early study shows that, unlike MPN, none of the subjects included with post-MPN AML had a normal karyotype.[12] Analyzing paired samples from several groups has yielded several genes that are mutated at the time of transformation, which are summarized in **Table 1.1**. In contrast to these genes, which have different mutation status before and after leukemic transformation, mutations in other genes, such as P53 and CBL, were found to exist in both clones. Upregulation of WT1 and EVI1 has also been documented in transformation.[36] Our laboratory, in two successive papers, performed mutational profiling of 17 paired samples in which dominant clones were shown to acquire mutations over the course of transformation in *TET2*[30] as well as in *TP53* and *KRAS*,[25] and further studies of this data have implicated IDH mutation in this event.

Table 1.1: Genetic mutations from studies comparing pre- and post- transformation

Study	Mutated Gene Identified	Total Paired Samples	Total Candidate Genes
Ding 2009[32]	RUNX1/AML1	18	7
Beer 2010[36]	RUNX1/AML1	16	11
Zhang and Rampal 2012[25]	TET2, TP53, KRAS	17	22
(Abdel-Wahab 2010[30])		(14)	(4)
Green 2010[40]	IDH1/2	5	2

Given this evidence, there is a compelling argument to investigate cooperation between activation of the JAK-STAT pathway and induction of *IDH*/*TET2* mutation in the pathogenesis of post-MPN AML. *JAK2* mutation is not sufficient to predict leukemic transformation,[31] but it is a pathognomonic feature of MPN and many post-MPN AMLs do maintain this mutation. In transforming to AML, studies to date have reported acquisition of mutations in *TET2*, *IDH1*, and *IDH2* in up to 50% of patients.[41] To this end, IDH mutation has, independent of *JAK2*-mutational status, been shown to significantly reduce leukemia-free survival; this is significantly further reduced when the mutations exist in combination[31](**Figure 1.3.A)** Our lab has shown frequent acquisition of *TET2* mutations, which are functionally related to IDH mutations, at the time of leukemic transformation,[25,30] and Green et al. in a recent study identified IDH mutations five paired samples from *JAK2*^{V617F} -positive PV patients that progressed to leukemia.[40] Furthermore, examining our own cohort of post-MPN AML patients (**Figure 1.2.C**), we find that JAK-STAT activating mutations and *IDH/TET2* mutations co-occur in 20% of patients. With this evidence, we set out to create models combining these two pathways.

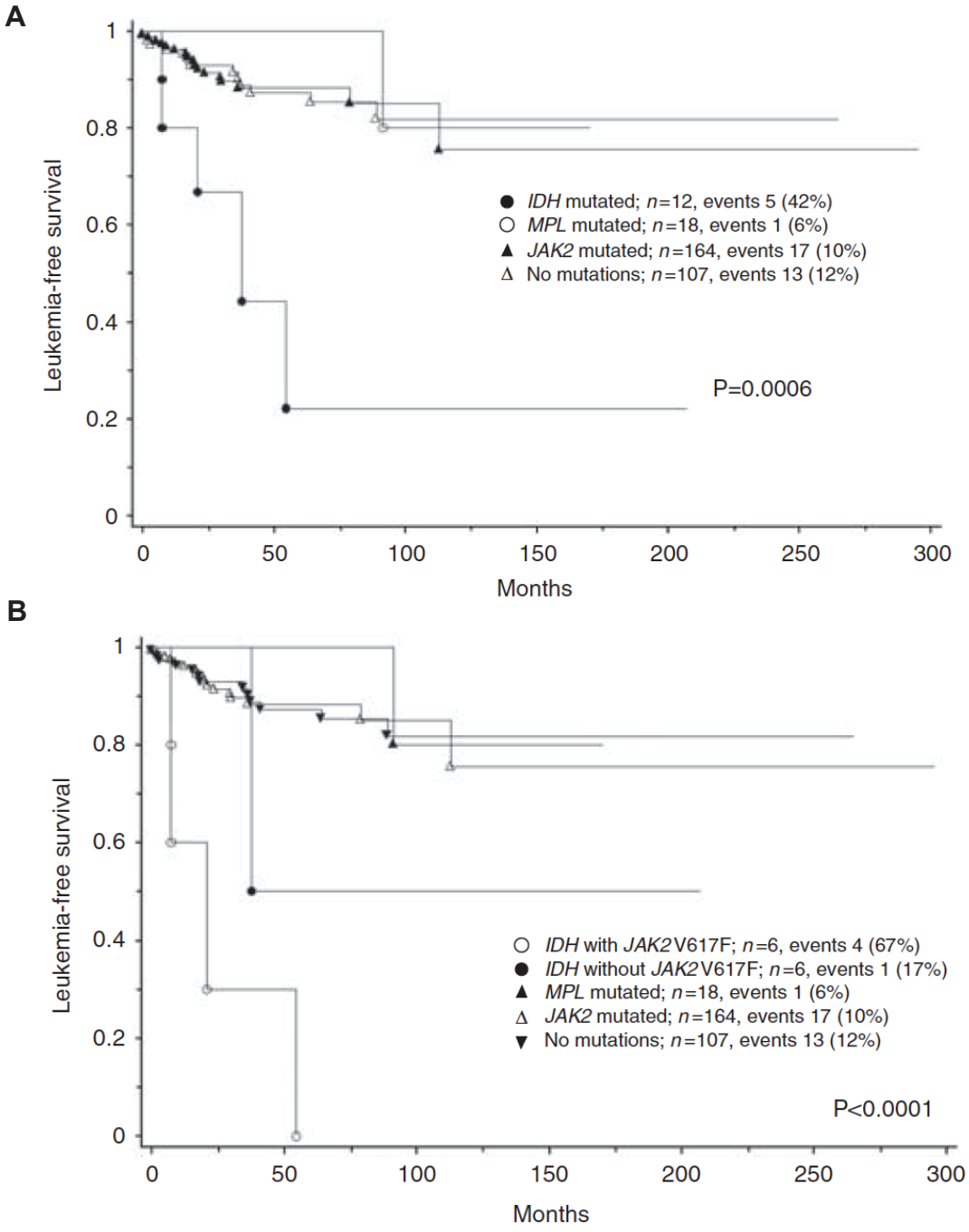

Figure 1.3: Patients with IDH mutation have shortened leukemia-free survival
Adapted from Tefferi A, Jimma T, Sulai NH, Lasho TL, Finke CM, Knudson RA, McClure RF, Pardanani A. IDH mutations in primary myelofibrosis predict leukemic transformation and shortened survival: clinical evidence for leukemogenic collaboration with JAK2V617F. Leukemia. 2012 Mar;26(3):475-80."

ISOCITRATE DEHYDROGENASE MUTATIONS

Isocitrate dehydrogenase (IDH) proteins catalyze the oxidative decarboxylation of isocitrate to α-ketoglutarate (α-KG, 2-oxoglutarate). IDH3 serves the classical role as an allosterically regulated, rate-limiting enzymatic step in the Citric Acid Cycle. The other isoforms, which are more commonly mutated in cancer, are thought to use this catalytic process in other roles, such as lipid metabolism and glucose sensing (in the case of IDH1), and regulation of oxidative respiration (in the case of IDH2).[42,43]

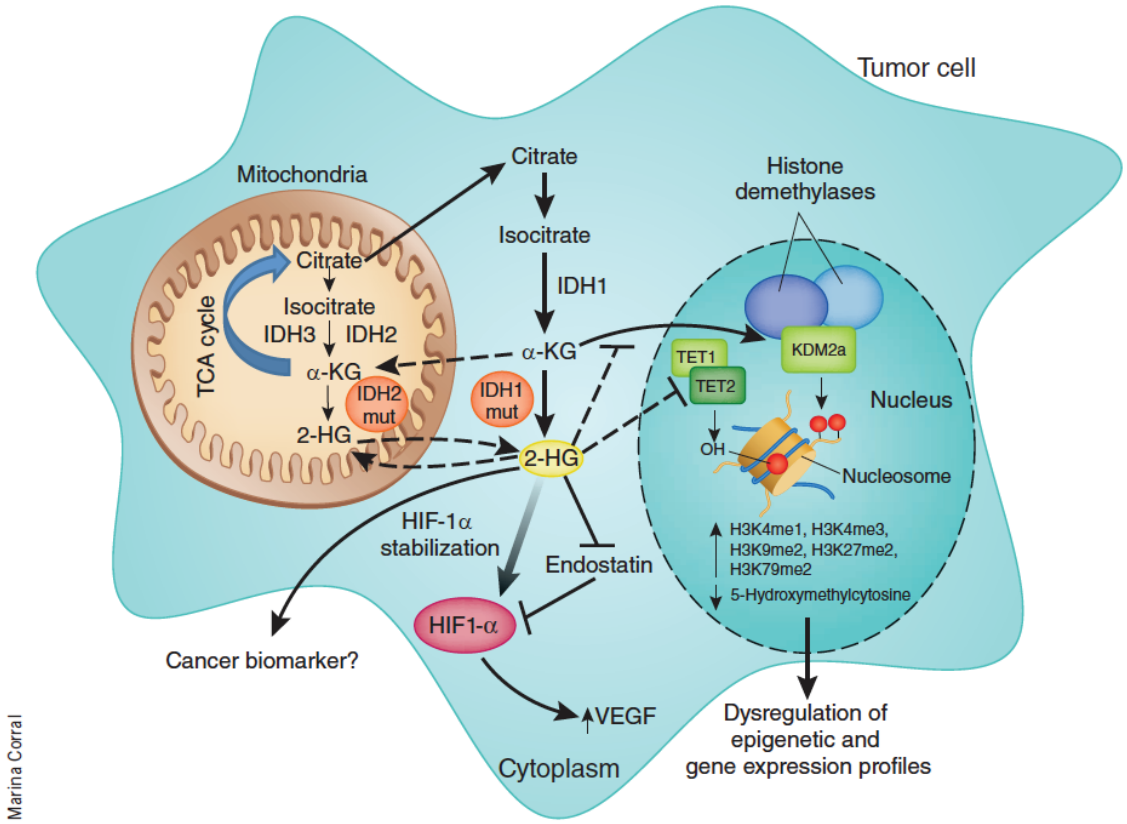

Figure 1.4: Mutant IDH activity and 2-HG signaling in cancer
Reprinted by permission from Macmillan Publishers Ltd: Nature Medicine 17(3), 291-3 copyright 2011.

Mutations in IDH1 were first identified in colorectal cancer[44] and gliomas.[45] Subsequently, whole genome sequencing studies in AML by Ley and colleagues led to the identification of IDH1 mutations in AML,[46] later confirmed by studies finding IDH1 and IDH2 mutations in cytogenetically normal AML (CN-AML) patients. Subsequent studies have identified IDH1/2 mutations in a spectrum of malignancies, including angioimmunoblastic T-cell lymphoma,[47] cholangiocarcinoma,[48] and chondrosarcoma,[49] suggesting that mutations in this pathway are a common mechanism of transformation across a wide spectrum of tumors. Notably, gliomas with IDH mutations are usually lower-grade, and are associated with relatively favorable outcome in brain tumors – this contrasts with the data in MPN/AML, in which IDH mutation is associated with transformation to AML and poor outcome.[50]

	IDH1	IDH2
Brain	R132H	R172K
	R132C	R172M
	R132S	R172G
	R132G	R172S
	R132L	R172W
	R132V	
	R132H	R140Q
	R132G	R140W
AML	R132C	R140L
	V71I	
	R132S	R172K
	R132L	R140Q
	R132H	R140Q
MDS	R132C	R140L
	R132L	R172K
	R132G	
	R132S	R140Q
MPN	R132C	R140W
	R132G	R172G
Prostate	R132H	
	R132C	
B-ALL	R132C	
Melanoma		V294M
Paraganglioma	R132C	
	R132H	
Thyroid	V71I	
	G123R	
Colorectal	G97D	
	R132C	

Figure 1.5: IDH1 and IDH2 mutations associated with different cancer types
Reprinted from Trends in Molecular Medicine, 16(9), Lenny Dang, Shengfang Jin, Shinsan M. Su, IDH mutations in glioma and acute myeloid leukemia, 387-97, Copyright 2010, with permission from Elsevier.

Given the prognostic significance of IDH mutations in glioma, the implications of IDH mutations in AML is of great interest. In AML, patients with the *IDH1*^{R132H} mutation have lower overall survival. [51,52] Patients with *IDH2*^{R172K} mutation have lower rates of compete remission,[53] and patients with this mutation have a worse prognosis than those with *IDH2*^{R140Q} mutations.[54] However, the relevance of IDH mutations to outcome in AML is more complex than it first appears. In one study of newly diagnosed patients, IDH mutations were associated with older age and higher platelet levels, but the mutations themselves were not independent predictors of survival.[55] In CN-AML, *IDH2* mutations have no influence on treatment outcome,[56] and IDH1 mutations remain stable over the course of disease, are not acquired at relapse, and do not have any independent impact on survival.[57] In childhood AML, IDH mutations were actually associated with increased overall survival, though this was not an independent predictor of survival.[58] Recently, *IDH2*^{R140Q} mutations have been associated with favorable outcomes in younger adults treated with dose-intensive therapy.[26,54] By contrast, IDH mutations, particularly *IDH2*^{R172K} mutations, are associated with adverse outcome in older adults with AML, suggesting an age-dependent relevance of IDH mutations to outcome in AML.[53] All together, these data suggest that the prognostic relevance of IDH mutations may depend on the specific allele, patient age, and treatment regimen.[59]

Loss of function mutations in other Krebs Cycle components have also been linked to cancer. Mutation of fumarate hydratase (FH) have been linked to hereditary leiomyomatosis and renal cell cancer,[60,61] and mutations in and succinate dehydrogenase (SDH) have been linked to pheochromocytoma, paraganglioma, renal cell carcinoma, and papillary thyroid cancer,[62-64] respectively. As such, many hypothesized that IDH1/2

mutations would result in loss of metabolic activity, and indeed, early enzymatic studies confirmed that the mutant protein loses the ability to catalyze conversion of isocitrate to α-ketoglutarate. However, these mutations were also characterized as somatic, heterozygous mutations at highly conserved positions, which is more consistent with gain-of-function mutations. This dissonance was resolved when metabolic profiling showed that IDH1 and IDH2 mutant proteins catalyze a reaction that converts α-KG to 2-hydroxyglutarate (2-HG).[65] This metabolite is a normal intermediate of hemoglobin synthesis; 2-HG is present in trace quantities in normal cells but accumulates in mutated cells, as shown in IDH-mutant AML and glioma cells.[65] Subsequently, Thompson, Caroll, and colleagues (including our laboratory) measured 2-HG production and compared it to targeted IDH1/2 mutational analysis in AML patients and observed that all AML patients with either *IDH1*^{R132} or *IDH2*R^{172} mutations had marked elevations in 2-HG. Furthermore, by recognizing a subset of samples with 2-HG elevations (but no known IDH1/2 mutations,) they identified a novel mutation in *IDH2*^{R140}, which is the most common IDH mutation seen in AML.[53,66]

IDH mutations are broadly associated with a differentiation block. This has been shown *in vitro* in hematopoietic cell lines that lose their capacity to differentiate in the presence of specific cytokines.[67] It has been observed in neural cell lines and patient samples as mediated by aberrant histone methylation.[68] It has also been observed in conditional mouse models of conditional *IDH2* mutation in hepatobiliary cells through suppression of transcription factor HNF-4α.[69] Together, these data indicate the neomorphic mutant's ability to confer a stem-like state to cells undergoing leukemic transformation.

TET2 MUTATIONS

TET2 was initially associated with MPN through genome-wide SNP arrays that identified an MPN patient with a microdeletion containing the gene, and this was followed by identification of somatic missense, nonsense, and frameshift *TET2* mutations in patients with MDS, MPN, AML and other myeloid malignancies.[70-73] This, together with the observation that missense *TET2* mutations result in loss of TET2 catalytic function,[74] are consistent with a tumor suppressor function in myeloid malignancies.

TET1 was first identified as a partner of MLL-translocated AML,[75,76] but the function of the TET gene family and its role in leukemogenesis remained unknown until TET1 was shown to catalyze α-KG-dependent addition of a hydroxyl mark to methylated cytosines.[77] This action leads to DNA demethylation and resultant epigenetic control.[77-84] Additionally, TET enzymes have been shown to catalyze conversion of methylated cytosine (5mC) to formylcytosine (5fC) or carboxylcytosine (5cC.)[85,86] These data suggest that loss of TET2 enzymatic function can lead to aberrant cytosine methylation and resultant epigenetic silencing in malignant settings.

ROLE OF 2-HG IN REGULATION OF CELLULAR PROCESSES

The role of 2-HG in malignant transformation has not been fully delineated. 2-HG accumulation is observed in patients with 2-hydroxyglutaric aciduria, and some of these patients have increased incidence of brain cancers.[87,88] However, this subset does not correlate with patients identified to have IDH2 mutations. More recently, 2-HG has been examined as a biomarker for leukemic disease activity and response to therapy.[89]

2-HG was first hypothesized to impact specific enzymatic processes in oncogenesis when a collaborative group observed that *TET2* mutations were mutually exclusive from mutations in *IDH1/2* in AML.[90,91] Further studies confirmed this association and delved into the functional relationship between these mutant IDH proteins and the function of TET2, implying a role for 2-HG. Increased global hypermethylation of DNA and transcriptional silencing of genes with hypermethylated promoters characterize *IDH/TET2*-mutant patient samples. Quantification *in vitro* and *in vivo* further confirmed that the expression of these mutant *IDH* alleles results in increased 5mC and reduced 5hmC, and impairs TET2 function.[90] Then, in biochemical assays, 2-HG was shown to directly inhibit TET2 as well as other α-KG dependent enzymes.[92]

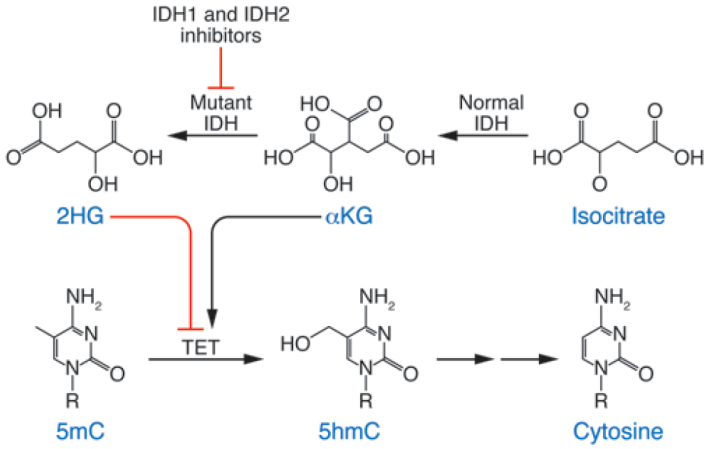

Figure 1.6: Oncometabolite 2-HG produced by mutant IDH blocks TET-mediated cytosine hydroxymethylation

Reproduced with permission of American Society for Clinical Investigation via Copyright Clearance Center. Original publication: McKenney AS, Levine RL. Isocitrate dehydrogenase mutations in leukemia. J Clin Invest. 2013 Sep;123(9):3672-7.

Several cellular enzymes have α-KG dependent activity, and many groups have investigated whether IDH-mutant mediated production of 2-HG inhibits the function of other enzymes involved in transformation (**Figure 1.04**). These include the JmjC family of histone demethylases, which are uniquely capable of demethylation of mono-, di-, and tri-methylated histone lysines. These enzymes use a highly conserved PHD domain to coordinate binding to histone tails while the JmjC domain coordinates demethylation, [93,94] and they have been shown to remove H3K4 mono-, H3K27 di-, H3K4 tri-, H3K9 di-, and H3K79 di-methylation.[92,95,96] 2-HG has been shown to block function of JmJC demethylases through competitive inhibition.[92,97] Consistent with these data, expression of IDH mutations in normal adipocytes, astrocytes, and hematopoietic cells leads to significant alterations in histone methylation, in particular in H3K27me3 and in H3K9me3. Moreover, these effects lead to altered chromatin markers with a resultant block in differentiation.[68] Of note, there are likely other mutations in metabolic enzymes which affect epigenetic patterning, as recent studies have shown that mutations which result in the accumulation of succinate and fumarate also result in reduced activity of JmjC histone demethylases.[98]

The prolyl 4-hydroxylases (P4H) also require α-KG for enzymatic function. In normoxic settings, P4H regulate Hypoxia Inducible Factor (HIF) by enabling the Von Hippel Lindau (VHL) protein to target HIF for degradation. The HIF transcription factor pathway has been implicated in tumor angiogenesis. The P4H also regulate post-transcriptional modifications of collagen species, as they act to oxidize proline to hydroxyproline. 2-HG has been shown to inhibit the function of P4H enzymes,[92] and overexpression of glioma-derived IDH1 mutations has been shown to cause accumulation

of HIF1α in cell lines (**Figure 1.04**).[92,99] Most importantly, these effects likely contribute to *in vivo* effects of IDH mutations, as brain-specific expression of IDH1 mutations blocks proper collagen maturation and basement membrane function *in vivo*.[100] Similarly, reduced function or loss of SDH or FH inhibit the function of HIF-α specific hydroxylases.[101,102] Recently 2-HG produced by IDH mutations was shown to stimulate the activity of the ELGN family of P4H, thus leading to reduced HIF levels and increased proliferation in astrocytes.[103]

JAK-STAT PATHWAYS

Janus Kinase (JAK) Proteins are nonreceptor tyrosine kinases which were named for the Roman god with two heads, in recognition of their unique structure with two kinase domains.[104] They were first identified in studies of cell lines with defective interferon (IFN) signaling using complementation assays with HeLa genomic material.[105] Four members of the JAK family have been identified (JAK1, JAK2, JAK3, and TYK2), and each is capable of associating with many different cytokine receptors, which may occur constitutively or be augmented by ligand binding. Classically, JAKs are required for the activation of the DNA-binding and regulatory functions of STATs.[104,106] Activation of STAT proteins, by somatic mutation or by increased upstream signaling, has been implicated in oncogenesis, and there is some evidence that dominant negative STAT3 can abrogate transformation of AML in cell lines.[107] SOCS proteins are associated with JAK2 proteins, may be activated by STATs, and act to suppress JAK-STAT signaling pathways.[108,109] JAK2 is also known to associate with insulin-related receptors and activate downstream targets, implicating JAK and SOCS in potential mechanisms of insulin resistance in metabolic syndrome.[110-112]

JAK2 is essential for myeloid hematopoiesis, based on an obligate role for JAK2 enzymatic function in erythropoietin (EPO), thrombopoietin (TPO) and GM-CSF receptor signaling. JAK2 signaling is essential for normal hematopoietic differentiation, and germline deletion of Jak2 in mice is homozygous lethal with severe anemia. This block in signaling is severe; for example, in comparison to Epo receptor knockout mice, JAK2 knockouts had a more severe block in erythroid differentiation.[113] Myeloid progenitors from JAK2 knockout mice fail to respond to erythropoietin, thrombopoietin, IL3, and GM-CSF, while response to other cytokines including GM-CSF is relatively intact.[114] The essential role for JAK-STAT signaling in normal erythropoiesis and more broadly in normal myeloid differentiation was underscored with the discovery of JAK2/MPL mutations in MPN patients, and likely explains the anemia and thrombocytopenia seen with JAK kinase inhibitors in MPN patients.[115,116]

Recent work has shown that in addition to its role in the canonical JAK-STAT pathway, activated JAK2 itself can translocate to the nucleus and alter chromatin state independent of STAT activation. *JAK2*^{V617F} was shown to directly phosphorylate Y41 on histone H3, with resultant displacement of HP1-α and derepressed expression of oncogenic targets, including LMO2. The effects of JAK2 on histone phosphorylation and gene activation were reversible, as they were inhibited with exposure to JAK2 inhibitors.[117] The *JAK2*^{V617F} mutant kinase has also been shown to phosphorylate PRMT5 (originally identified as JAK-binding protein 1), which inactivates the function of this arginine methyltransferase. This was also reversible with JAK2 inhibitors.[118] Nuclear JAK2 may also serve a role in NF1-C2 and RUSH-1α phosphorylation.[119] When examined by immunohistochemistry, patient samples of Philadelphia-chromosome-

negative MPNs show elevated nuclear accumulation of JAK2 in JAK2-mutant patients. Additionally, this accumulation is more evident in $CD34^+$ cells compared to granulocytic, megakaryocytic, or erythroid cells, suggesting a more prominent role for nuclear JAK2 in stem/progenitor function in MPN patients.[120]

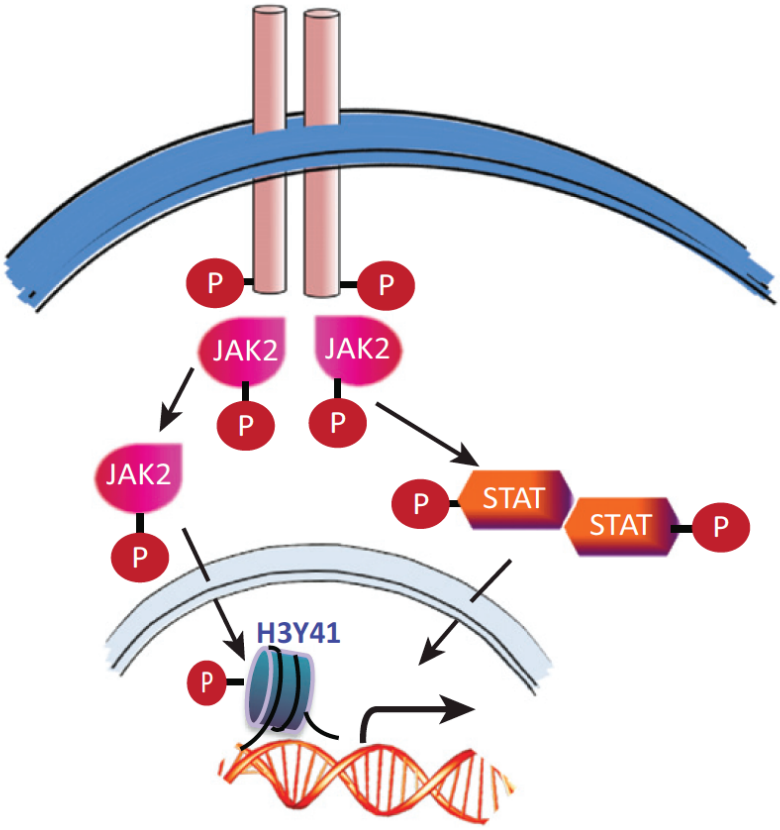

Figure 1.7: JAK can activate a multitude of signaling pathways including STAT
Reprinted from Trends in Pharmacological Sciences, 33(11), LaFave LM, Levine RL, JAK2 the future: therapeutic strategies for JAK-dependent malignancies, 574-82, Copyright 2012, with permission from Elsevier.

Chapter 2 : Modeling combined IDH and JAK2 mutant disease in mice

MURINE MODELS OF JAK-STAT PATHWAY ACTIVATION

In vivo murine bone marrow transplantation (BMT) models found that retroviral overexpression of *JAK2* or *MPL* alleles results in a fully penetrant, short latency MPN. However, as in human disease, these alleles confer different disease phenotypes. Expression of *JAK2*^{V617F} or *JAK2* exon 12 alleles results in a PV/PMF-like phenotype.[5,121-124] Expression of *MPL*^{W515L} causes disease resembling human ET/PMF, manifesting marked splenomegaly, thrombocytosis, and leukocytosis, with only mild effects on hematocrit. Notably, this model did not show a significant increase in cKit positive populations.[6]

The most physiologic models of *Jak2*^{V617F}-mediated disease,express the mutation in the endogenous locus, and result in PV with progression to MF, characterized by elevated hematocrit (HCT) and splenomegaly.[125,126] This MPN is serially transplantable, but disease does not show competitive advantage against wild type cells in reconstitution assays. This disease has its cell of origin in the LSK (Lin^- $Sca1^+$ $cKit^+$) long term hematopoietic stem cell (LT-HSC) compartment, but JAK2 inhibitor treatment does not eradicate the disease initiating capacity of this population.[125]

MURINE MODELS OF IDH/TET MUTATION IN HEMATOPOIETIC CELLS

Based on the genetic and functional data described above, several groups have begun to investigate the hematopoietic effects of conditional *TET2* loss and IDH mutant

expression *in vivo* through conditional knockout/knockin models. In these studies, loss of *Tet2* expression was shown to increase leukemic self-renewal as assessed by methylcellulose replating assays, and resulted in significant extramedullary hematopoiesis, myeloid progenitor production in the form of Granulocyte/Macrophage Progenitors (GMP), and ability to outcompete wild type marrow in competitive transplant.[127] These mice develop chronic myeloid expansion with features of chronic myelomonocytic leukemia (CMML), but they do not develop AML. These data are comparable to groups who have reported the phenotype of TET2 gene-trap/catalytic mutant mice.[128-130]

Mouse models of IDH mutation have been characterized as well. Mak and colleagues reported the phenotype of conditional *IDH1*^{R132H} expression in the hematopoietic[131] and neural compartments.[100] Another group has characterized the role of mutant IDH1 in hepatobiliary development and cancer,[69] and shown the effects of ubiquitously expressed mutant IDH2 on cardiac and neural integrity.[132] Mice with hematopoietic-specific expression of *IDH1*^{R132H} are characterized by hematopoietic stem/progenitor expansion, including increased numbers of LSK cells and myeloid progenitors. In addition, expression of mutant IDH in the hematopoietic compartment was associated with a DNA methylation signature with promoter hypermethylation similar to that observed in primary AML patients.[131] As in the cases of hematopoietic-specific *Tet2* loss, these mice did not develop overt AML, indicating a requirement for cooperating disease alleles to induce leukemic transformation. These data indicate that hematopoietic expression of mutations in the *TET2/IDH* pathway lead to alterations in self-renewal and differentiation and contribute to transformation.

Models have also been characterized that combine IDH/TET mutation with mutation in the receptor tyrosine kinase *Flt3*. One murine model developed in our group combines *Tet2* knockout and *Flt3*^{ITD} and demonstrates that these alleles cooperate to induce AML. In this model, the LSK Multipotent Progenitor (MPP) cells propagate this disease and this portion of the LSK compartment is relatively expanded.[133] Similar results have been obtained in a combined *Idh2*^{R140Q} *Flt3*^{ITD} model (data not published.) Another group was able to use *IDH2*^{R140Q} mutation in cooperation with overexpression of HoxA9, Meis1a, and mutant FLT3 to precipitate leukemia with evidence of blocked differentiation.[134]

Finally, a model combining *Jak2*^{V617F} mutation with *Tet2* knockout was recently characterized. This model manifested a fulminant MPN with invasive features, including specific expansion of granulocytic compartments and competitive advantage in the bone marrow niche. Ultimately, these data indicate that these pathways may cooperate phenotypically. However, they also indicate that the combination of *Jak2* and *Tet2* mutations is not sufficient to induce transformation to AML.[135]

MATERIALS AND METHODS

Retrovirus Production and Transduction for Overexpression

Retroviral overexpression vectors containing human cDNA for *IDH1*, *IDH1*^{R132H}, *IDH2*, and *IDH2*^{R140Q} on the MSCV promoter with IRES GFP were kindly provided by Patrick Ward and Craig B. Thompson (Memorial Sloan Kettering Cancer Center.) Vectors containing *MPL* and *MPL*^{W515L} on the MSCV promoter with IRES GFP or IRES human CD4 (OKT4, BioLegend) were previously described or cloned directly from

previously described vectors[6,136] and verified by Sanger sequencing and Western Blot (data not shown).

Retrovirus was produced using FuGENE® 6 Transfection Reagent (Promega, Cat E2311) according to manufacturer specifications with VSVG envelope protein in 293T-HEC cell lines, collected, and flash frozen for future use. Transduction was performed using 6.7 μg/mL polybrene (American Bioanalytical, Cat AB01643), 1mL virus, and 1 x 10^6 cells /mL for 5 hours using spinfection technique, and then cells were resuspended in fresh media overnight.

Stable expression of Cell Lines

Ba/F3, 32D, and TF1 cell lines were transduced simultaneously with *IDH* MSCV *GFP* vector and *MPL* MSCV *CD4* vector twice at two-day intervals with an additional week of recovery. FACS sorting was performed on GFP and using antibodies against human CD4 and allowed to recover for one week before evaluation and further sorting.

Transgenic Animals

The conditional *Jak2*^{V617F} mice were previously described.[125] Conditional transgenic *IDH1*^{R132H} mice,[69,132] were kindly provided by Kwok-Kin Wong (Dana Farber Cancer Institute) and conditional *Idh2*^{R140Q} mice were kindly provided by Craig B. Thompson (Memorial Sloan Kettering Cancer Center). At induction, mice received five intraperitoneal injections of polyI:polyC (Amersham) of 200 μL of a 1 mg per mL solution. Peripheral blood was collected via cheek bleeding using heparinized microhematocrit capillary tubes (Thermo Fisher Scientific). Peripheral blood counts were obtained using a HemaVet according to standard manufacturer's instructions.

Excision at two weeks post-induction was confirmed using PCR. Animals were humanely sacrificed when they were moribund. All animal procedures were conducted in accordance with the Guidelines for the Care and Use of Laboratory Animals and were approved by the Institutional Animal Care and Use Committees at Memorial Sloan Kettering Cancer Center.

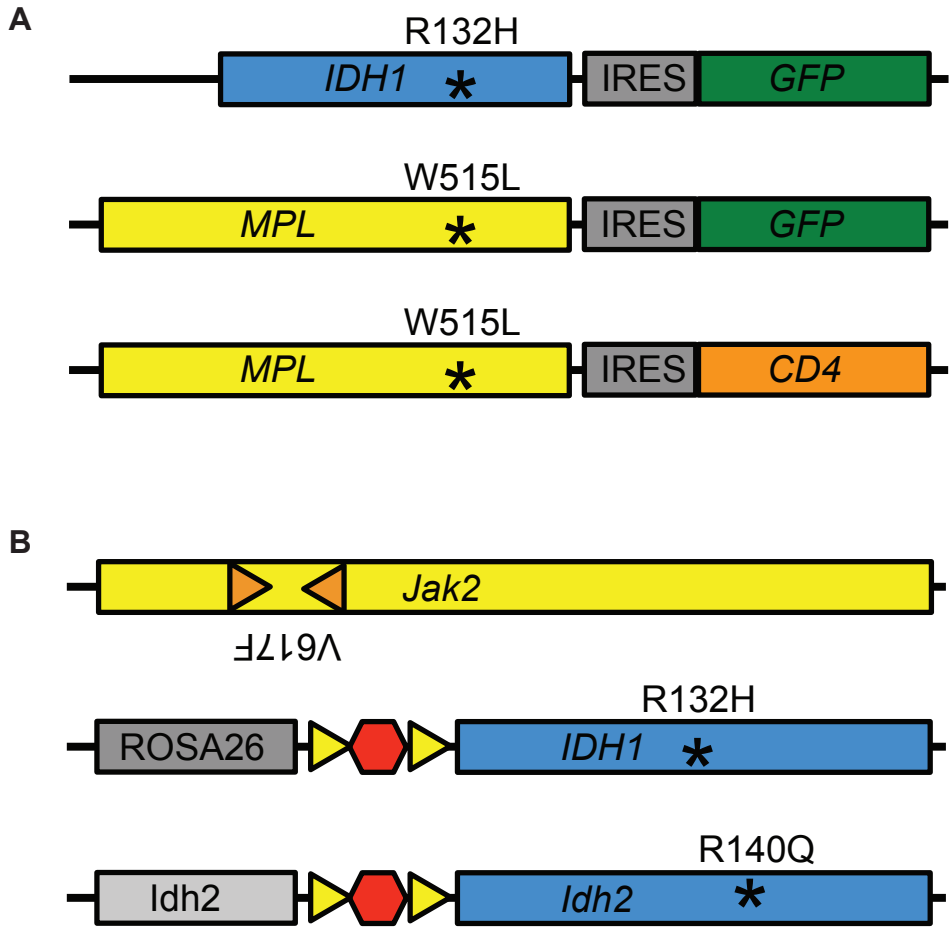

Figure 2.1: Schematic constructions of vectors and mouse models used in this study
(A) Construction of retroviral vectors used in adoptive transfer and in vitro experiments. (All retroviral vectors used an MSCV promoter.) (B) Construction of transgenic and knockin mice used in primary experiments.

Histology

Pathology was obtained after fixation in 4% paraformaldehyde (PFA); blood smears and bone marrow cytospins were performed on the day of sacrifice. Sections were stained with hematoxylin and eosin stain or Wright Giemsa stain as appropriate. Immunohistochemical staining was performed on a Leica Bond™ RX using the Bond™ Polymer Refine Detection Kit (Cat. No. DS9800). The sections stained with CD34 (Abcam, Cat. Ab8158 diluted 1:50) were pre-treated using heat mediated antigen retrieval with Citrate, pH6 (Leica Biosystem Epitope Retrieval 1, Cat. No. AR9961) for 20min. DAB was used as the chromogen, counterstained with hematoxylin and mounted.

Bone Marrow Transplant and Retroviral Adoptive Transfer Studies

Dissected femurs and tibias were isolated. Bone marrow was flushed into PBS + 2%BSA or RPMI + 10% FCS using a syringe or by centrifuge spin. Spleens were isolated and single cell suspensions made by mechanical disruption using glass slides. All harvested cells were passed through a 70 mm strainer. Red blood cells (RBCs) were lysed in ammonium chloride-potassium bicarbonate lysis buffer for 10 min on ice.

Donors for retroviral adoptive transfer transplants were dosed by intraperitoneal injection (IP) with 150 mg per kg 5-Fluorouracil 5-7 days before sacrifice. Bone marrow cells were maintained overnight in transplant media (RPMI, 10% FCS, P/S, 6 ng/mL recombinant mouse IL3 (R and D systems, Cat 403-ML), 10 ng/mL recombinant mouse SCF (R and D Systems, Cat 1832-01), 10 μg/mL recombinant human IL-6 (Gemini, Cat 300-155P)) and transfected as described above twice on consecutive days before cells were injected into recipients.

For secondary transplants, cells were transplanted by via tail vein injection into lethally irradiated (2 x 550 Rad) CD45.1 host mice. For noncompetitive transplants, $1x10^6$ total cells were transplanted; for competitive transplants including drug studies, $1x10^6$ total donor cells were injected in a mixture with $1x10^6$ cells from a congenic CD45.1 donor; for cell of origin transplants, injection number was determined based on the lowest yield after sort to inject approximately 100,000 MPP or 300 LT-HSC with 300,000 whole bone marrow cells from a CD45.1 donor.

Flow cytometry and fluorescence-activated cell sorting for murine tissues

Cells were stained with antibodies in FACS Buffer (2% Bovine Serum Albumin in phosphate-buffered saline (PBS)) for 30 min on ice. Donor and support chimerism was assessed using antibodies against CD45.1 (Clone A20, Biolegend) and CD45.2 (Clone 104, BioLegend).

For hematopoietic stem and progenitor staining, cells were stained with a lineage cocktail including CD4 (clone RM4-5, BioLegend), CD3 (clone 17A2, BioLegend), B220/CD45R (clone RA3-6B2, BioLegend), NK1.1 (clone PK136, BioLegend), Gr-1 (clone RB6-8C5, BioLegend), Mac1/CD11b (clone M1/70, BioLegend) and Ter119 (cat no. 116223, BioLegend), allowing for mature lineage exclusion from the analysis. Cells were also stained with antibodies specific to c-Kit/CD117 (clone 2B8, BioLegend), Sca-1 (clone D7, BioLegend), FcγRII/III/CD16/32 (clone 2.4G2, eBiosciences) and CD34 (clone RAM34, eBiosciences) or SLAM/CD150 (TC15-12F12.2, BioLegend) and CD48 (HM48-1, eBiosciences). To assess mature cell lineages we used a combination of antibodies against Mac1, Gr-1, B220, CD3, cKit/CD117, CD45.1, and CD45.2.

To assess erythroid and megakaryocyte progenitors we stained unlysed tissues with a lineage cocktail including CD4, CD8, B220/CD45R, Mac1/CD11b, Gr-1, IL7R/CD127 (A7R34, BioLegend), CD49b (DX5, BioLegend). Antibodies were also used against c-Kit/CD117, Sca-1, SLAM/CD150, CD48, FcγRII/III/CD16/32, CD41 (eBioMWReg30, eBioscience), CD105 (MJ7/18, BioLegend), CD71 (RI7217, BioLegend), and Ter119 and gated as previously described.[137]

Before cell of origin transplants, sorting was performed on bone marrow with enrichment for cKit/CD117-positive cells using CD117 MicroBeads (Miltenyi). For expression analysis, sorting was performed on bone marrow that had been depleted of mature cells using Progenitor Cell Enrichment Kit (STEMCELL Technologies).

Metabolomic analysis

2-HG was extracted from cells and tissue culture media using 80% aqueous methanol, as previously described.[138] For cell extraction, 2×10^6 cells were suspended in -80°C 80% methanol. All extracts were spun at 13,000 rpm at 4°C to remove precipitate, dried at room temperature, and stored at -80°C. Metabolite levels were determined by ion-paired reverse-phase LC coupled to negative mode electrospray triple-quadrupole mass spectrometry using multiple reactions monitoring, and integrated elution peaks were compared with metabolite standard curves for absolute quantification.[65]

Expression analysis

$CD45.2^+$ LSK cells were sorted into ice cold FACS Buffer, pelleted, and stored in Triazol until extraction of RNA using phenol-chlorophorm. The library was produced

using SMARTer amplification (Clontech) amplify and create the library. Illumina sequencing was performed using Paired-End 50 bp at 40 x 10^6 reads per sample.

Statistical analysis

Data are displayed as mean ± SEM. Prism software was used to conduct the statistical analysis of all data. Multiple comparisons were performed using an ordinary one-way ANOVA, using Tukey's correction for post-hoc comparisons. Comparisons of survival were performed using the log-rank (Mantel-Cox) test. Statistical interaction calculated for influence of *Jak2* mutation status and IDH mutation status combined using two-way ANOVA. Paired t-tests were used to compare results in mice before and after treatment. Longitudinal chimerism data was modeled as log-log curves assuming constant y-intercept and performing hypothesis testing for equal slopes. Correlations were examined by calculating Pearson's correlation coefficient and its corresponding significance. All comparisons are two-tailed. $P < 0.05$ was considered to be significant. *$P < 0.05$, **$P < 0.01$, ***$P < 0.001$, ****$P < 0.0001$.

RESULTS

Combined IDH and JAK2 mutant mice develop lethal MPN with preleukemic features

To create a preliminary model of phenotypic cooperativity between IDH and JAK-STAT activating mutations, we employed a retroviral adoptive transfer (RAT) model using vectors expressing *MPL*^{W515L} or *IDH1*^{R132H} cDNA with an IRES GFP reporter. Retrovirus was transduced into bone marrow from primary mice conditionally expressing *Jak2*^{V617F} or *IDH1*^{R132H} and marrow was transplanted into recipients.

MPL^{W515L} adopted into *IDH1*^{R132H} resulted in a sudden, dramatic phenotype as early as 20 days and combined mutant mice reached death (or moribund state) within 4 weeks. At this endpoint, combined mutant mice displayed splenomegaly (**Figure 2.2.A**). Notably, leukocytosis and thrombocytosis were significantly greater and polycythemia was significantly lesser in combined mutants than in than in MPL-mutant alone mice (**Figure 2.2.B**). Pathological observation revealed that peripheral blood of combined mutant mice was typical MPN, while the bone marrow of combined mutant mice showed atypical blasts which were not seen in *MPL*^{W515L} mice alone (data not shown.)

Mice in which *IDH1*^{R132H} was adopted into *Jak2*^{V617F} had a longer course of disease with all mice remaining in the cohort at least 115 days. Endpoint data was suggestive of increased splenomegaly in double mutants in comparison to Jak2-mutant alone mice (**Figure 2.2.C**), although this observation was limited by small sample size. Over time, combined mice showed leukocytosis and polycythemia similar to that of JAK2-mutant mice (**Figure 2.2.D**).

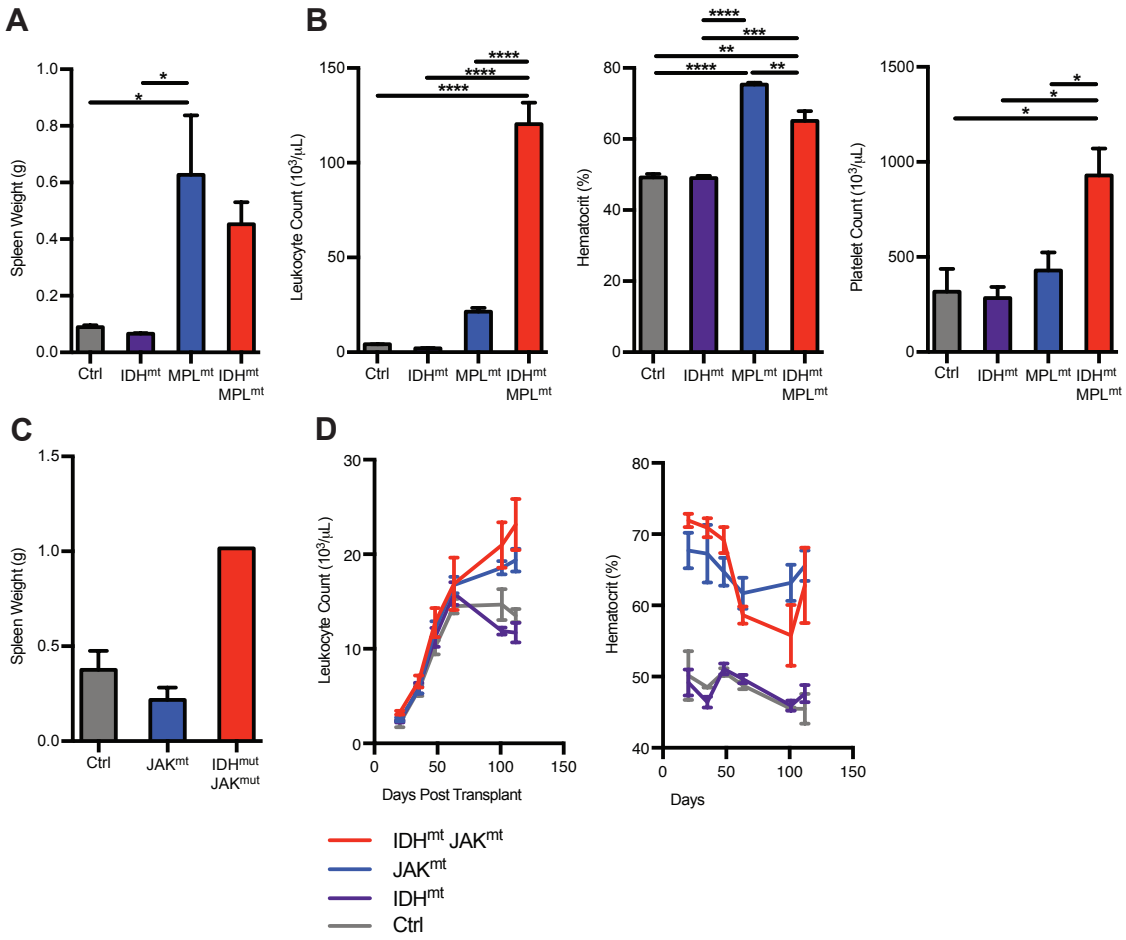

Figure 2.2: Retroviral adoptive transfer recipients of combined JAK-STAT and mutant IDH1 develop MPN

(A-B) Phenotype of recipients of retrovirally-induced *MPL*^{W515L} expression in *IDH1*^{R132H}-expressing murine bone marrow cells. (A) Spleen weights at sacrifice, and (B) complete blood count quantification of leukocytosis, polycythemia, and thrombocytosis 20 days post transplant.

(C-D) Phenotype of recipients of retrovirally-induced *IDH1*^{R132H} expression in *Jak2*^{V617F}-expressing murine bone marrow cells. (C) Spleen weights at sacrifice, and (D) longitudinal measurements of complete blood counts after adoptive transfer.

To create a more faithful model of phenotypic cooperativity between IDH and JAK2 mutations, we crossed mice to combine inducible transgenic *IDH1*^{R132H} or conditional knockin *Idh2*^{R140Q} with *Jak2*^{V617F} and Mx1-cre. We aged a primary cohort of *IDH1*^{R132H} *Jak2*^{V617F} mice after cre induction, and combined mutant primary mice showed similar survival to Jak2-mutant controls, which both have significantly reduced survival compared to IDH mutant and control mice (**Figure 2.3.A**). Combined mutant mice show an MPN phenotype with leukocytosis and polycythemia similar to that of Jak2-mutant mice (**Figure 2.3.B**). At endpoint, combined mutant mice show splenomegaly (**Figure 2.3.C**) and trend toward leukocytosis and polycythemia (**Figure 2.3.D**). In timed sacrifices at approximately 100 days, combined mutants show robust splenomegaly (**Figure 2.4.A**) and leukocytosis while trending toward polycythemia (**Figure 2.4.B**), similar to *Jak2*-mutant controls. Histological examination of these mice revealed combined mutant spleens showed increased loss of normal architecture beyond that of *Jak2*^{V617F} mice, and the appearance of blast-like cells with open chromatin and large nucleoli could be observed in the spleen of combined mice but not in *Jak2*^{V617F} mice. In the bone marrow and cytospins, atypical megakaryocytes were observed, and CD34 staining in the bone marrow revealed that these cells showed stronger staining than in single mutant mice. (**Figure 2.4.C**) These histological changes were accompanied by pallor in hematopoietic organs in comparison to *Jak2*^{V617F} (data not shown).

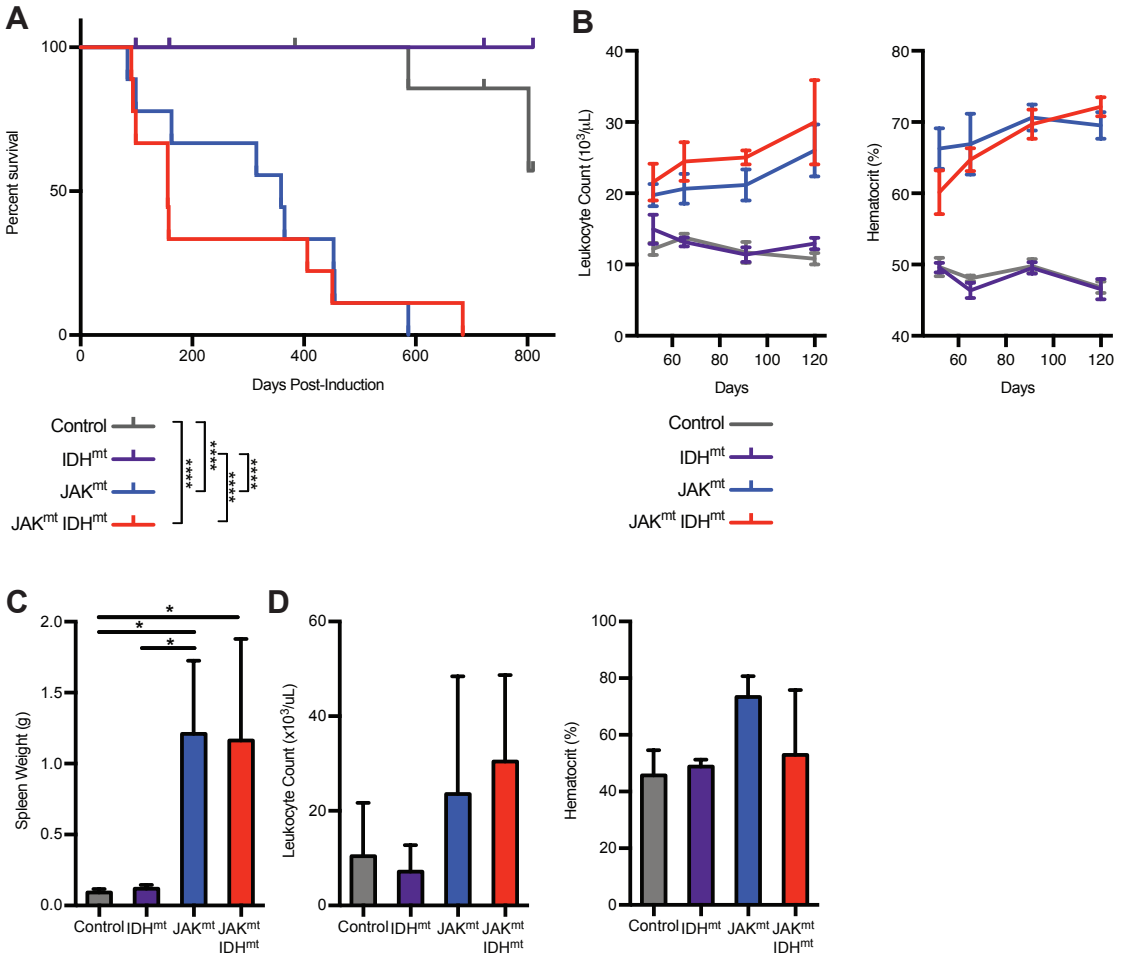

Figure 2.3: Primary mice expressing *IDH1*^{R132H} and *JAK2*^{V617F} develop lethal MPN
(A-B) Longitudinal measurements of primary mice after polyI-polyC induction of recombination: (A) Kaplan-meier survival curve, (B) complete blood count quantification of leukocytosis and polycythemia in peripheral blood.
(C-D) Phenotypic measurements in primary mice at endpoint: (C) Spleen weights, and (D) complete blood count quantification of leukocytosis and polycythemia in peripheral blood.

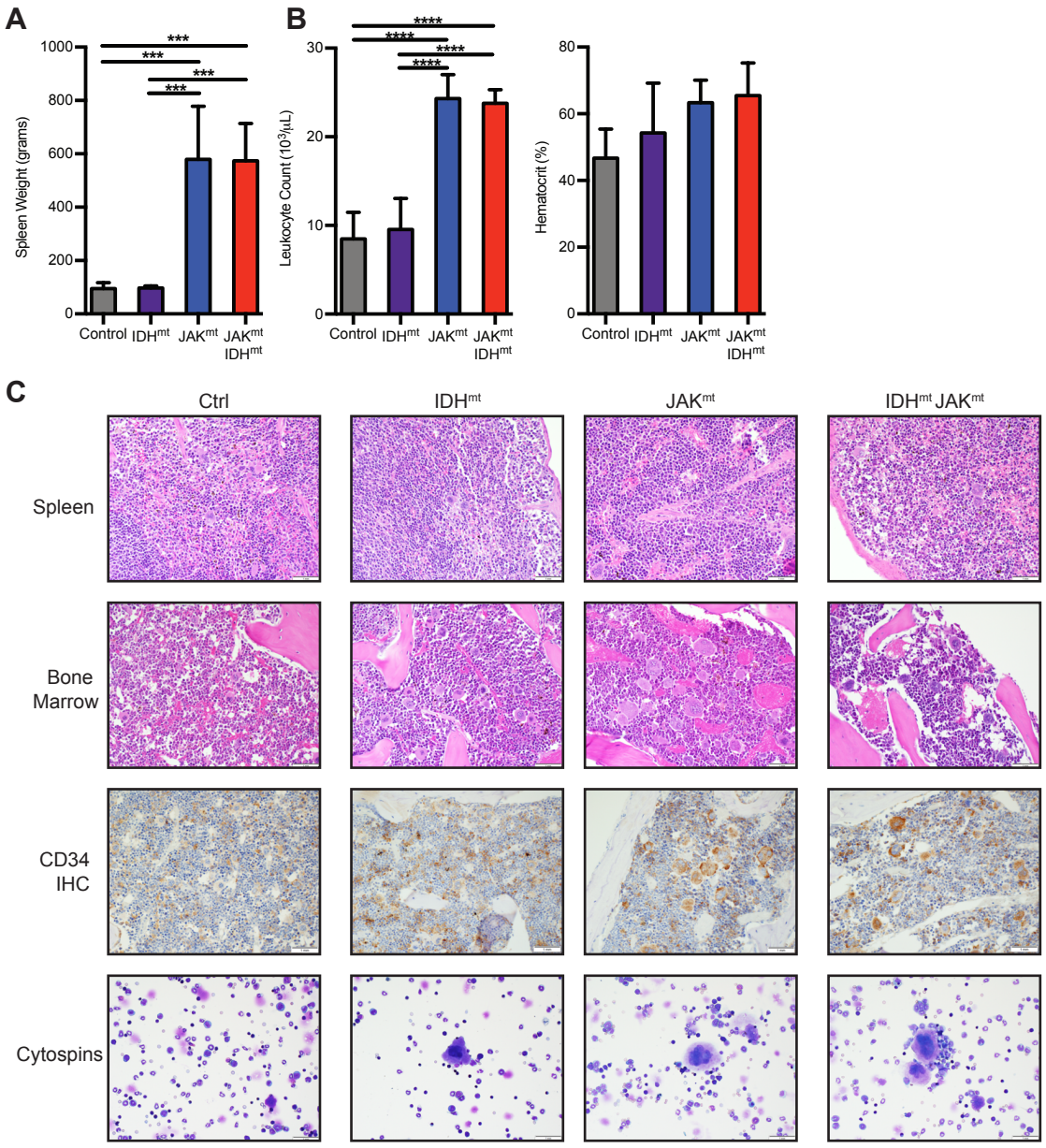

Figure 2.4: Primary IDH1R132H Jak2V617F mice develop lethal MPN with preleukemic histology

(A-C) Characterization of disease in primary mice sacrificed approximately 100 days after recombination by polyI:polyC induction. (A) Spleen weights at sacrifice, and (B) complete blood count quantification of leukocytosis, and polycythemia. (C) Representative images of histological sections from hematopoietic organs.

Mice expressing combined *Idh2*^{R140Q} and *Jak2*^{V617F} showed splenomegaly (**Figure 2.5.A**), leukocytosis and polycythemia (**Figure 2.5.B**) similar to that of *Jak2*^{V617F} mice, at timed sacrifices at approximately 100 days. Histologically, these mice also show significantly disrupted spleen architecture with blast-like cells that are not present in *Jak2*^{V617F} mice. Megakaryocyte-like cells also show noticably stronger immunohistochemical staining of CD34 in these mice than in single mutant mice, and bone marrow cytospins show a variety of abnormal myeloid elements with a strongly elevated M:E ratio (**Figure 2.5.C**). These data indicate that combined mutant mice have a lethal myeloproliferative neoplasm with histological preleukemic features.

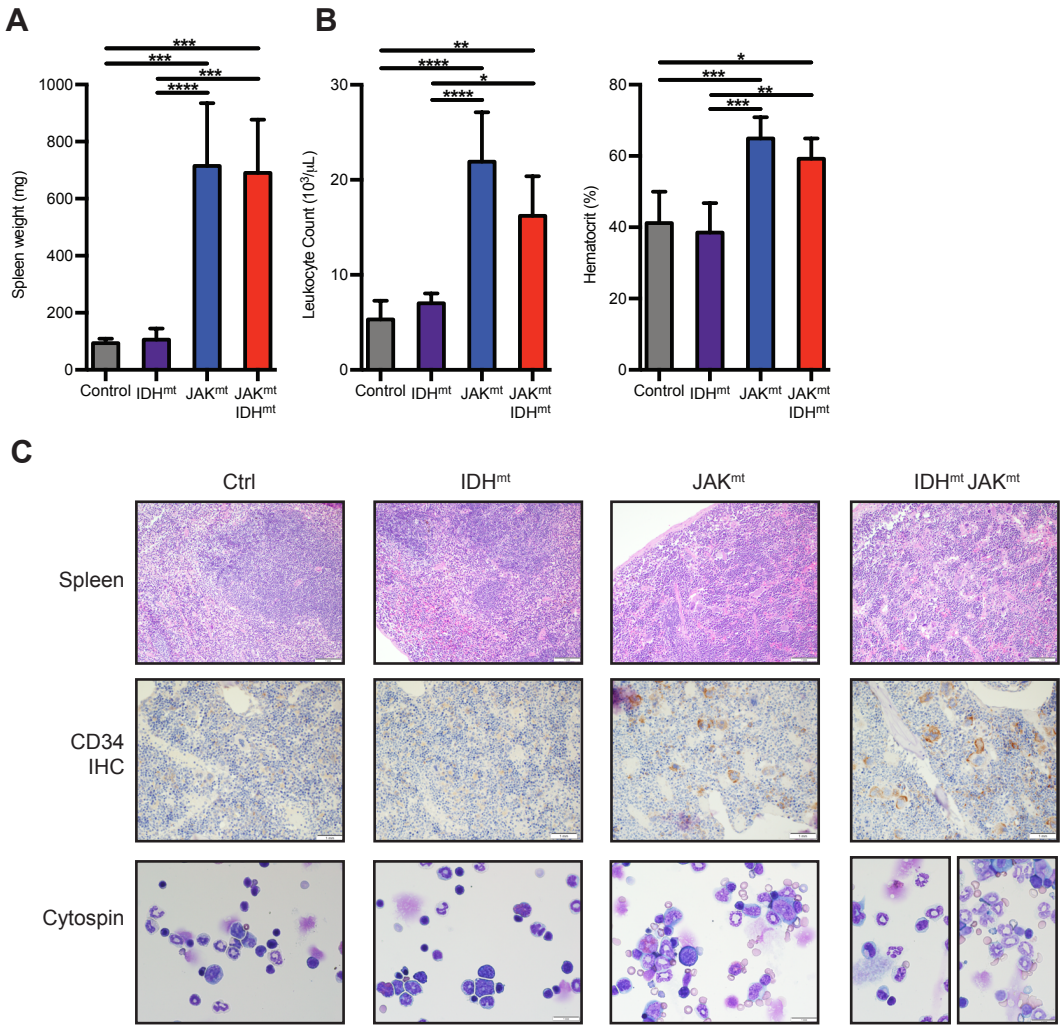

Figure 2.5: Primary *Idh2*^{R140Q} *Jak2*^{V617F} mice develop lethal MPN with preleukemic histology

(A-C) Characterization of disease in primary mice sacrificed approximately 100 days after recombination by polyI:polyC induction. (A) Spleen weights at sacrifice, and (B) complete blood count quantification of leukocytosis and polycythemia. (C) Representative images of histological sections from hematopoietic organs.

To test the functional aspects of this preleukemic phenotype we performed secondary transplants of bone marrow from *IDH1*^{R132H} *Jak2*^{V617F} primary mice into lethally irradiated recipients. These combined mutant mice had significantly shorter survival than *Jak2*^{V617F} mice (**Figure 2.6.A**), indicating that this disease accelerates upon transplantation. The recipients of combined bone marrow also developed myeloproliferative neoplasm with leukocytosis and thrombocytosis similar to recipients of *Jak2*^{V617F} bone marrow (**Figure 2.6.B**).

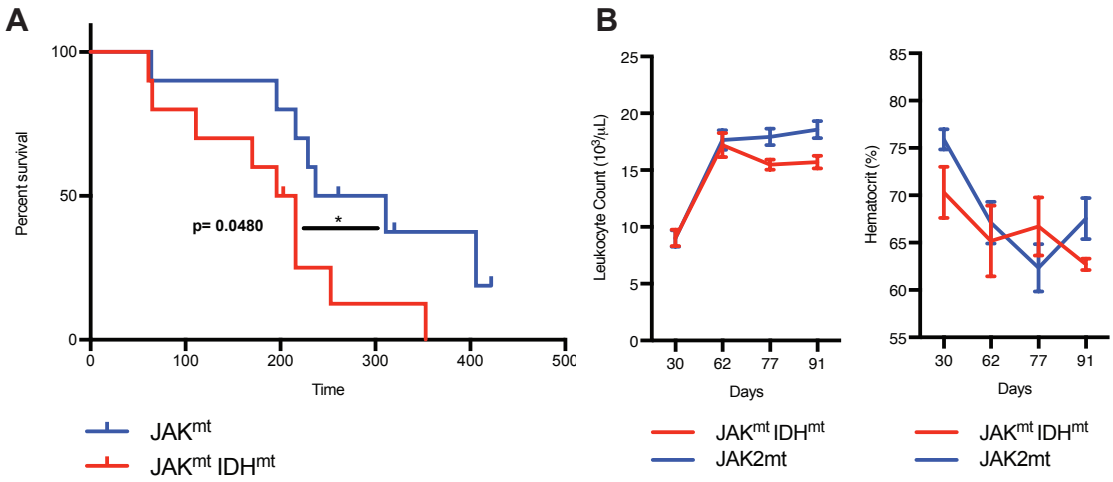

Figure 2.6: Secondary transplant recipients of *IDH1*^{R132H} *Jak2*^{V617F} bone marrow develop accelerated lethal MPN

(A-B) Longitudinal characterization of disease in recipients of primary bone marrow: (A) Kaplan-Meier survival curves and (B) complete blood count quantification of leukocytosis and polycythemia.

IDH1 combined mutant MPN shows non-cell autonomous synergistic elevation of serum 2-HG with JAK-STAT activating mutation

Interestingly, measurement of the oncometabolite 2-HG in serum of the primary and adoptive transfer models above showed a synergistic relationship between expression of IDH mutation and JAK2 mutations. This was true for our *MPL*^{W515L} into *IDH1*^{R132H} model (**Figure 2.7.A**), our *IDH1*^{R132H} into *Jak2*^{V617F} model (**Figure 2.7.B**), and our primary *IDH1*^{R132H} *Jak2*^{V617F} model mice (**Figure 2.7.C**), indicating that it is not simply an artifact of one model system. However, we did not observe this cooperation in our primary *Idh2*^{R140Q} *Jak2*^{V617F} models (**Figure 2.7.D**), which show much higher levels of 2-HG in the serum on induction.

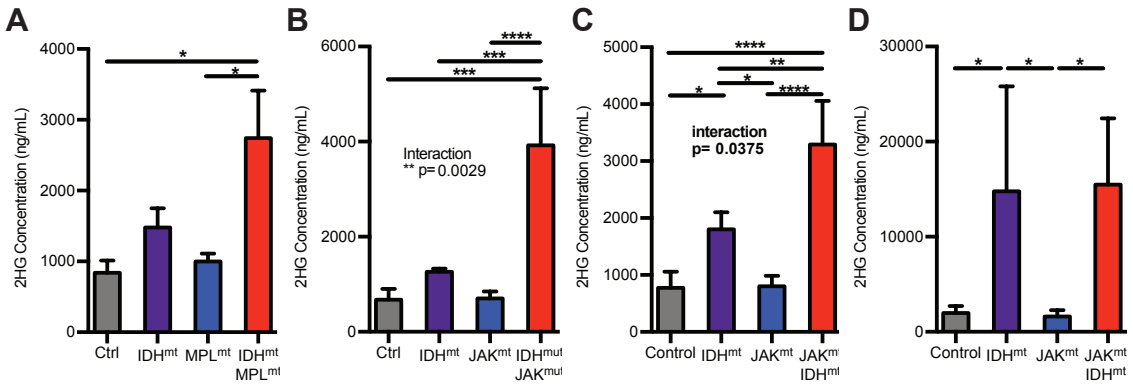

Figure 2.7: Serum 2-HG quantification reveals synergistic relationship between *IDH1* and JAK-STAT mutations

(A-D) Quantification of 2HG in serum in the following mouse models: (A) recipients of retrovirally-induced *MPL*^{W515L} expression in *IDH1*^{R132H}-expressing murine bone marrow cells, (B) recipients of retrovirally-induced *IDH1*^{R132H} expression in *Jak2*^{V617F}-expressing murine bone marrow cells, (C) primary *IDH1*^{R132H} *Jak2*^{V617F} mice, and (D) primary *Idh2*^{R140Q} *Jak2*^{V617F} mice.

In an effort to delineate the mechanism for this synergy, we correlated serum 2-HG with other measurements taken at the time of serum collection. In *IDH1*^{R132H} into *Jak2*^{V617F} mice, we did not see a correlation between 2-HG and proportion of GFP-positive cells, indicating that this elevation is not simply associated with increased presence of the mutant clone. Instead, a mild correlation was seen with leukocyte counts and excellent correlation (r^2 = 0.9584, p=0.036) with hematocrit levels in each mouse (**Figure 2.8.A**). Accordingly, in *IDH1*^{R132H} *Jak2*^{V617F} primary mice, there was a strong negative correlation (r2 = 0.9508, p=0.0249) between 2-HG and proportion of common myeloid progenitors (CMP; $Lin^- Sca1^+ cKit^- CD16/32^- CD34^+$), a negative correlation with granulocyte-macrophage progenitors (GMP; $Lin^- Sca1^+ cKit^- CD16/32^+$), and a strong positive correlation (r^2 = 0.929, p= 0.0362) with megakaryocyte-erythroid progenitors (MEP; $Lin^- Sca1^+ cKit^- CD16/32^- CD34^-$) (**Figure 2.8.B**).

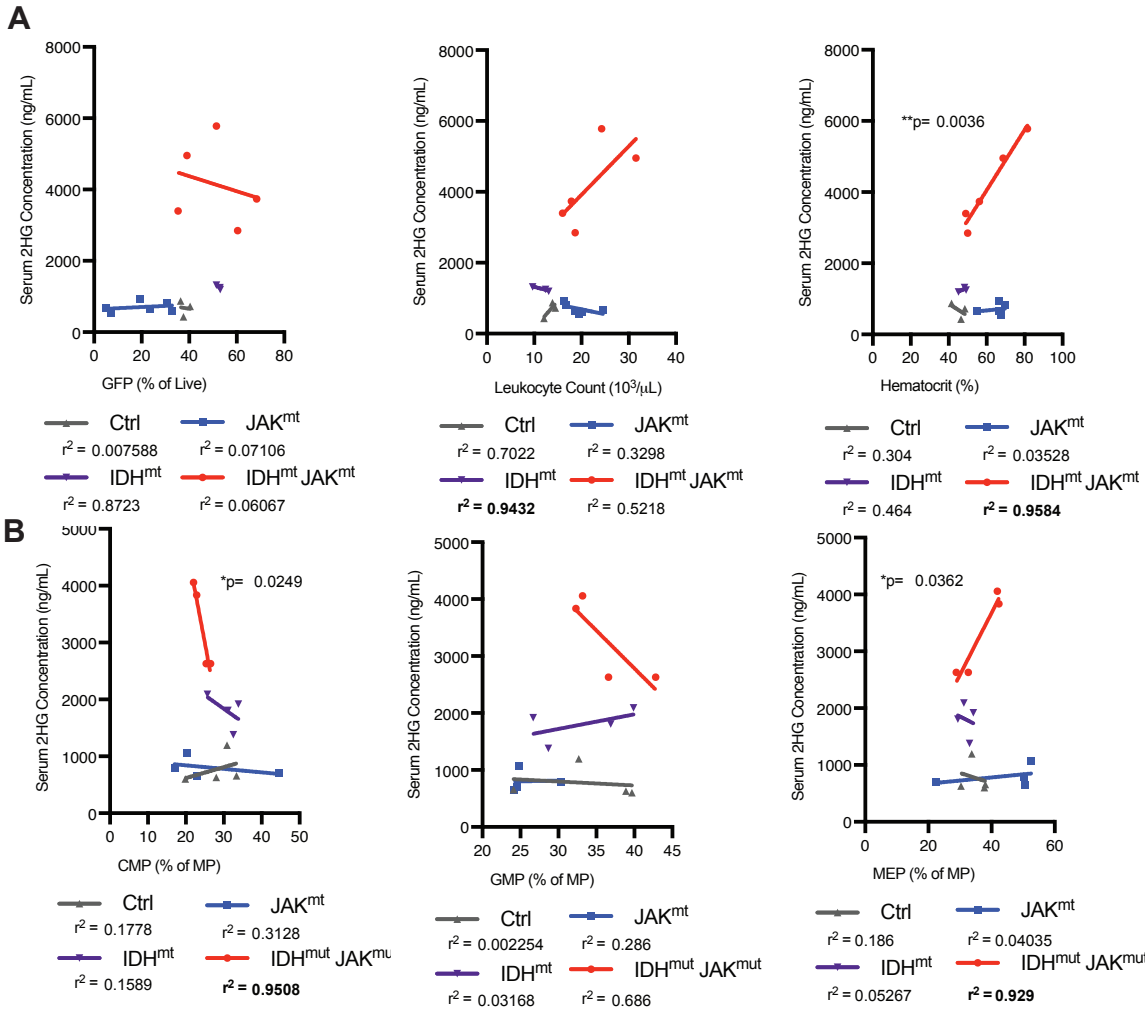

Figure 2.8: Strong positive correlations are observed between serum 2-HG and erythroid development

(A) Correlation between serum 2-HG and peripheral blood measurements in recipients of retrovirally-induced *IDH1*^{R132H} expression in *Jak2*^{V617F}-expressing murine bone marrow cells.

(B) Correlation between serum 2HG and peripheral blood measurements in *IDH1*^{R132H} *Jak2*^{V617F} primary mice

Because metabolomics assays currently require large numbers of cells, we sought to reproduce this finding in various murine and human cell lines using retroviral overexpression vectors with fluorescent reporters. In the lymphoblastic murine Ba/F3 cell line, although expression of *IDH1*^{R132H} elevated 2-HG, the presence of *MPL*^{W515L} did not appear to elevate this level either intracellularly (**Figure 2.9.A**) or in the supernatant media (**Figure 2.9.B**). Western blots confirmed overexpression of the relevant proteins (**Figure 2.9.C**). In the myeloblastic murine 32D cell line, overexpression of *IDH2*^{R140Q} also elevated intracellular 2-HG levels but this did not increase with the presence of *MPL*^{W515L} (**Figure 2.9.D**). Western blots confirmed overexpression of appropriate proteins in this cell line (**Figure 2.9.E**). Finally, in the human myelo/erythroblastic TF1 cell line, similar results were obtained (**Figure 2.9.F**) despite adequate levels of expression markers (**Figure 2.9.G**). We concluded that the relevance of this system to the preleukemic phenotype we observe in mice might be limited.

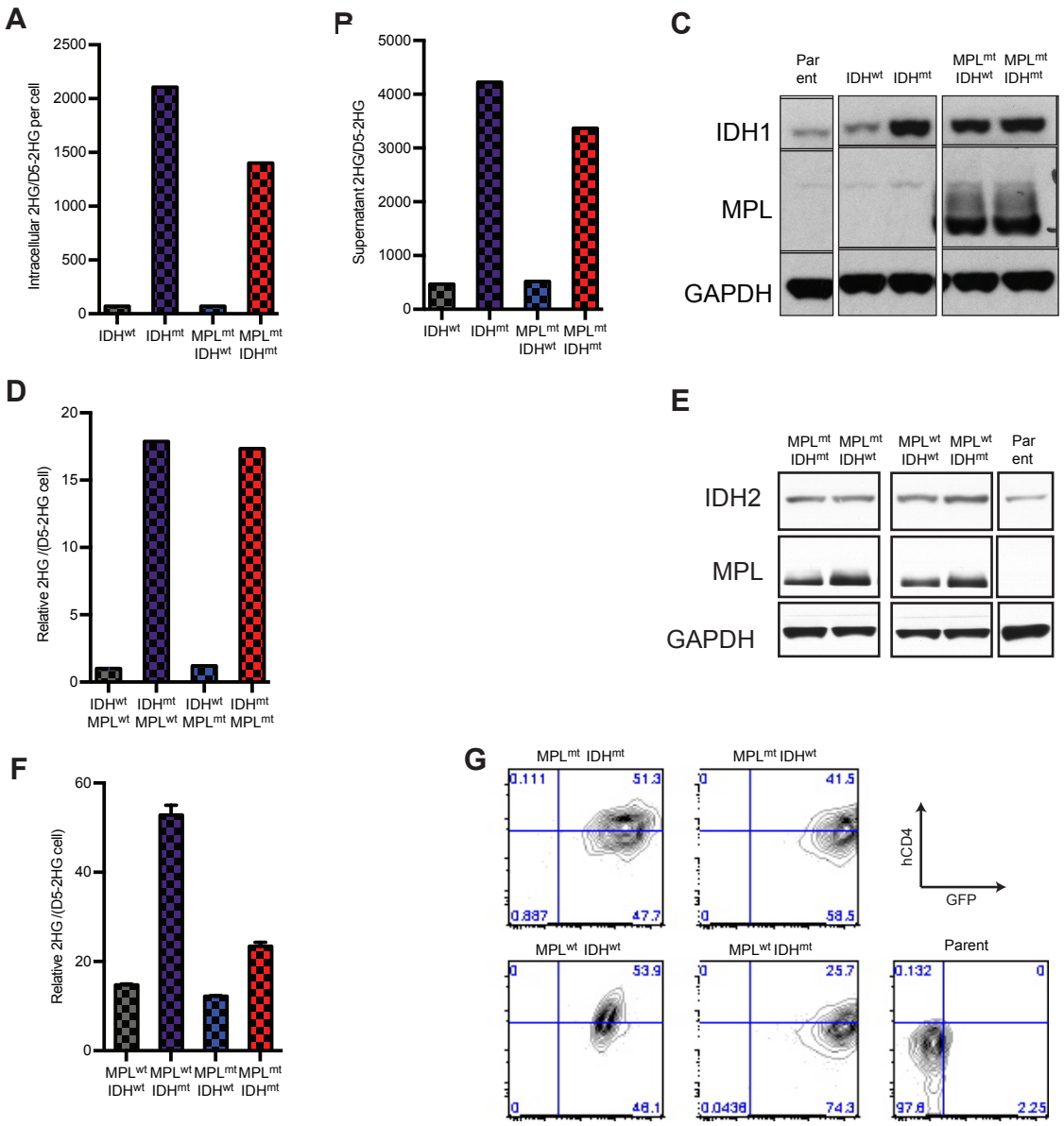

Figure 2.9: Activating JAK-STAT mutations do not synergistically elevate 2-HG production by mutant IDH in vitro

(A-C) Ba/F3 cell lines overexpressing *MPL*^{W515L} and *IDH1*^{R132H}, evalutated with respect to (A) intracellular 2-HG, (B) 2-HG accumulation in supernatant media, and (C) overexpression of transduced proteins.

(D-E) 32D cell lines overexpressing *MPL*^{W515L} and *IDH2*^{R140Q}, evaluated with respect to (D) intracellular 2-HG, and (E), overexpression of transduced proteins.

F-G) TF1 cell lines overexpressing *MPL*^{W515L} and *IDH2*^{R140Q}, evaluated with respect to (D) intracellular 2-HG, and (E), surface staining of expression markers.

Combined IDH and JAK2 mutant mice have altered stem cell and progenitor phenotype

We sought to explore the stem/progenitor cell population of transmission of this disease. *IDH1*^{R132H} and *Jak2*^{V617F} bone marrow was sorted into LSK (Lin$^-$ CD117/cKit$^+$ Sca1$^+$) long-term hematopoietic stem cell (LT-HSC; LSK CD48$^-$ CD150$^+$) and multipotent progenitor (MPP; LSK CD48$^+$ CD150$^-$) populations (**Figure 2.10.A**) and injected into primary recipients. Disease transplanted from the LT-HSC was lethal, and *IDH1*^{R132H} and *Jak2*^{V617F} recipients showed similar survival to controls with *Jak2*^{V617F} (**Figure 2.10.B**). Disease chimerism, (**Figure 2.10.C**) polycythemia, and thrombocytosis were conferred overwhelmingly in recipients of LT-HSC but not MPP marrow (**Figure 2.10.D**). We infer based on these data that the combined mutant preleukemic MPN has its cell of origin in the LT-HSC compartment.

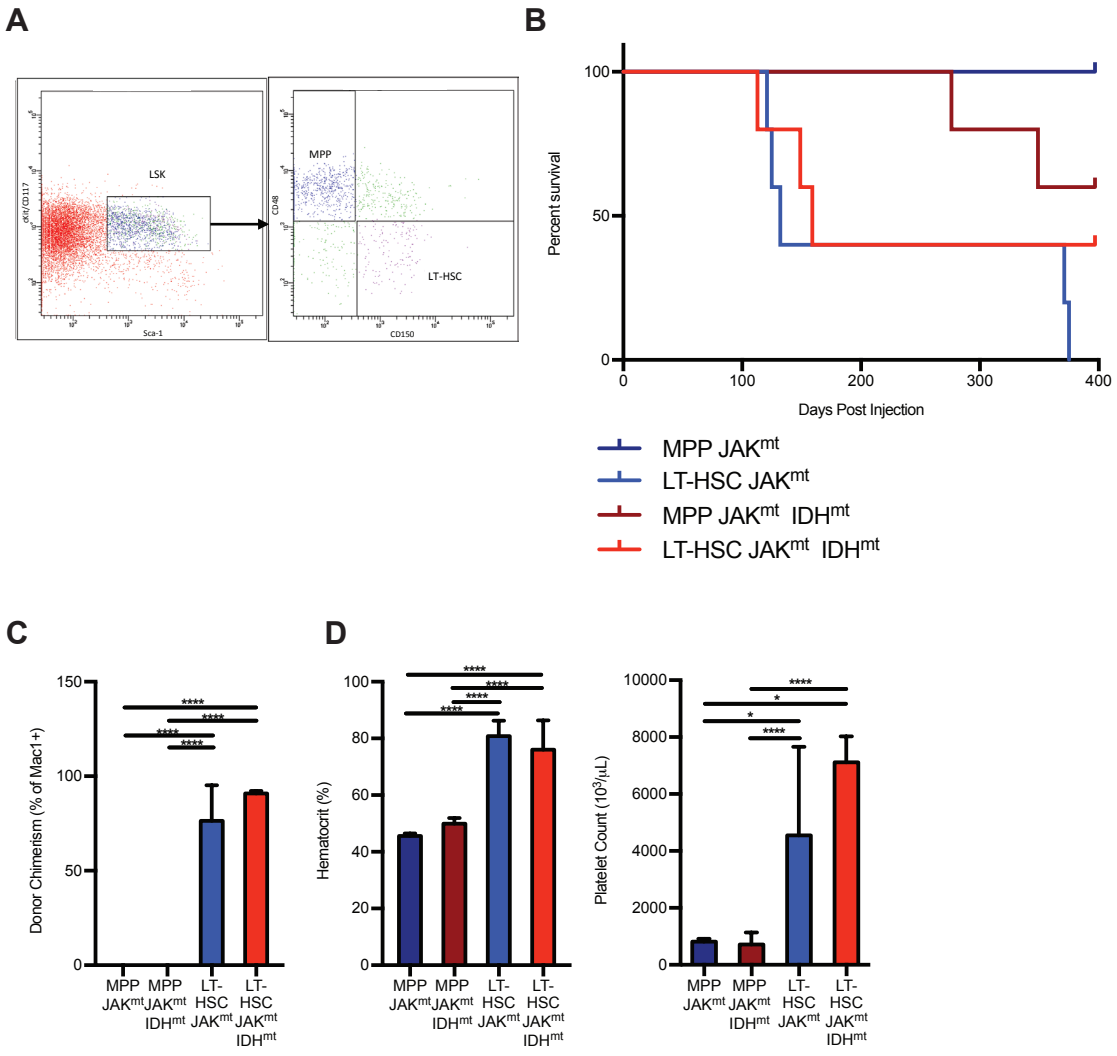

Figure 2.10: The cell of origin in *IDH1*^{R132H} *Jak2*^{V617F} MPN resides in LT-HSC compartment

(A) Representative image of gating of lineage negative bone marrow for FACS sorting.
(B) Kaplan-Meier survival curves of recipients after injection of sorted cells.
(C-D) Characterization of disease in peripheral blood of recipients approximately 100 days after transplant: (C) FACS quantification of donor (CD45.2^{+}) chimerism and (D) complete blood count quantification of leukocytosis and polycythemia.

Since combined mutant disease has its cell of origin in the LSK LT-HSC compartment, we explored other stem cell phenotypes that may exist in this combined mutant MPN. In the retroviral transfer experiments overexpressing *MPL*^{W515L} in *IDH1*^{R132H} marrow, we found that the presence of IDH mutation coincided with an increase the level of the MPL GFP marker in the peripheral blood (**Figure 2.11.A**). Similarly, in *IDH1*^{R132H} into *Jak2*^{V617F} marrow adoptive transfer experiments, cells containing the IDH1-mutant gained presence in the peripheral blood over time, while those overexpressing the wild type IDH1 did not (**Figure 2.11.B**). We tested the competitive abilities of *Idh2*^{R140Q} mouse bone marrow using competitive transplants by injecting marrow from donors with a CD45.2 cell surface marker mixed equally with marrow from wild type mice expressing a congenic CD45.1 marker. In doing this, we found that the presence of the IDH2 mutant improved the competitive capacity of the donor bone marrow regardless of *Jak2* mutant status (**Figure 2.11.C**), and this difference was statistically significant (**Figure 2.11.D**). Transplant recipients developed a phenotype very similar to primary mice including polycythemia and thrombocytosis. Notably, leukocytosis was greater in recipients of *Idh2*^{R140Q} *Jak2*^{V617F} marrow in comparison to *Jak2*^{V617F} alone (**Table 2.11.E**) further confirming the preleukemic disease observed in these mice.

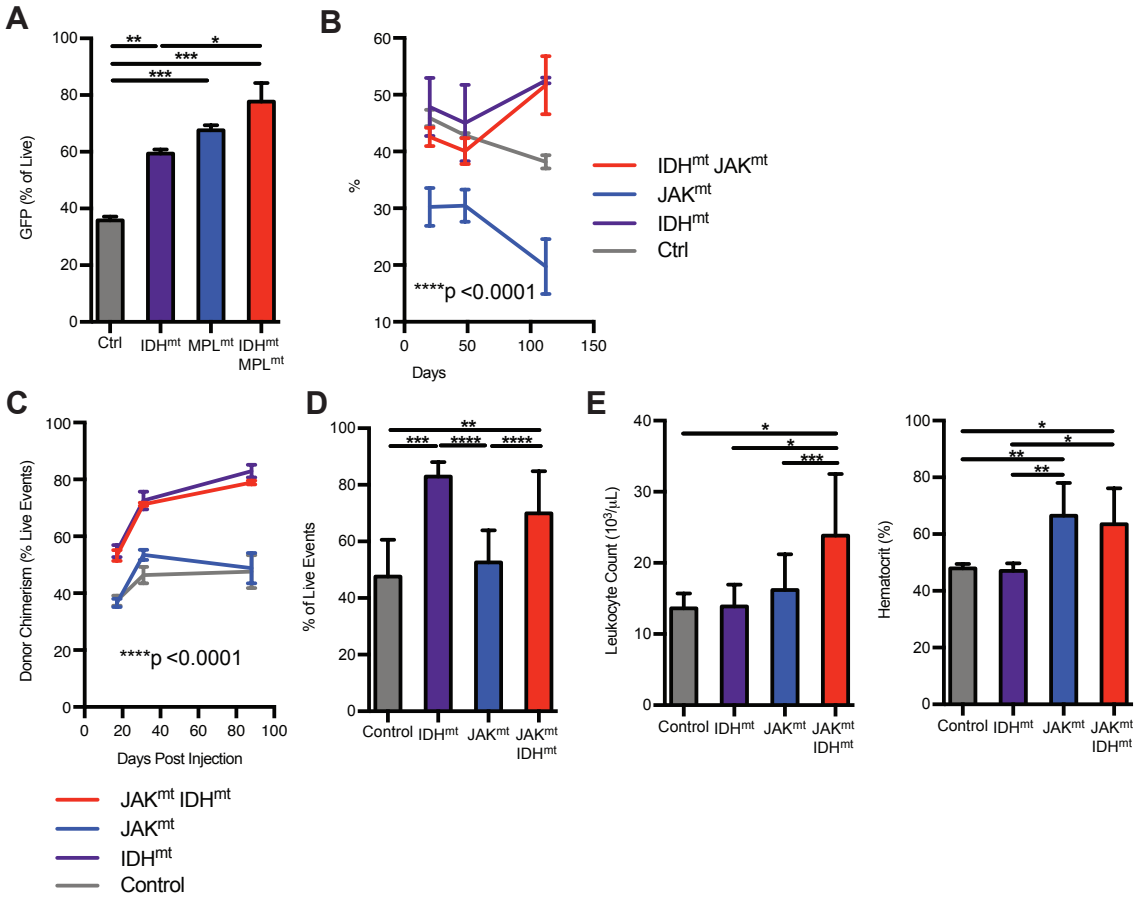

Figure 2.11: IDH mutant-expressing bone marrow has competitive advantage in hematopoietic niche

(A) Peripheral blood cells detected with GFP expression marker in recipients of retrovirally-induced *MPL*^{W515L} expression in *IDH1*^{R132H}-expressing murine cells, 20 days post transplant..

(B) Peripheral blood cells detected with GFP expression marker in recipients of retrovirally-induced *IDH1*^{R132H} expression in *Jak2*^{V617F}-expressing murine cells, displayed longitudinally after transplant.

(C-E) Observation of peripheral blood of recipients of equally mixed *Idh2*^{R140Q} *Jak2*^{V617F} (CD45.2^{+}) and wild type (CD45.1^{+}) bone marrow: (C) CD45.2^{+} chimerism observed longitudinally post transplant, (D) CD45.2^{+} chimerism observed approximately 12 weeks post transplant, and (E) complete blood count quantification of leukocytosis and polycythemia observed approximately 12 weeks post transplant.

Given this observation that IDH mutation improves the ability of bone marrow to expand within the hematopoietic niche, we sought to further characterize the stem cell phenotype of these mice. In models of overexpression of *MPL*^{W515L} in *IDH1*^{R132H} bone marrow, we found significantly elevated proportions of cKit/CD117^{+} cells (**Figure 2.12.A**) – this finding is not seen in the *MPL*^{W515L} model.[6] Looking into this cKit^{+} population, we observed that the presence of IDH mutation altered the distribution of LSK subpopulations by expanding the LT-HSC and ST-HSC compartments at the expense of the MPP compartment (**Figure 2.12.B**). Accordingly, the presence of MPL mutation expanded the GMP compartment at the expense of the MEP compartment (**Figure 2.12.C**).

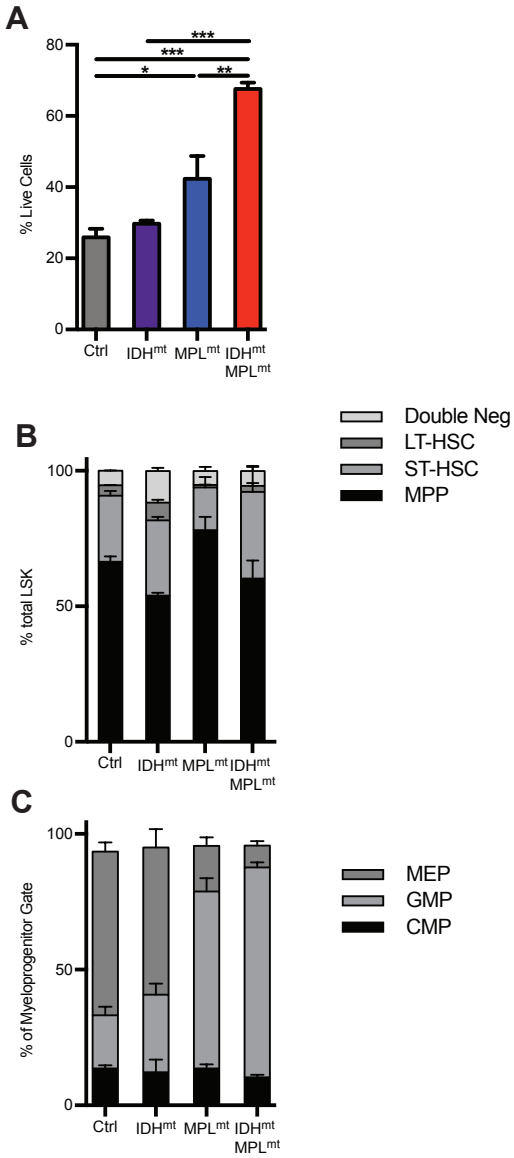

Figure 2.12: Retroviral transplant recipients of combined JAK-STAT and IDH mutation have aberrant stem cell populations

(A-C) Phenotype of recipients of retrovirally-induced *MPL*^{W515L} expression in *IDH1*^{R132H}-expressing murine bone marrow cells. (A) Proportion of live cells in bone marrow expressing high levels of cKit/CD117, (B) LSK cells quantified proportions of LSK subcompartments, (C) myeloprogenitors quantified by proportions of myeloprogenitor subcompartments

In primary *IDH1*^{R132H} *Jak2*^{V617F} mice, we observed marked expansion of the LSK compartments in both the bone marrow and spleen. In the bone marrow, the trend was toward expansion of the MPP (**Figure 2.13.A**), while in the spleen this population showed the opposite trend (**Figure 2.13.B**). Myeloid progenitor numbers were greatly affected by Jak2 mutation, though there was some trend toward reduction of MEP populations with the addition of IDH mutation in bone marrow (**Figure 2.13.C**) and the spleen (**Figure 2.13.D**).

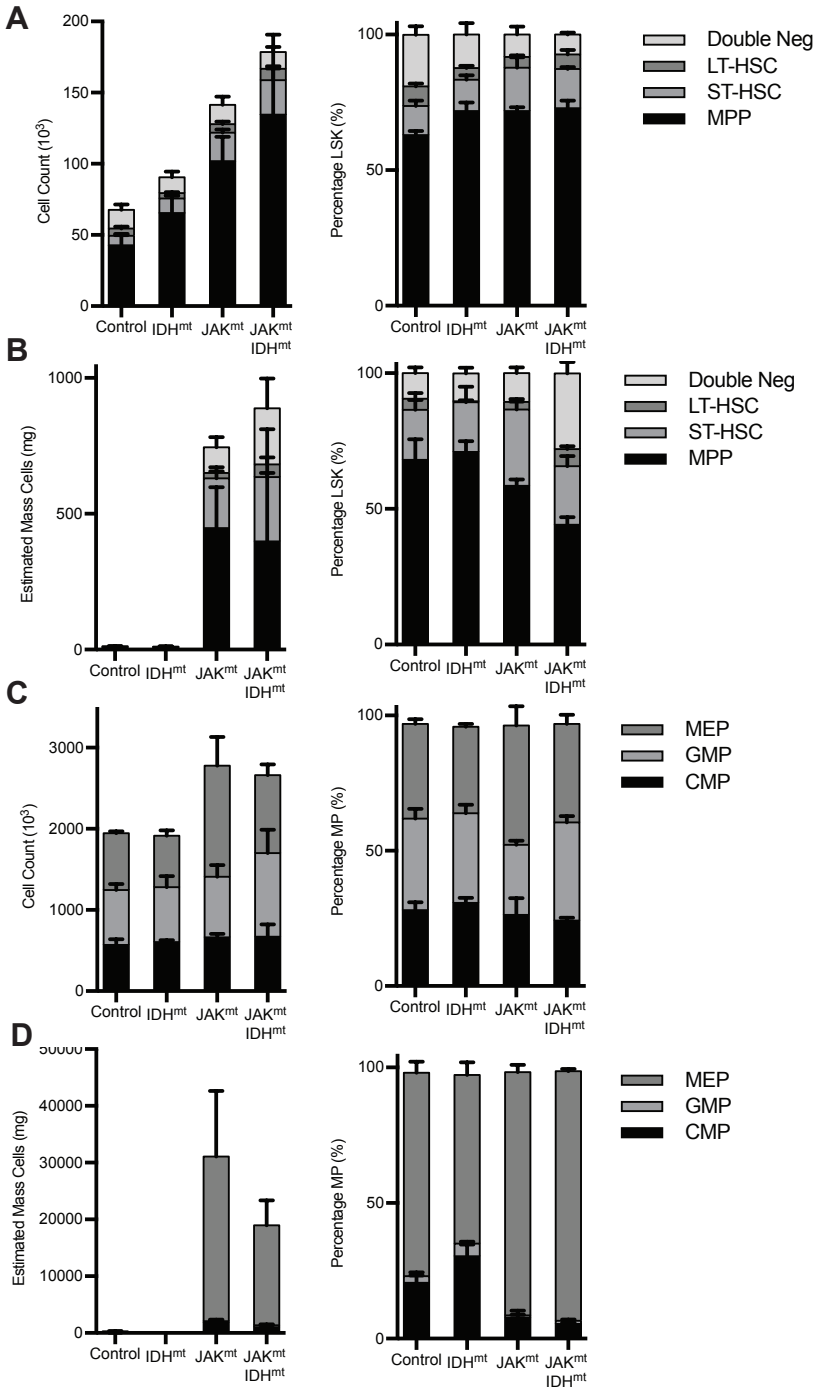

Figure 2.13: Primary *IDH1*^{R132H} *Jak2*^{V617F} mice have perturbed stem and progenitor compartments

(A) FACS characterization of total LSK and proportions of LSK subcompartments in bone marrow. (B) FACS characterization of total LSK and proportions of LSK subcompartments in splenocytes. (C) FACS characterization of total myeloprogenitors and proportions of myeloprogenitor subcompartments in bone marrow. (D) FACS characterization of total myeloprogenitors and proportions of myeloprogenitor subcompartments in splenocytes.

Similar studies in *Idh2*^{R140Q} *Jak2*^{V617F} primary mice also demonstrated expansion of the LSK population with a trend away from the MPP population both in bone marrow (**Figure 2.14.A**) and in spleen (**Figure 12.14.B**). There is a trend towards expansion of the myeloprogenitor population in these mice, and the addition of IDH mutant attenuated the MEP population size in comparison to *Jak2*^{V617F} alone mice in bone marrow (**Figure 2.14.C**) and in spleen (**Figure 2.14.D**).

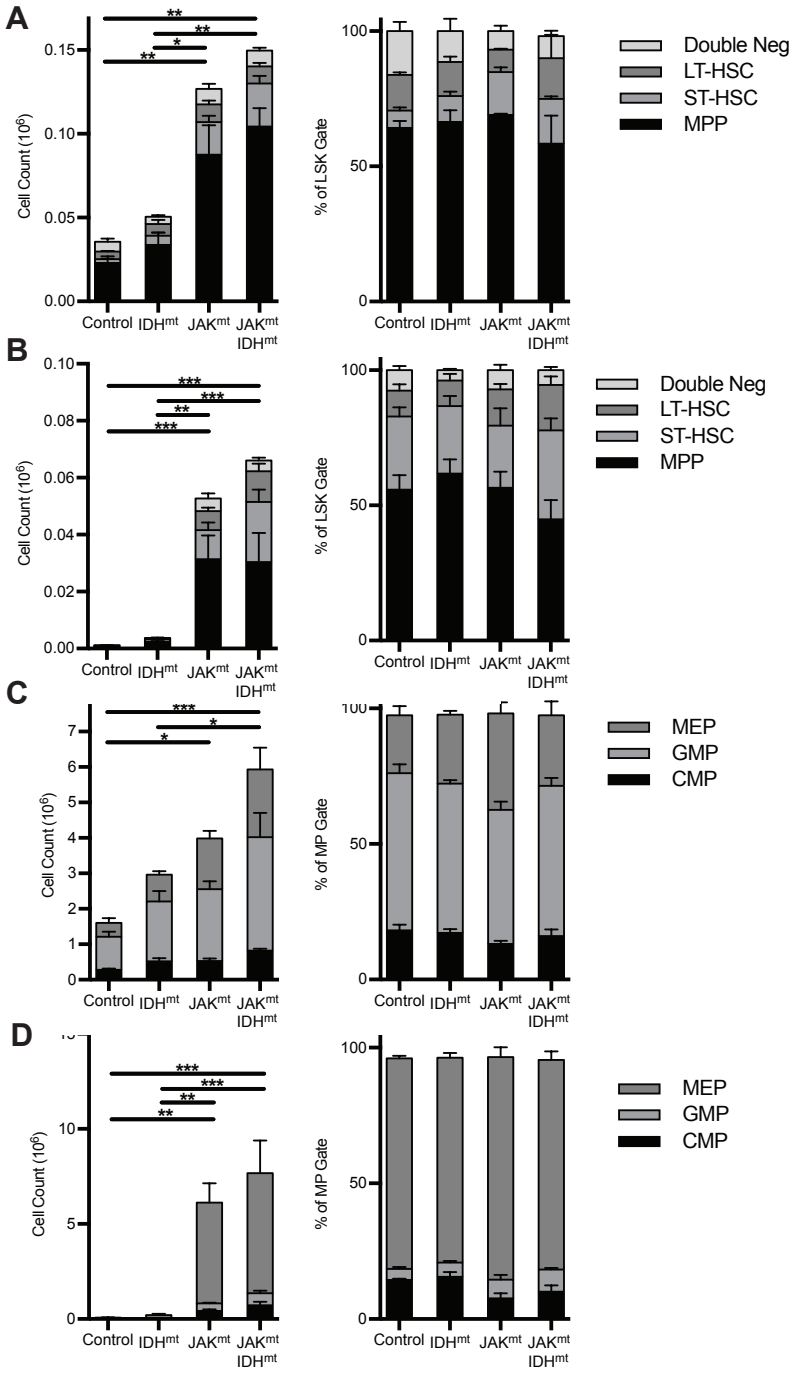

Figure 2.14: Primary *Idh2*^{R140Q} *Jak2*^{V617F} mice have perturbed stem and progenitor cell compartments

(A) FACS characterization of total LSK and proportions of LSK subcompartments in bone marrow. (B) FACS characterization of total LSK and proportions of LSK subcompartments in splenocytes. (C) FACS characterization of total myeloprogenitors and proportions of myeloprogenitor subcompartments in bone marrow. (D) FACS characterization of total myeloprogenitors and proportions of myeloprogenitor subcompartments in splenocytes.

Given our previous studies of erythroid development, we made a more granular examination of megakaryocyte and erythroid populations. This allowed us to find THAT induction of Jak2-mutant expression expanded GMP (in this experiment defined as Lin^- $cKit^+$ $Sca1^-$ $CD41^-$ $CD16/32^+$ $CD150^-$) populations, with a coordinate reduction in less differentiated pre-granulocyte-macrophage progenitors (Pre-GM; Lin^- $cKit^+$ $Sca1^-$ $CD41^-$ $CD16/32^-$ $CD150^-$ $CD105^-$) (**Figure 2.15.A**). Jak2-mutant associated expansion of megakaryocyte progenitors (MkP: Lin^- $cKit^+$ $Sca1^-$ $CD150^+$ $CD41^+$) while presence of IDH mutation appears to greatly accentuate a reduction in pre-megakaryocyte populations (Pre-MegE: Lin^- $cKit^+$ $Sca1^-$ $CD41^-$ $CD16/32^-$ $CD150^+$ $CD105^-$) (**Figure 2.15.B**). In examining early erythroid populations, CFU-E (Lin^- $cKit^+$ $Sca1^-$ $CD41^-$ $CD16/32^-$ $CD150^-$ $CD105^+$ $Ter119^-$) populations were reduced while pre-erythrocytes (Lin^- $cKit^+$ $Sca1^-$ $CD41^-$ $CD16/32^-$ $CD150^-$ $CD105^+$ $Ter119^+$) trended toward expansion in *Idh2*^{R140Q} mutants regardless of Jak2 status (**Figure 2.15.C**).

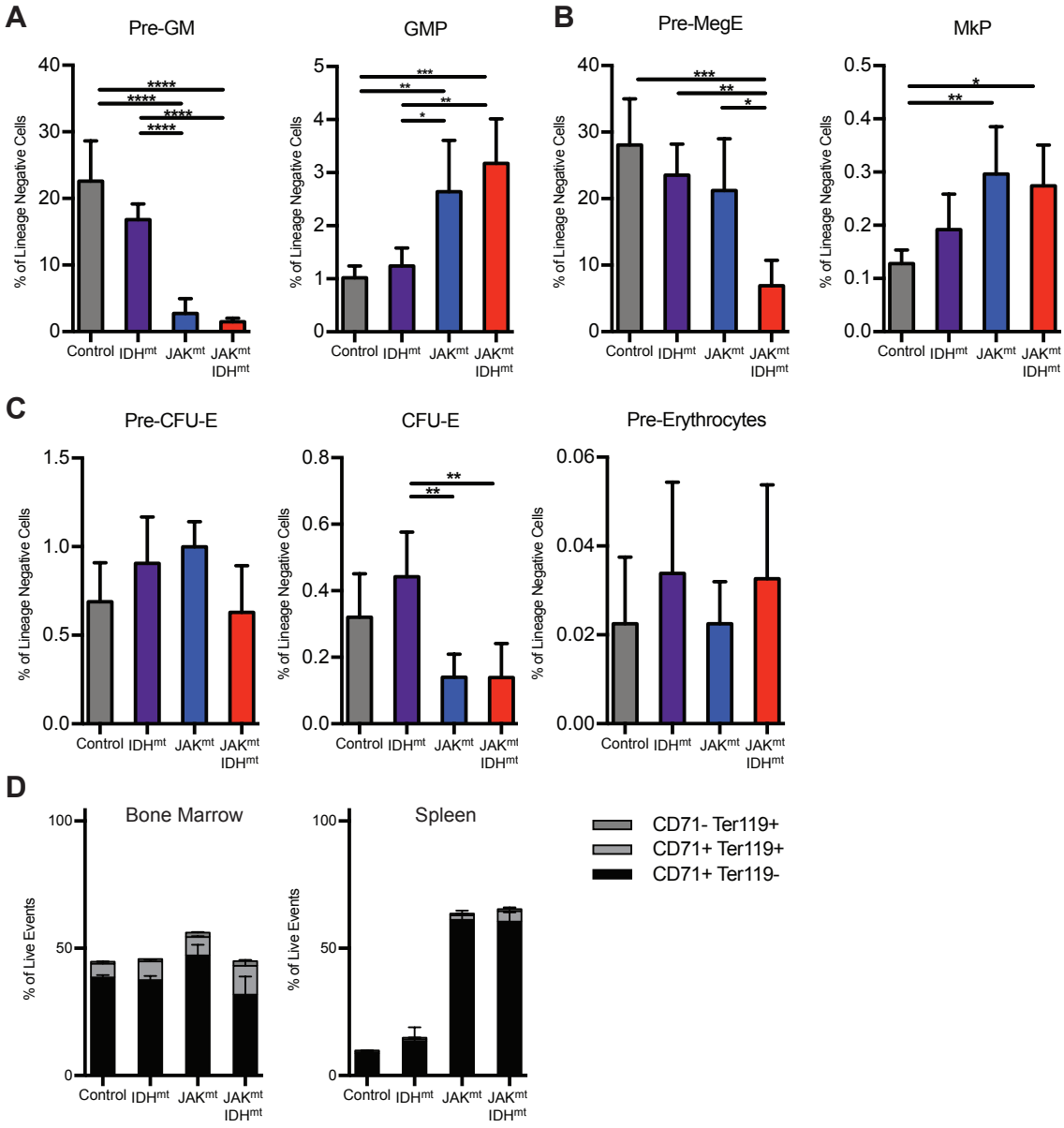

Figure 2.15: Primary *Idh2*^{R140Q} *Jak2*^{V617F} mice have perturbed myeloid differentiation

(A-D) FACS characterization of bone marrow poulations: (A) Pre-GM and GMP populations as a proportion of lineage negative cells, (B) Pre-MegE and MkP as a proportion of lineage negative cells, (C) Pre-CFU-E, CFU-E, and Pre-Erythrocytes as a proportion of lineage negative cells, (D) maturing erythrocyte compartments as a proportion of live cells.

Combined IDH and JAK2 mutant mice have characteristic disease expression pattern

Since both IDH-mutant and JAK2 proteins have significant functions in transcriptional regulation, we sought to explore the expression profiles of LSKs in combined mutant stem/progenitor cells. To do this, we performed RNA-Seq analysis on CD45.2^{+} LSK cells from combined mutant recipients and wild type controls. This analysis identified a setof genes that are able to effectively cluster combined mutant mice separately from wild type mice (**Figure 2.16**). Examining this gene list further, we observe enrichment for several gene sets that are relevant to our systems, including those activated in Wilms Tumor 1, which can alter TET2 function[139] (**Figure 2.17.A**). This gene list also enriches for signatures consistent with myelopoiesis including VEGF and PDGF (**Figure 2.17.B**). Finally, several signatures related to oncogenic metabolism were enriched, including positive correlations with *KRAS*^{V600} mutation, and negative correlations with PTEN and mTOR inhibition (**Figure 2.17.C**).

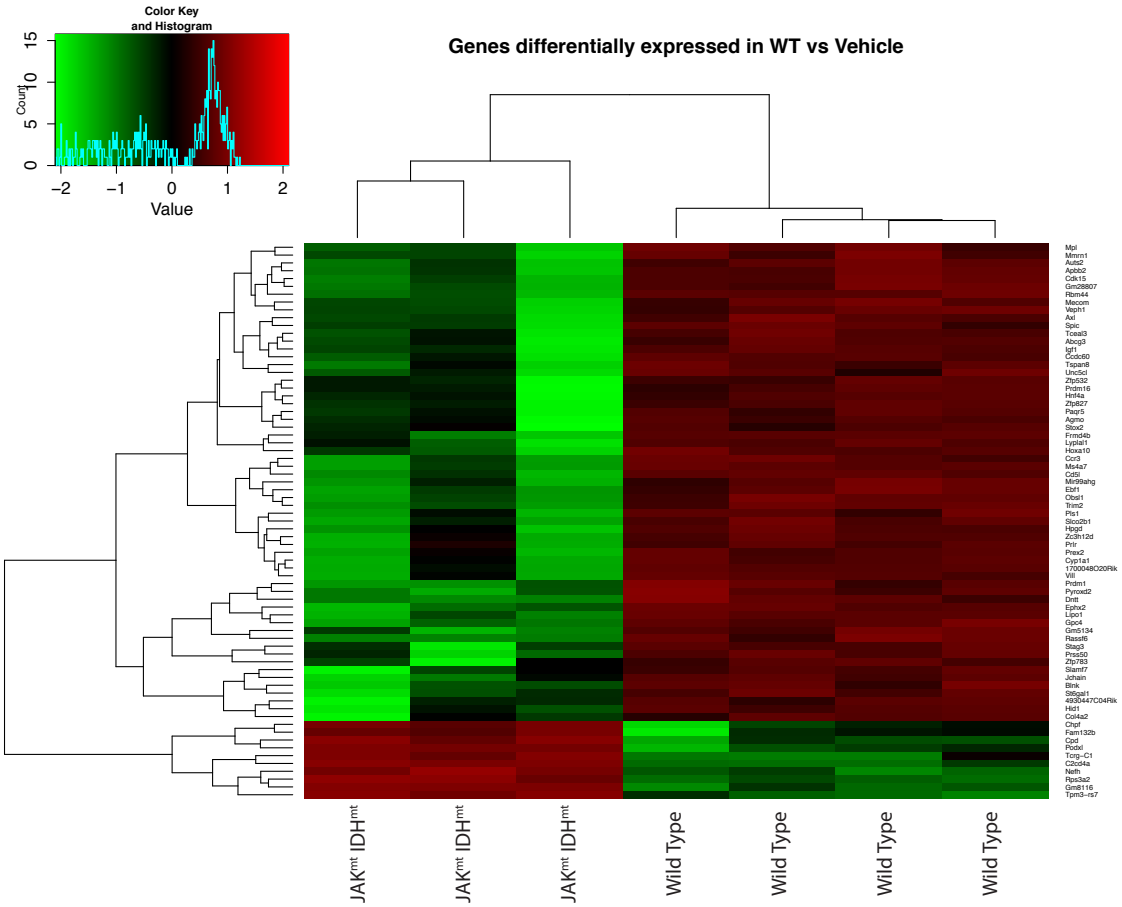

Figure 2.16: Donor LSK from *Idh2*^{R140Q} *Jak2*^{V617F} mice have RNA-Seq expression patterns distinct from wild type mice

Heatmap showing supervised clustering of RNA-Seq expression analysis of CD45.2^{+} LSK based on most differentially expressed genes.

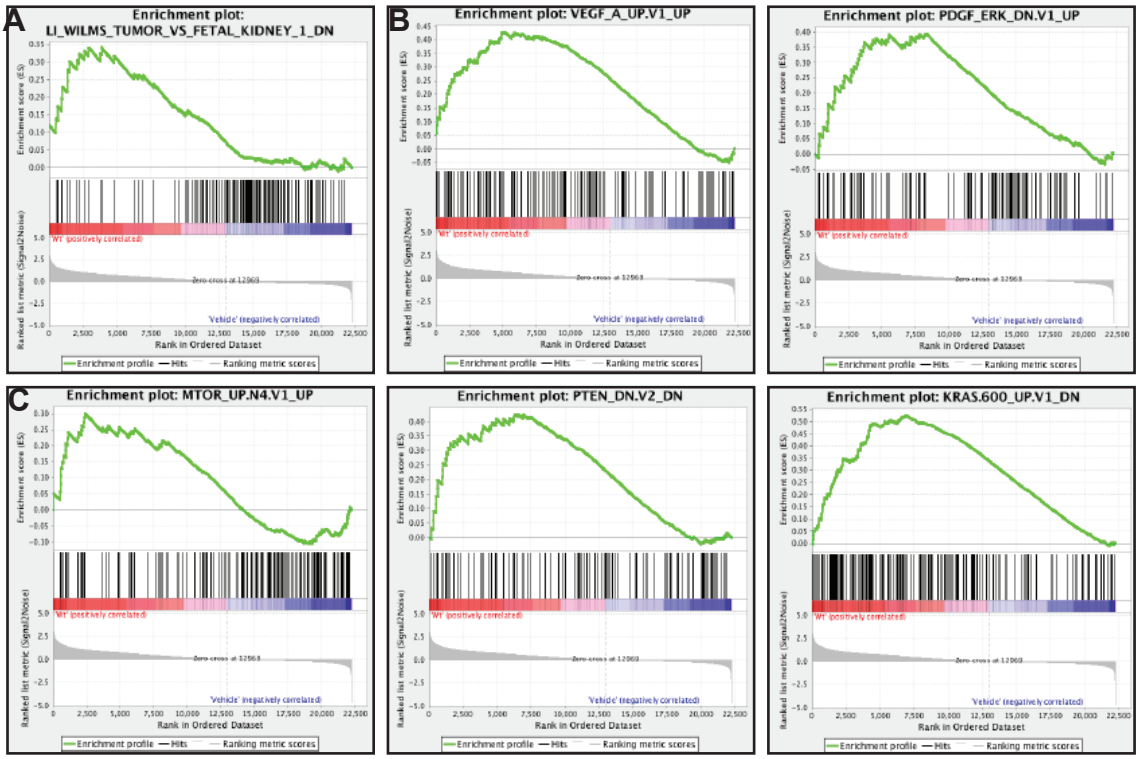

Figure 2.17: Donor LSK from Idh2R140Q Jak2V617F mice have enrichment for gene sets over wild type

(A-C) Highly enriched GSEA in most differentially expressed genes from RNA-Seq expression patterns of CD45.2^{+} LSK, related to (A) IDH/TET2 function, (B) erythrocyte and platelet development, and (C) oncogenic metabolic pathways.

DISCUSSION

Together, these data indicate that in the hematopoietic system, IDH mutations cooperate with JAK-STAT activating mutations to escalate a lethal MPN to a more advanced state with preleukemic features. This is evidenced by slightly elevated blood counts, acceleration of disease on transplant, and a competitive advantage in the hematopoietic niche in comparison to JAK-STAT mutant mice. This coincides with expansion of early stem cell populations and disturbances in several megakaryocyte and erythroid progenitor populations. Our single mutant MPN results are consistent with previously reported MPL- and Jak2-mutant models[6]

Our description of the combined IDH and Jak2 mutations is consistent with recently reported data regarding cooperation between *Jak2* and *Tet2* mutations.[135] Although the overt phenotype in the described model is less subtle, this may be due to the fact that Tet2 is just one of many proteins whose activity affected by 2-HG. In contrast, the mutation of IDH in our model will affect several pathways simultaneously, which may interact. This Jak2/Tet2 phenotype may also be affected by this group's use of a cre-recombinase that is expressed early in development. Our study instead used a recombinase that must be induced after birth, which we believe to be more physiologically relevant given the age and progression of human patients with combined mutant disease.

Our results contrast strikingly with data combining *Tet2/Idh2* mutation with mutations in the tyrosine kinase *Flt3*.[133,134] Both of these models found that the combination of these mutations result in an AML phenotype, which was not the case for

our model. Additionally, both of these models report aberrant stem cell populations and expansion of LSKs, but the cell of origin in the *Idh2* mutant leukemia appears to be found in the MPP LSK population. In contrast, our model's cell of origin appears to be maintained in the LT-HSC LSK population. Our results are consistent with a block in differentiation that maintains the cell of origin SEEN in *Jak2* mutant disease, and show evidence for specificity for cooperativity between different kinases.

Curiously, we are not aware of another combination of mutations that appears to synergistically elevate 2-HG levels in the serum, as seen in our models. This finding is consistent across different *in vivo* IDH1 models. It was not reproduced in primary *Idh2*^{R140Q} *Jak2*^{V617F} mutants. However, we believe this may be due to already very high levels of 2-HG with single mutation that may become lethal for cells if elevated – further experimentation is necessary in mice with a less potent IDH2 mutation to test this hypothesis. This elevated 2-HG in IDH1 combined mutant mice was highly correlated with phenotypic measures of erythroid development as early as the MEP compartment, so future experimentation would ideally explore the metabolic state of these cells despite very small cell numbers. Unfortunately, this finding was not reproduced effectively in cell lines, which we believe to be a consequence of this synergy occurring in a highly undifferentiated cell in the bone marrow niche. All together, these data suggest that JAK2 potentiates the production of 2-HG in a physiological context, but further research is necessary to explore this relationship and delineate a mechanism for interaction.

Further experimentation is also needed to understand why these mice with combined mutations do not acquire leukemia, while humans with combined JAK and

IDH mutations clearly have a high risk of progression shortly after observation of IDH mutation. One method to achieve this would be to combine these mutations with a third allele based on mutations that coincide in our human cohort. Additionally, the use of human xenografts may help isolate any differences in physiology between mice and humans. Human data from paired samples can also be explored including retrospective clinical data, to see if they also appear to harbor an MPN with preleukemic features.

Chapter 3 : Combined targeted inhibition in combined mutant samples from mice and men

DEVELOPMENT OF JAK/STAT PATHWAY INHIBITORS

The remarkable efficacy of targeted therapies to inhibit the BCR-ABL tyrosine kinase in CML[140] and the identification of JAK2/MPL mutations in PV, ET, and PMF resulted in great interest in the development of JAK2 kinase inhibitors. As a result, several JAK2 inhibitors have been investigated in preclinical settings.[115,141-143] JAK2 inhibitor therapy results in marked reductions in spleen size and improvement in constitutional symptoms in patients; this led to the FDA approval of ruxolitinib, a selective JAK1/JAK2 inhibitor, for the treatment of MF.[144] Although ruxolitinib does not lead to pathologic or molecular remissions, recent randomized clinical trial data suggest that patients had improved survival and a reduced leukemic transformation rate as compared to placebo.[145] There are a spectrum of other JAK kinase inhibitors being tested in different clinical settings, and recent studies have suggested that HSP90 inhibition[146]or HDAC inhibition[147] may be promising in combination with ruxolitinib. It is thought that ruxolitinib's effectiveness may lie, at least in part, in its ability to lower circulating cytokine levels, thus reducing systemic inflammation, splenomegaly, and generalized symptoms. This also has implications on resistance mechanisms, and to this end, point mutations that confer resistance *in vitro* have not been corroborated in patient samples.[144] Instead, recent work has postulated that, in the presence of inhibitor, *Jak2*^{V617F} is able to recruit heterodimeric partners in the JAK family to induce constitutive JAK-STAT signaling and persistence of neoplastic clones.[148]

Although most JAK kinase inhibitor studies have been limited to patients with chronic phase MPN, there are limited data regarding the efficacy of JAK kinase inhibition in acute leukemias. In patients with post-MPN AML, ruxolitinib induced complete remission in three out of 18 patients.[149] This study indicates that JAK kinase inhibitors are active in post-MPN AML, but that combination therapies with JAK inhibitors and other therapies are needed.

DEVELOPMENT OF IDH1 and IDH2 INHIBITORS

Preclinical development of IDH inhibitors has emerged as an important goal, both to test the viability of mutant IDH1/2 as a therapeutic target and as a tool to help dissect the IDH/2-HG pathway in different malignant contexts. One compound under investigation is compound 35, which is active against *IDH1*^{R132H} mutants, and preclinical tests have indicated that its application reduces 2-HG production in cell lines and mouse xenograft models.[150] A similar selective compound was more recently used in combination with an exogenous 2-HG system to show that the cellular phenotype induced by IDH mutation is reversed by this drug, whereas the cellular phenotype induced by exogenous 2-HG production is not.[67] A specific inhibitor of IDH1, AGI-5198, was reported to delay glioblastoma xenograft growth. However, notably, treatment with this compound was reported to induce differentiation of cells as evidenced by increased expression of neural differentiation markers.[151]

Recently, compounds targeting mutant IDH2 have been explored in leukemia cell lines[152] and glioma cell models.[151] In both cases, IDH inhibitors were found to reduce 2-HG production and inhibit the growth of leukemia or glioma cells in a mutant-specific

manner. In addition, IDH inhibition led to global changes in DNA methylation/histone state and to induction of hematopoietic/neural differentiation, suggesting that these agents might induce differentiation in IDH-mutant cells through alterations in the epigenetic state.

In vivo murine models of IDH2 mutation in leukemia have been shown to be susceptible to deinduction of IDH2 with a differentiation expression phenotype.[134] However, extensive *in vivo* studies in IDH-mutant transformation models remain to be reported, and the role of IDH in malignant cells after oncogenic transformation requires additional, extensive investigation. [59]

Early reports of Phase I/II clinical trials for the selective IDH2 inhibitor AG221 have shown potential for this therapeutic in humans with de novo AML, relapsed-refractory AML, and other myeloid malignancies. The composite complete remission rate among AML patients is 28.6%, and a substantial subset of the patients were reported to show resolution of abnormal myelopoiesis and partial remission through significant reduction of myeloblasts. Additionally, the investigators provide evidence that persistence of the mutant clone was associated with differentiation of cells in the myeloid lineage as measured by recovery in absolute neutrophil counts.[153-155]

MATERIALS AND METHODS

Therapeutic Assays in Secondary Transplants: AG221 and INC424

Approximately two months after competitive transplant, peripheral blood analysis was performed by HemaVet and FACS for donor chimerism. Mice were matched using HCT(%), WBC(K/μL), donor chimerism, and body weight, and they were randomized within matching groups using a random number generator. Drugs were administered BID by gavage for 21-28 days. INC424 (James Bradner, Dana Farber Cancer Institute) was administered 60 mg per kg; AG221 (Agios Pharmaceuticals) was administered at 100 mg per kg or 40 mg per kg. Final doses were administered approximately 1.5 hours before sacrifice.

Human Tissues

Approval was obtained from the Institutional Review Board at Memorial Sloan-Kettering Cancer Center. Tissues were collected in partnership with the Human Oncology Tissue Bank, and all patients provided informed consent. Fresh peripheral blood was collected into heparinized collection tubes, and separation of peripheral blood mononuclear cells (PBMC) was performed using hetastarch and a Ficoll gradient with subsequent red blood cell lysis.

Human Colony Forming Assays

Frozen or fresh PBMCs were plated in Methocult H4435 (Stem Cell) with penicillin and streptomycin in triplicate wells. MPN patient cells were plated after enrichment using CD34 Microbeads (Miltenyi) at 1,000 cells per well; AML patient

cells were plated without enrichment at 100,000 cells per well. AG221 and INC424 were dissolved into samples at 400nM concentration and DMSO was dissolved into controls.

Patient Derived Xenograft (PDX) Models

1 x 10^6 Peripheral Blood Mononuclear Cells (PBMCs) from an AML patient were injected into sublethally irradiated NSG mice and mice were maintained in a xenograft facility. Engraftment was monitored monthly in peripheral blood and bone marrow aspirates for up to 12 months or engraftment was observed.

Therapeutic Assays in PDX Models: AGI5198 and INC424

After chimerism was detected in peripheral blood or bone marrow, mice were randomized using a random number generator. Drugs were administered by gavage for 28 days. INC424 (James Bradner, Dana Farber Cancer Institute) was administered twice per day at 60 mg per kg; AGI5198 (Agios Pharmaceuticals) was administered once per day at 450 mg per kg. Final doses were administered approximately 1.5 hours before sacrifice.

Flow Cytometry for Human Tissues

To observe erythroid differentiation in human tissues we stained with a combination of CD117/cKit (YB5.B8, eBiosciences), CD34 (581, BioLegend), CD38 (HIT2, BioLegend), CD36 (5-271, BioLegend), CD71 (OKT9, eBiosciences), and CD235a (HIR2, eBiosciences). To observe monocytic and granulocytic differentiation, antibodies against CD117/cKit, CD34, CD38, CD15 (HI98, eBiosciences), CD14 (HCD14, BioLegend), and CD16 (3G8, BioLegend) were used. To observe engraftment and clone differentiation in PDX models, antibodies against mouse Ter119, mouse

CD45.1, human CD45 (HI30, BioLegend), human CD3 (OKT3, eBiosciences), human CD19 (HIB19, eBiosciences), human CD33 (WM53, BD), human CD34 (581, BioLegend), human CD38 (HIT2, BioLegend), and human CD117/cKit (YB5.B8, eBiosciences).

RESULTS

AG221 INC424 treatment in recipients of IDH2/JAK2 mutant MPN resolves disease phenotype, reduces size of all stem cell and progenitor populations

Due to the lack of therapeutic options for patients, we explored whether currently available inhibitors might be able to affect disease. Primary recipients of *Idh2*^{R140Q} *Jak2*^{V617F} bone marrow treated with AG221 showed reduction of plasma 2-HG to the level of wild type mice (**Figure 3.1.A**). Monotherapy with either AG221 or INC424 reduced splenomegaly, while combined treatment completely resolved splenomegaly (**Figure 3.1.B**). Combined therapy with AG221 and INC424 normalized polycythemia and leukocytosis to a level not seen with monotherapy (**Figure 3.1.C**). Histologically, treatment with monotherapy or combined therapy results in restoration from left-shifted cells in the bone marrow as well as the return of normal diletations in the bone. Treatment with AG221, but not INC424, resulted in reduction of CD34 immunohistochemical staining in cells with megakaryocyte morphology, while combined treatment eliminated the presence of these cells. In the spleen, cells identified morphologically as blasts are no longer present in single AG221 or combined treatment (**Figure 3.1.D**).

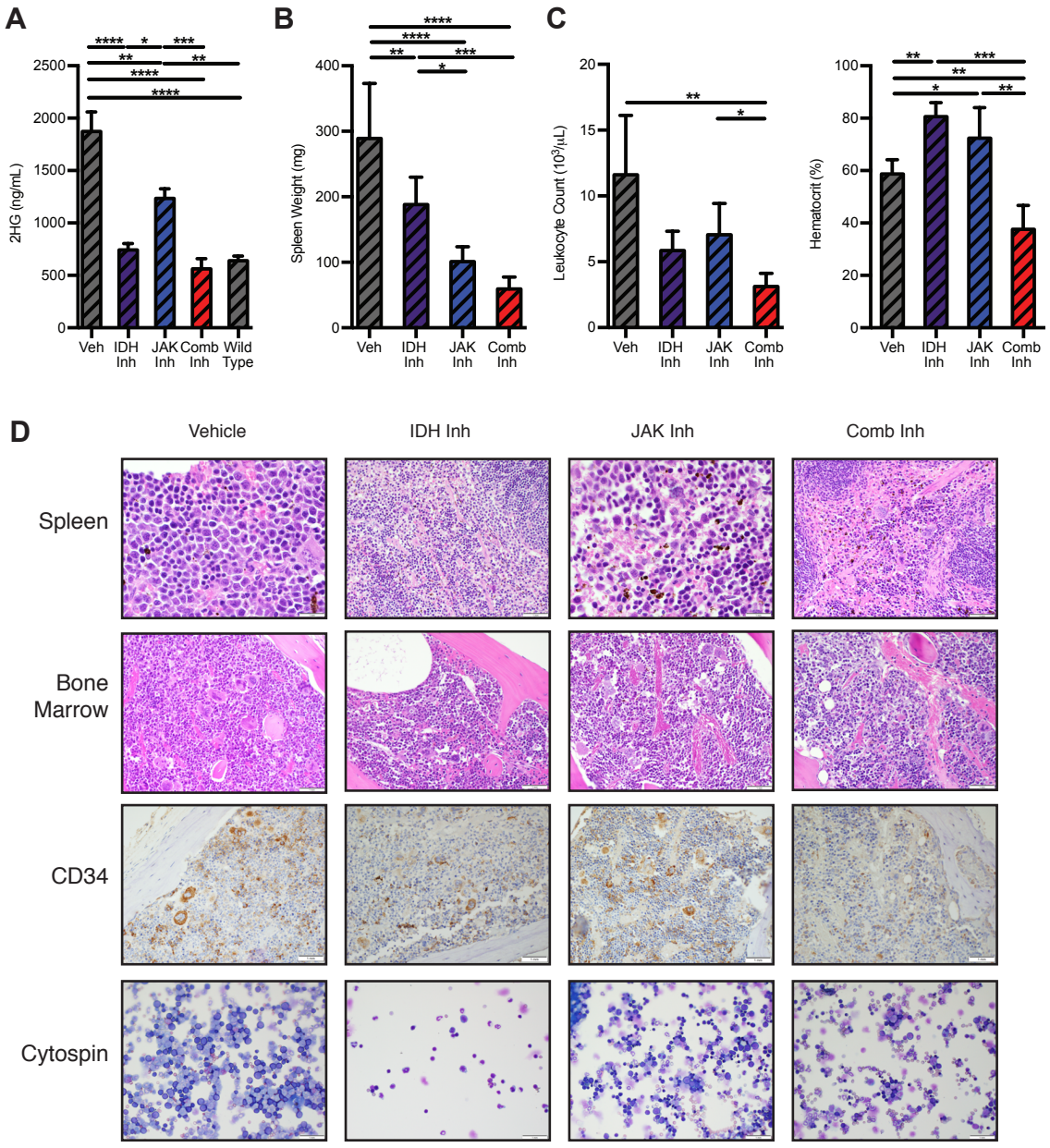

Figure 3.1: Treatment of Idh2^{R140Q} Jak2^{V617F} combined mutant mice with combined JAK2 and IDH2 inhibitors results in resolution of disease phenotype

(A-D), Disease phenotype in bone marrow recipients treated with targeted JAK inhibitor and high dose targeted IDH2 inhibitor. (A) 2HG quantification in plasma, (B) spleen weights, (C) hematocrit levels and leukocyte counts, and (D) representative images of histological stained sections.

Both monotherapy and combined therapy dramatically reduced the size of the LSK compartment in the bone marrow (**Figure 3.2.A**) and spleen (**Figure 3.2.B**), in a manner largely uniform across all populations. This is also true for myeloprogenitor populations, for which monotherapy and combined therapy reduced the total size of the compartment in the bone marrow (**Figure 3.2.C**) and spleen (**Figure 3.2.D**) in a uniform manner. Combined therapy or monotherapy reduced Pre-GM and GMP populations (**Figure 3.3.A**). Similarly, treatment with monotherapy reduced Pre-MegE populations while trending toward reduction in expanded MkP populations (**Figure 3.3.B**). Monotherapy or combined therapy reduced the proportions of Pre-CFU-E, CFU-E, and Pre-erythrocytes in the bone marrow (**Figure 3.3.C**). Notably, treatment with AG221 expanded the population of intermediate maturity erythrocytic precursors ($CD71^{-}$ $Ter119^{+}$) in the spleen. (**Figure 3.3.D**).

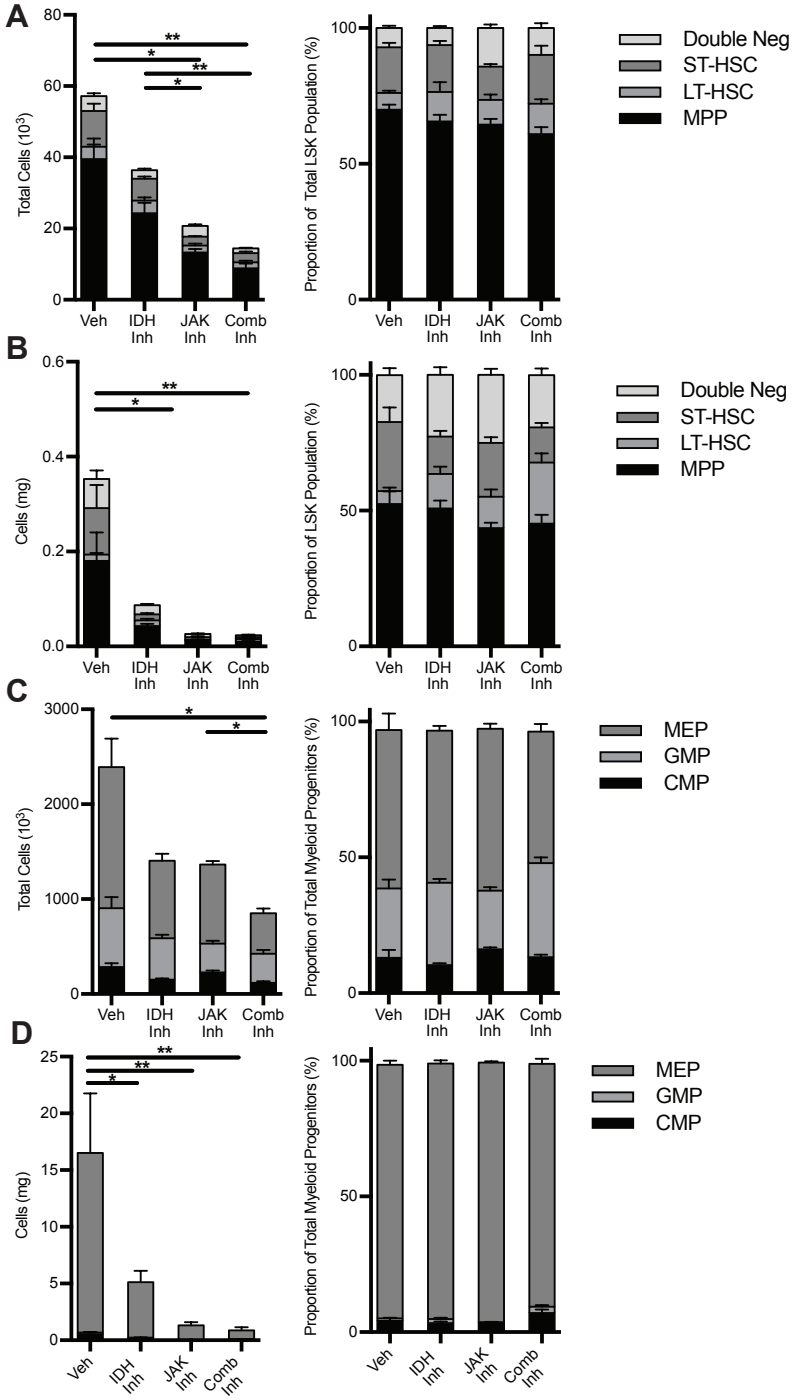

Figure 3.2: Treatment of combined mutant mice with combined JAK2 and IDH2 inhibitors results in contraction of expanded stem and progenitor compartments
(A-D), FACS characterization of stem cell phenotype in *Idh2*^{R140Q} *Jak2*^{V617F} bone marrow recipients treated with targeted JAK inhibitor and IDH2 inhibitor. (A) Total LSK and proportions of LSK subcompartments in bone marrow. (B) Total LSK and proportions of LSK subcompartments in splenocytes. (C) Total myeloprogenitors and proportions of myeloprogenitor subcompartments in bone marrow. (D) Total myeloprogenitors and proportions of myeloprogenitor subcompartments in splenocytes.

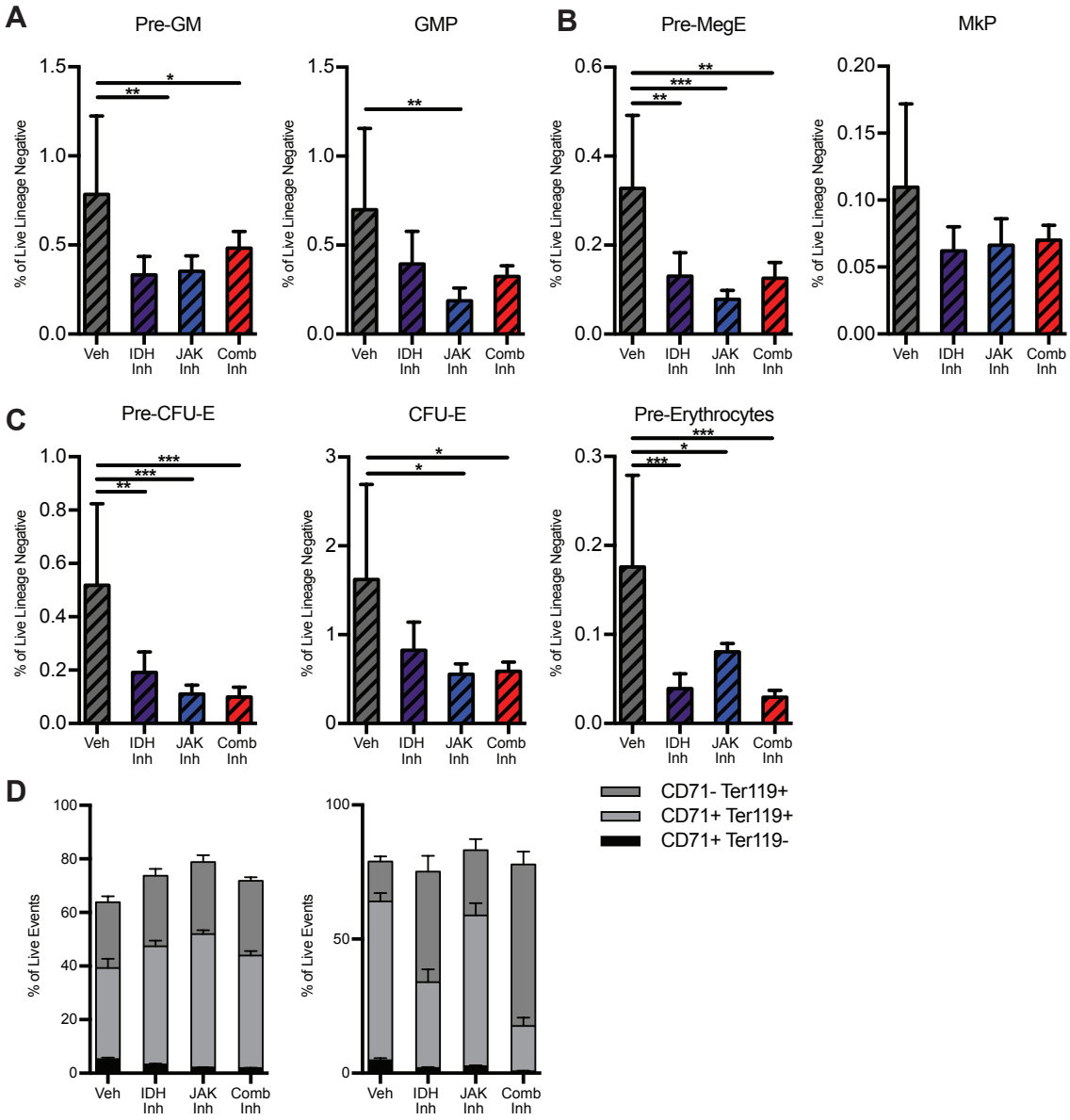

Figure 3.3: Treatment of combined mutant mice with combined JAK2 and IDH2 inhibitors results in contraction of other myeloid differentiation compartments
(A-D) FACS characterization of bone marrow poulations: (A) Pre-GM and GMP populations as a proportion of lineage negative cells, (B) Pre-MegE and MkP as a proportion of lineage negative cells, (C) Pre-CFU-E, CFU-E, and Pre-Erythrocytes as a proportion of lineage negative cells, (D) maturing erythrocyte compartments as a proportion of live cells.

AG221 treatment in recipients of IDH2/JAK2 mutant MPN reduces chimerism of combined mutant cells in a targeted fashion

Because JAK2 inhibitors have not been shown to reduce allele burden in JAK2-mutant disease, we examined specific effects on cells contributed from the *Idh2*^{R140Q} *Jak2*^{V617F} donor (CD45.2^{+}). In comparing peripheral blood from individual mice before and after treatment, we observed that mice treated with either AG221 or combined inhibitors showed significant reductions in mutant donor chimerism; in contrast, mice treated with either INC424 or vehicle showed significant expansion of the proportion of mutant derived clones (**Figure 3.4.A**). A trend toward reduction in chimerism was present in unfractionated, CD11b/Mac1^{+}, and CD117/cKit^{+} bone marrow (**Figure 3.4.B**), as well as in the spleen (**Figure 3.4.C**), and peripheral blood (**Figure 3.4.D**). Notably, the reduction of mutant allele burden was significant in whole bone marrow, Ckit/CD117^{+} bone marrow, CD11b/Mac1^{+} spleen, and CD11b/Mac1^{+} peripheral blood.

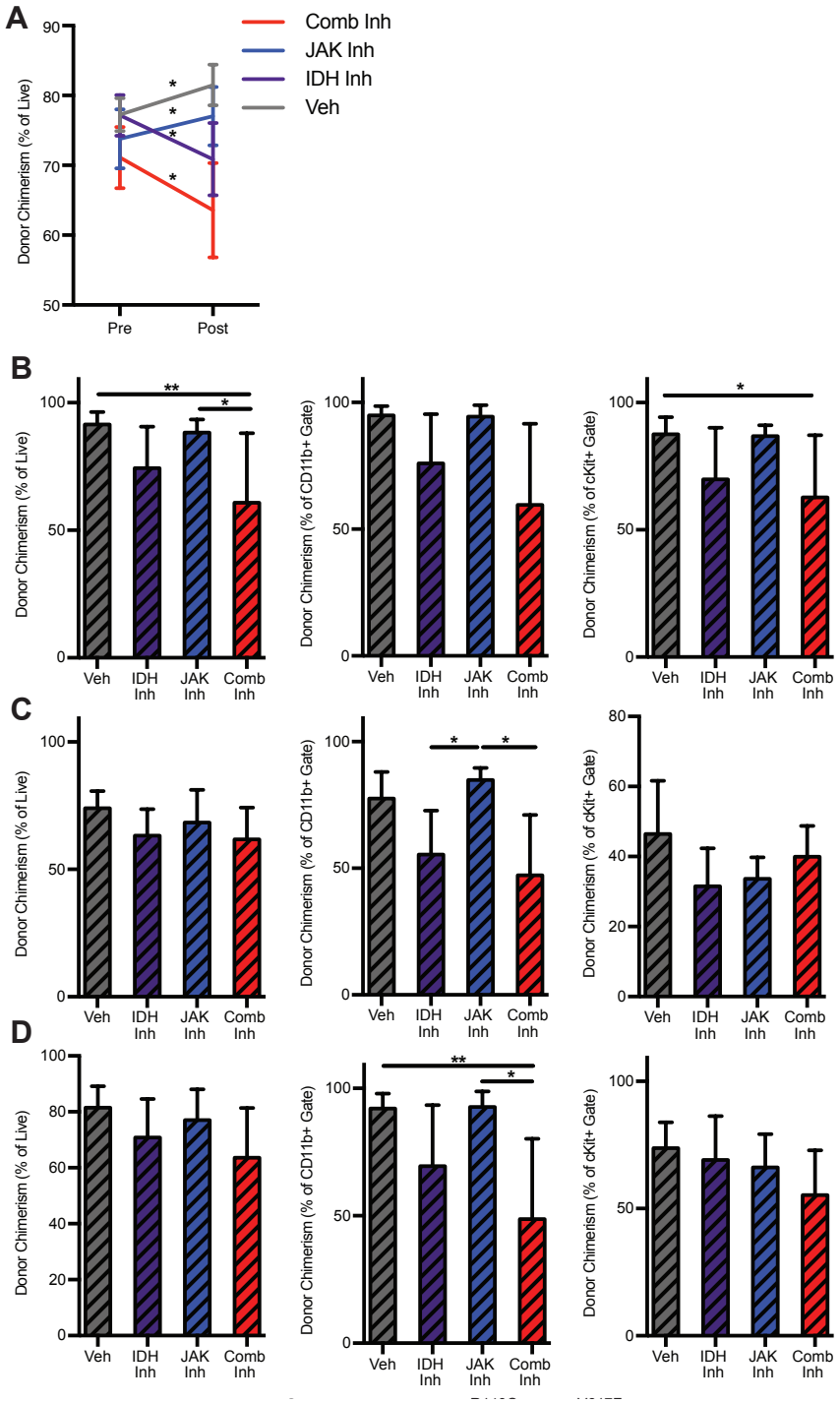

Figure 3.4: Treatment of combined mutant mice with IDH2 inhibitor results in reduction of donor chimerism

(A) Paired analysis of donor chimerism in peripheral blood of mice before and after treatment, highlighting statistically significant changes within each group.

(B-D) Donor chimerism as a proportion of all live cells, all myeloid (CD11b/Mac1^{+}), and all CD117/cKit^{+}) compartments of (B) bone marrow, (C) splenocytes, and (D) peripheral blood.

For practical reasons, we examined whether a reduction in dose of AG221 would be efficacious for future experiments. Dosage of mice with approximately half the dose still resolved serum 2-HG levels to that of wild type mice (**Figure 3.5.A**), resolved spleen weights (**Figure 3.5.B**), and trended toward reduction in leukocytosis and polycythemia (**Figure 3.5.C**).

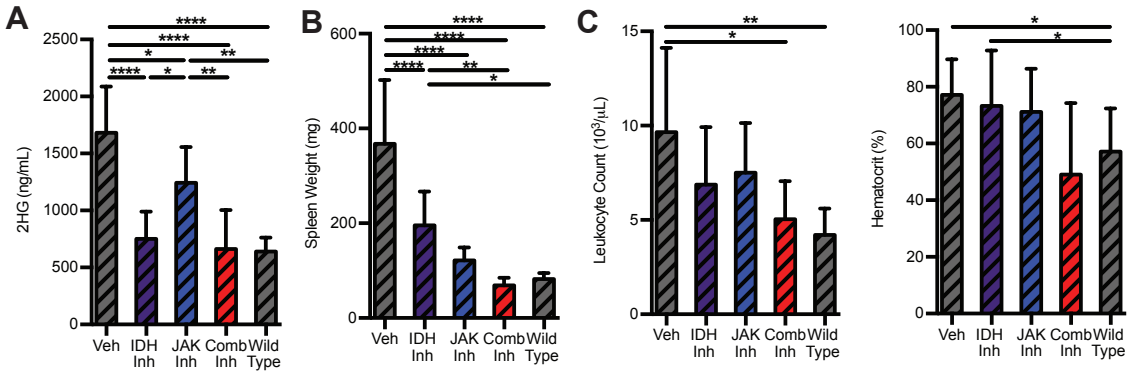

Figure 3.5: Treatment of combined mutant *Idh2*^{R140Q} *Jak2*^{V617F} mice with lower dose IDH2 inhibitor results in resolution of disease phenotype

(A-D), Disease phenotype in Idh2R140Q Jak2V617F bone marrow recipients treated with targeted JAK inhibitor and lower dose targeted IDH2 inhibitor. (A) 2HG quantification in plasma, (B) spleen weights, and (C) hematocrit levels and leukocyte counts.

Interestingly, within the donor compartment, monotherapy or combined therapy appeared to reduce the proportion of LSK significantly beyond wild type levels, through the proportions of each subpopulation trend toward that of a wild type mouse (**Figure 3.6.A**). The number of $CD45.1^+$ wild type cells is not significantly affected by treatment, indicating that this effect is specific to the mutant donor cells (**Figure 3.6.B**). Furthermore, mutant donor derived myeloid progenitor populations contract to wild type proportions. Within this compartment, the myeloid progenitor subpopulations also trend toward their wild type proportions (**Figure 3.6.C**). Again, while there was a slight trend toward expansion in the $CD45.1^+$ compartment (**Figure 3.6.D**), the effect of treatment appears to be specific to the donor cells. In the mutant donor compartment, erythroid progenitors ($CD71^+$ $Ter119^-$) cells are normalized with treatment, although this is accompanied by coordinate reduction in proportion of more mature erythroid cells (**Figure 3.6.E**).

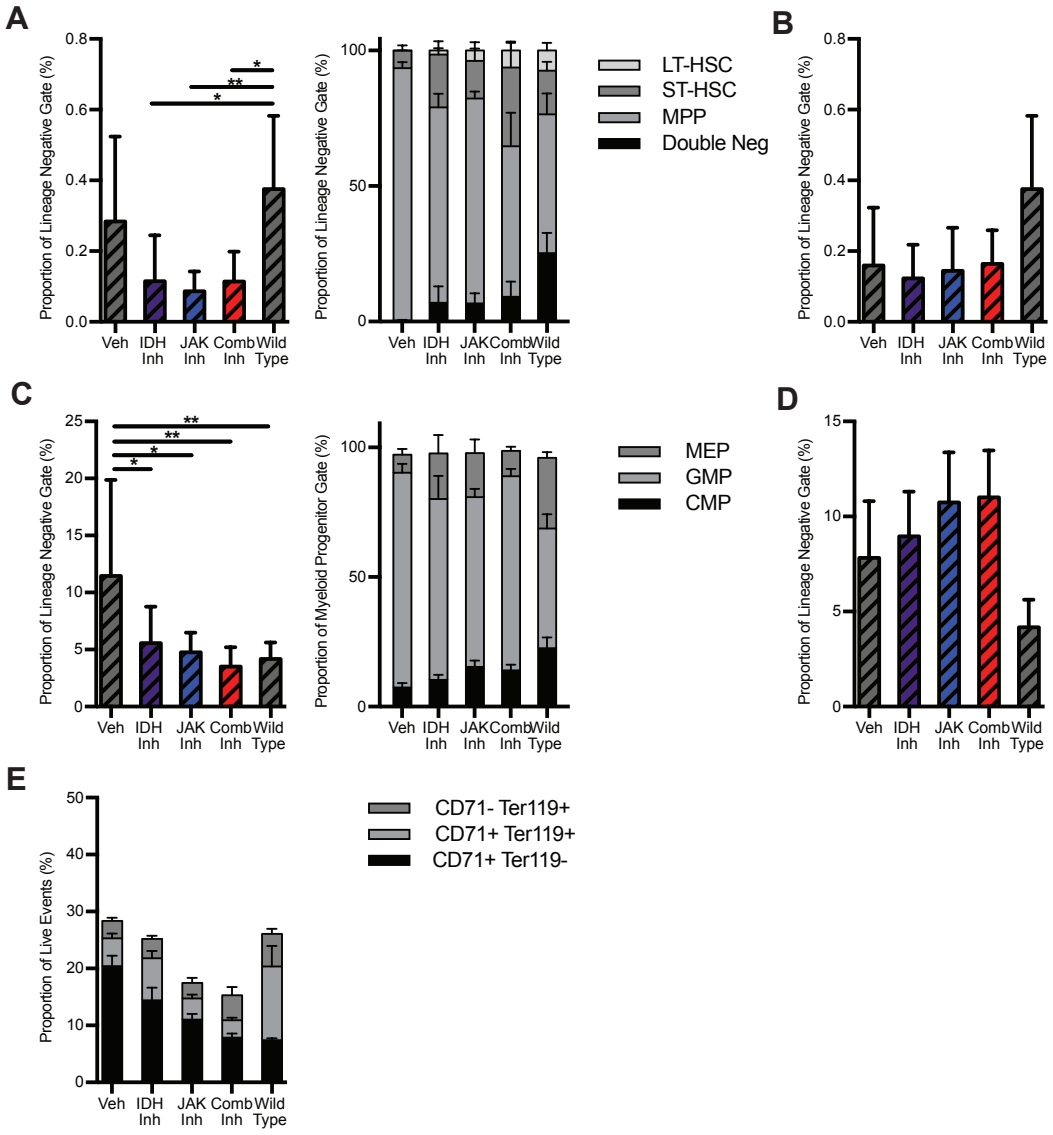

Figure 3.6: Treatment of combined mutant mice with combined inhibitors results in normalization of stem and progenitor proportions within the donor compartment

(A) FACS quantification within the donor-derived ($CD45.2^+$) population, LSK population as a proportion of lineage negative cells and LSK subpopulations as proportion of total cells

(B) Within the recipient-derived ($CD45.1^+$) population, LSK population as a proportion of lineage negative cells.

(C) FACS quantification within the donor-derived ($CD45.2^+$) population, Myeloprogenitor population as a proportion of lineage negative cells and myeloprogenitor subpopulations as proportion of total cells

(D) Within the recipient-derived ($CD45.1^+$) population, myeloprogenitor population as a proportion of lineage negative cells.

(E) Within the recipient-derived ($CD45.1^+$) population, immature erythroid populations as a proportion of live cells

Combined treatment of combined mutants resolves disease expression pattern

We further explored the effects of our therapeutic interventions on expression. In comparing the differential expression of each treatment arm to wild type mice, we found that while a large number of genes are affected by each monotherapy, even outside the untreated disease set, combined mutant mice show many fewer differentially expressed genes (**Figure 3.7.A**). Additionally, supervised clustering using the disease-derived gene list described above showed that combined treatment mice cluster with wild type mice (**Figure 3.7.B**). Together, these data indicate that combined treatment induces LSKs to return to a wild type pattern of gene expression.

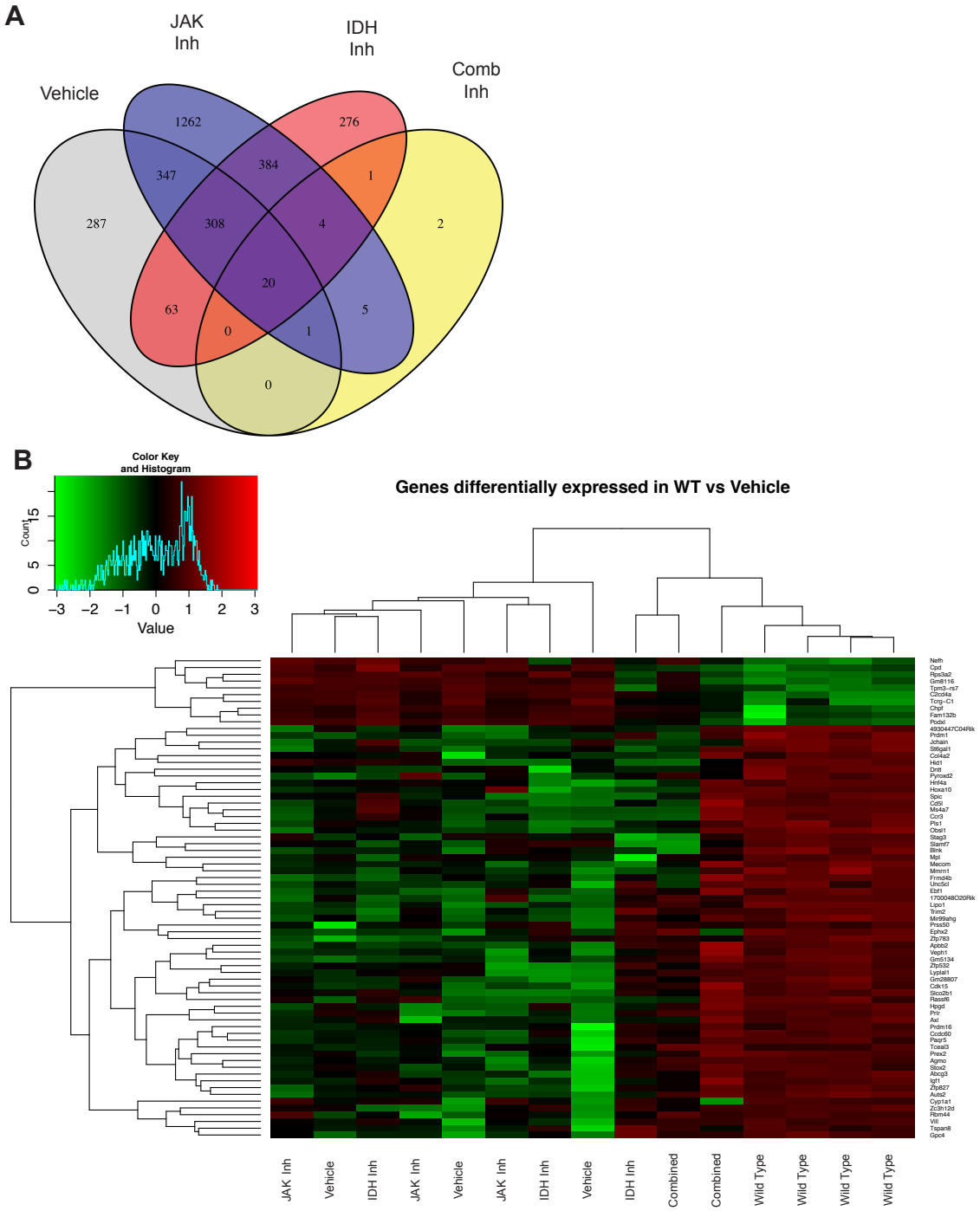

Figure 3.7: Donor LSK from Idh2R140Q Jak2V617F recipients treated with IDH2 inhibitor have RNA-Seq expression patterns very similar to wild type mice

(A) Venn diagram depicting lists of highly differentially expressed genes in CD45.2^{+} LSK in each treatment group in comparison to wild type.

(B) Heat map with supervised clustering based on gene list of highly differentially expressed genes in CD45.2^{+} LSK in combined mutant mice in comparison to wild type (as defined in Figure 2.15).

***Ex vivo* treatment of human combined IDH2/JAK2 mutants with combined therapy results in expansion of differentiated cells in culture**

To explore the relevance of these inhibitors in human disease we performed methylcellulose assays on patients with clinically determined MPN and post-MPN AML patients with *IDH2*^{R140Q} *JAK2*^{V617F} mutations. This included paired samples both tken from one patient before and after transformation (MPN 24 and AML 24, **Figure 3.8**). All of the patients showed a characteristic pattern of colony formation with marked expansion of colony number with IDH inhibitor treatment. This expansion was often accompanied by the presence of BFU-E colonies (**Figure 3.8.A**). On morphological examination, this expansion was also associated with the presence of large, well-differentiated colonies in comparison to controls (**Figure 3.8.B**).

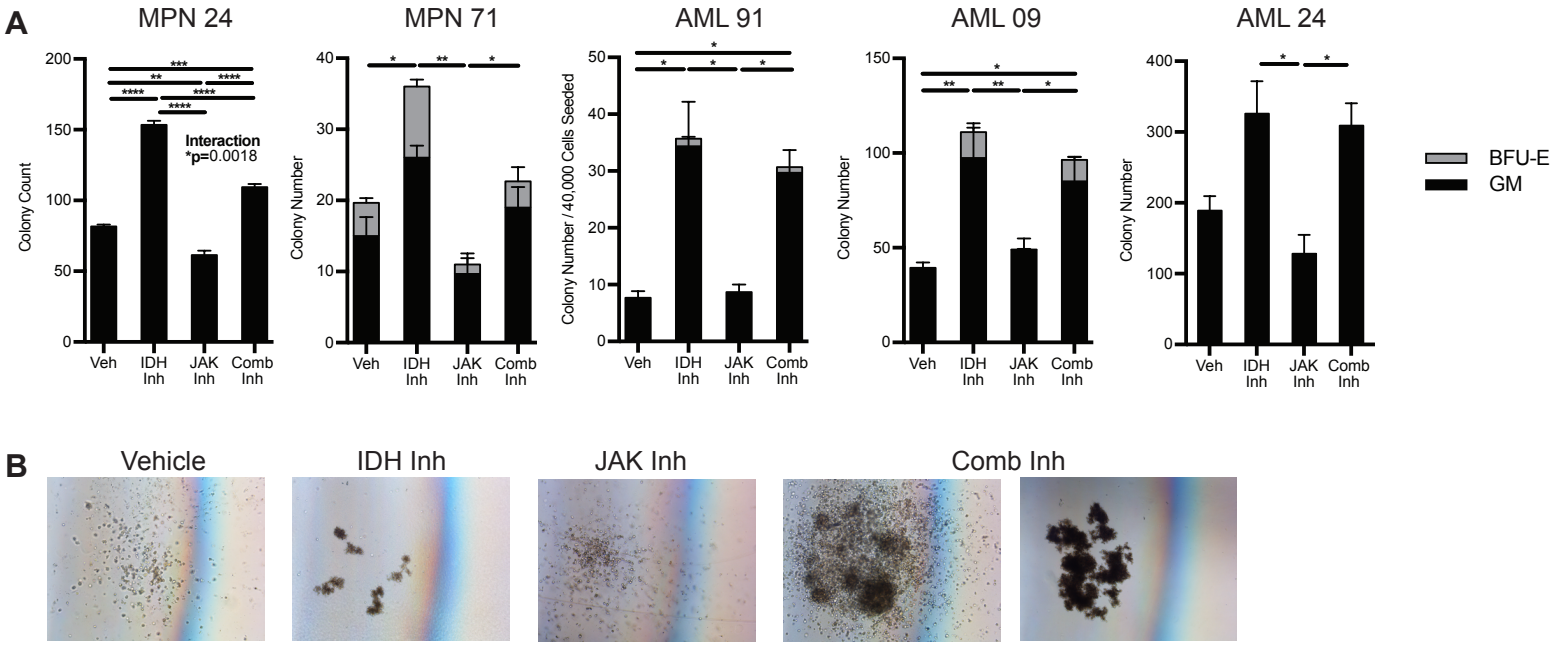

Figure 3.8: Human IDH2-mutant JAK2V617F MPN and AML samples in methylcellulose respond to IDH2 inhibitor therapy
(A) Colony counts of cultured cells from four different patients with MPN or AML classified by colony morphology.
(B) Representative images of colonies taken during culture of cells from MPN Patient 71.

FACS analysis showed that in all patients, IDH inhibitor treatment reduced surface expression of at least two of the three following immature markers: cKit/CD117 (**Figure 3.9.A**), CD34 (**Figure 3.9.B**), and/or CD38 (**Figure 3.9.C**). Observing differentiation markers in the myeloid lineage, we found that several patient samples showed increased surface expression of mature erythroid and/or granulocyte markers in the presence of IDH inhibitor. For example, MPN 24 downregulated erythroid markers CD36, CD71, and CD235a (**Figure 3.10**), but cells from this sample upregulated granulocytic markers CD15, CD14, and CD16 (**Figure 3.11**). In contrast, MPN 71 shows upregulation of CD36 and CD235a (**Figure 3.10**) and downregulation of granulocytic markers (**Figure 3.11**). AML 91 and AM L09 both show upregulation of both erythrocytic CD235a (and upregulation of CD14 and CD16.) AML 24 is the only patient sample in this dataset that did not show a specific differentiation phenotype according to these panels. Together, these observations indicate that treated samples may undergo differentiation in response to AG221 treatment.

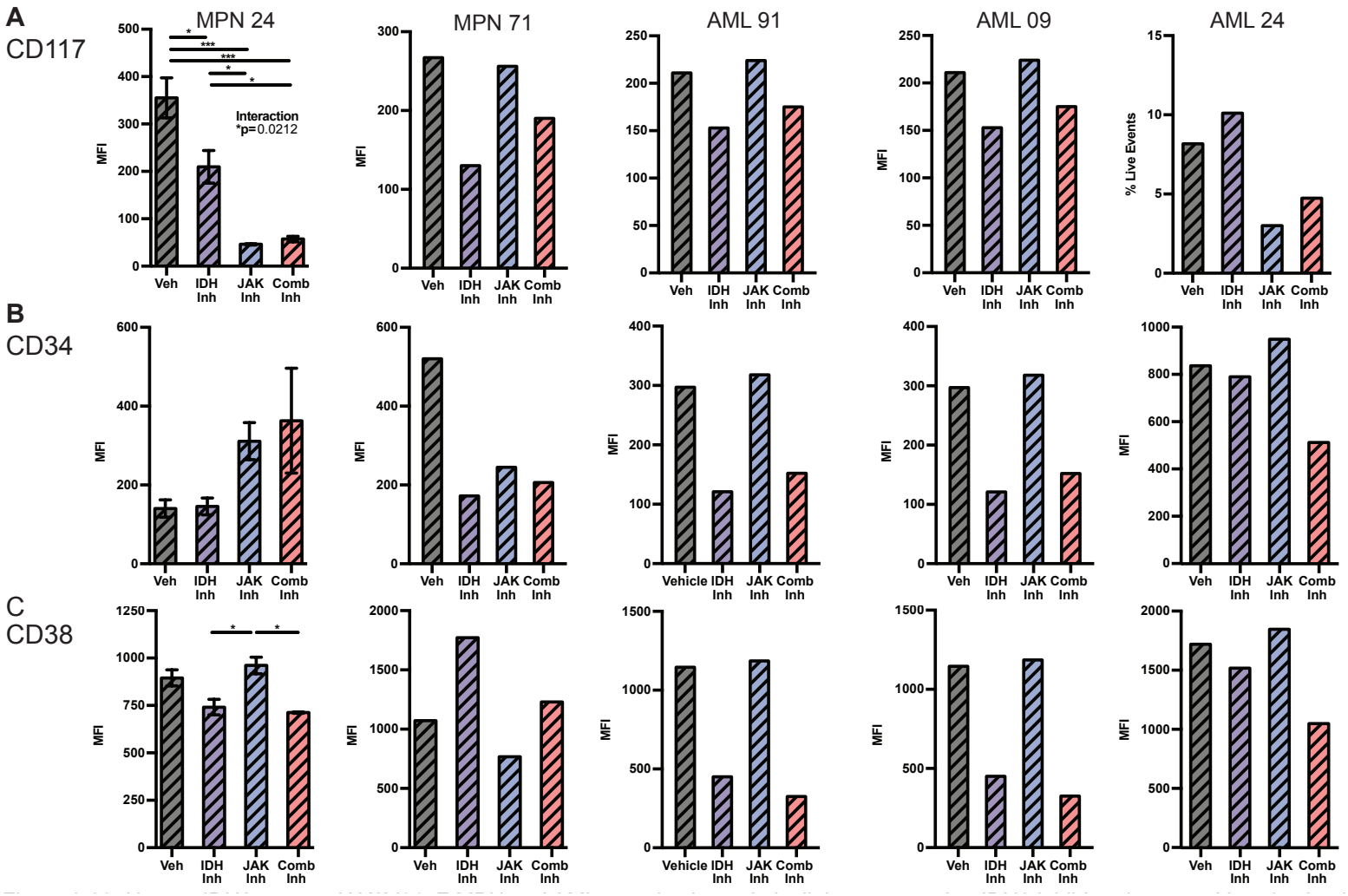

Figure 3.9: Human IDH2 mutant Jak2V617F MPN and AML samples respond to IDH2 inhibitor therapy with downregulation of canonical immature markers

Mean fluorescence intensity of (A) CD117/cKit, (B) CD34, and (C) CD38.

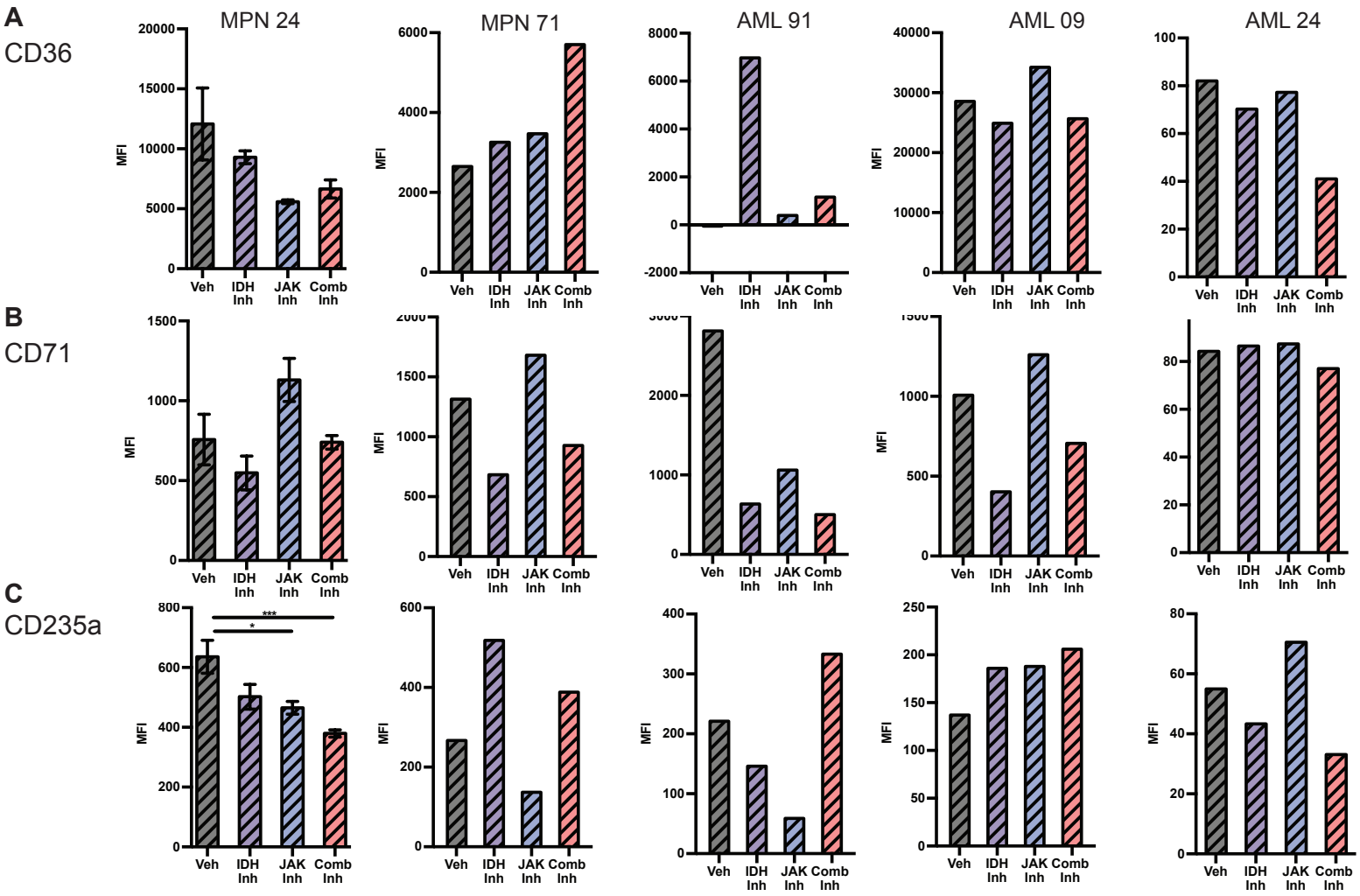

Figure 3.10: Some human *IDH2* mutant *JAK2*^{V617F} MPN and AML samples in methylcellulose respond to IDH2 inhibitor therapy with skew toward erythroid differentiation

Mean fluorescence intensity of (A) CD36, (B) CD17, and (C) CD235a

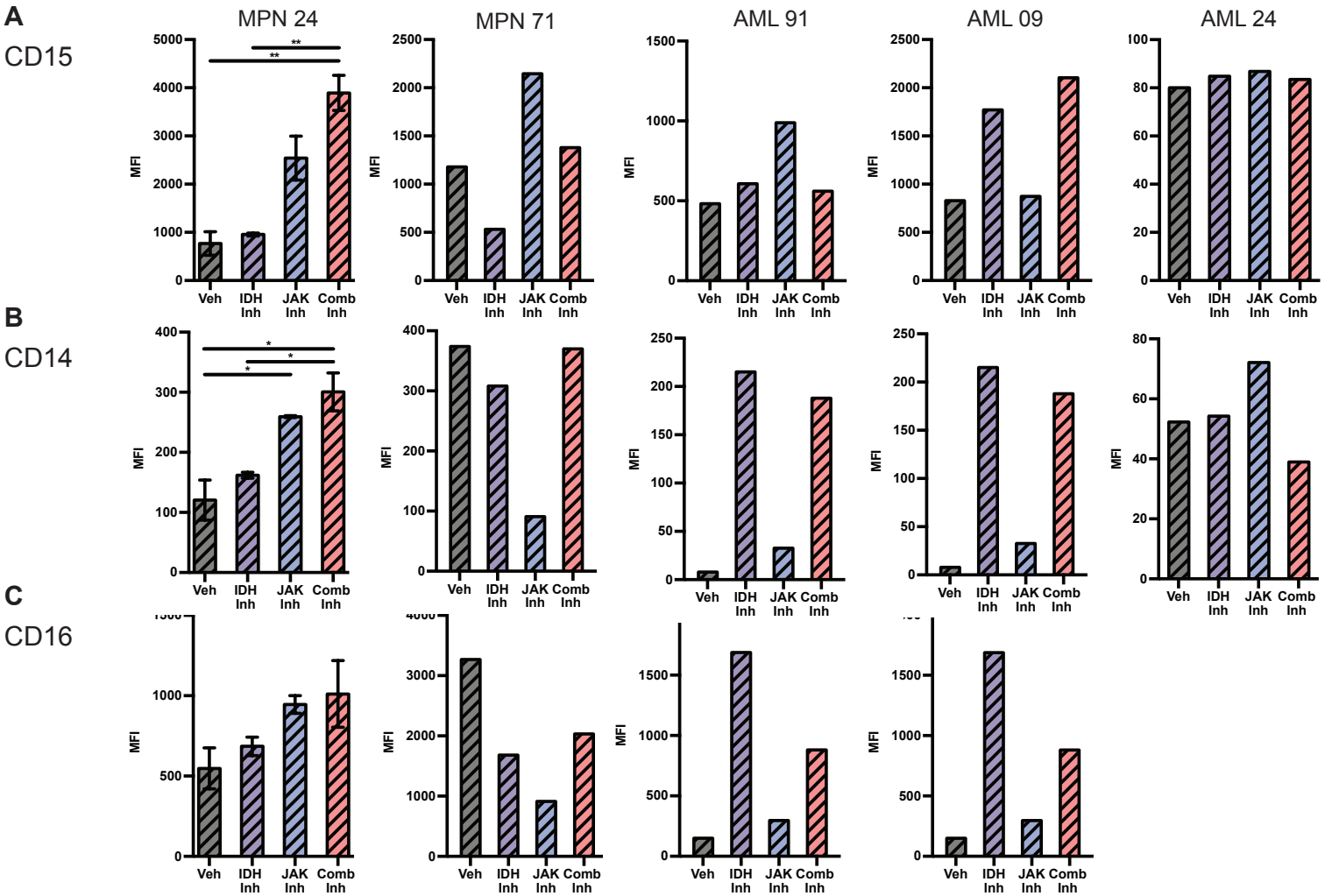

Figure 3.11: Some human IDH2 mutant JAK2V617F MPN and AML samples in methylcellulose respond to IDH2 inhibitor therapy with skew toward granulocytic differentiation

Mean fluorescence intensity of (A) CD15, (B) CD14, and (C) CD16.

Patient derived AML xenografts with IDH1/JAK2 mutation respond to AGI5198 treatment with expansion of chimerism of mature cells

In light of these results in *ex vivo* human samples, we sought to understand the response of patient derived xenografts to IDH inhibitor therapy. After engraftment of peripheral blood mononuclear cells from an AML patient harboring *IDH1*^{R132C} and *JAK2*^{V617F} mutations into NSG mice as detected by bone marrow aspirates, we treated with AGI-5198 and INC424. Consistent with AG221 treatment, treatment with AGI5198 reduced 2-HG levels in bone marrow cells (**Figure 3.12.A**). However, in contrast, treatment with IDH inhibitor expanded spleen size (**Figure 3.12.B**). This trend was true for human cell chimerism in bone marrow, spleen, and peripheral blood (**Figure 3.12.C**).

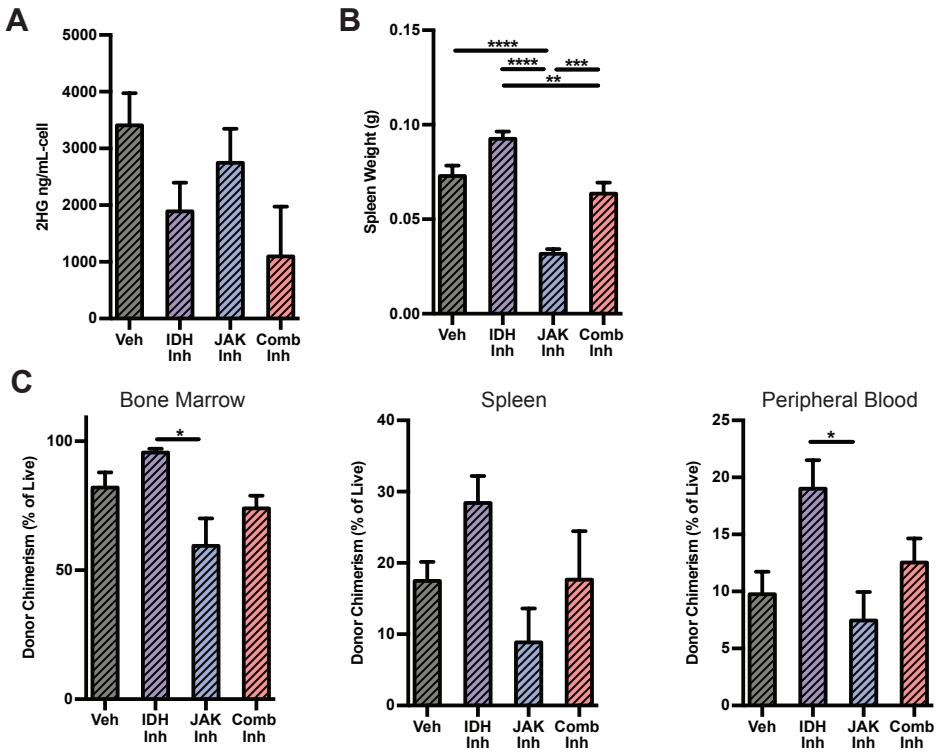

Figure 3.12: *IDH1* mutant *JAK2* mutant AML xenografts respond to IDH1 inhibitor treatment

(A-C) Analysis of treated xenograft mice at sacrifice: (A) quantification of 2HG in bone marrow cells normalized for human chimerism, (B) spleen weights, (C) proportion of human chimerism in cells isolated from bone marrow, spleen, and peripheral blood.

Observing the cell surface phenotype of these human cells in the bone marrow, spleen, and peripheral blood, we found that combined therapy reduced expression of immature / stem cell markers CD34 (**Figure 3.13.A**), CD38 (**Figure 3.13.B**), and CD117/cKit (**Figure 3.13.C**). At the same time, mature markers CD33 (**Figure 3.14.A**) and CD15 (**Figure 3.14.B**) were upregulated in these samples in comparison to the vehicle. Together, this indicates that this expansion of chimerism is in fact a differentiation phenotype induced by administration of the IDH inhibitor.

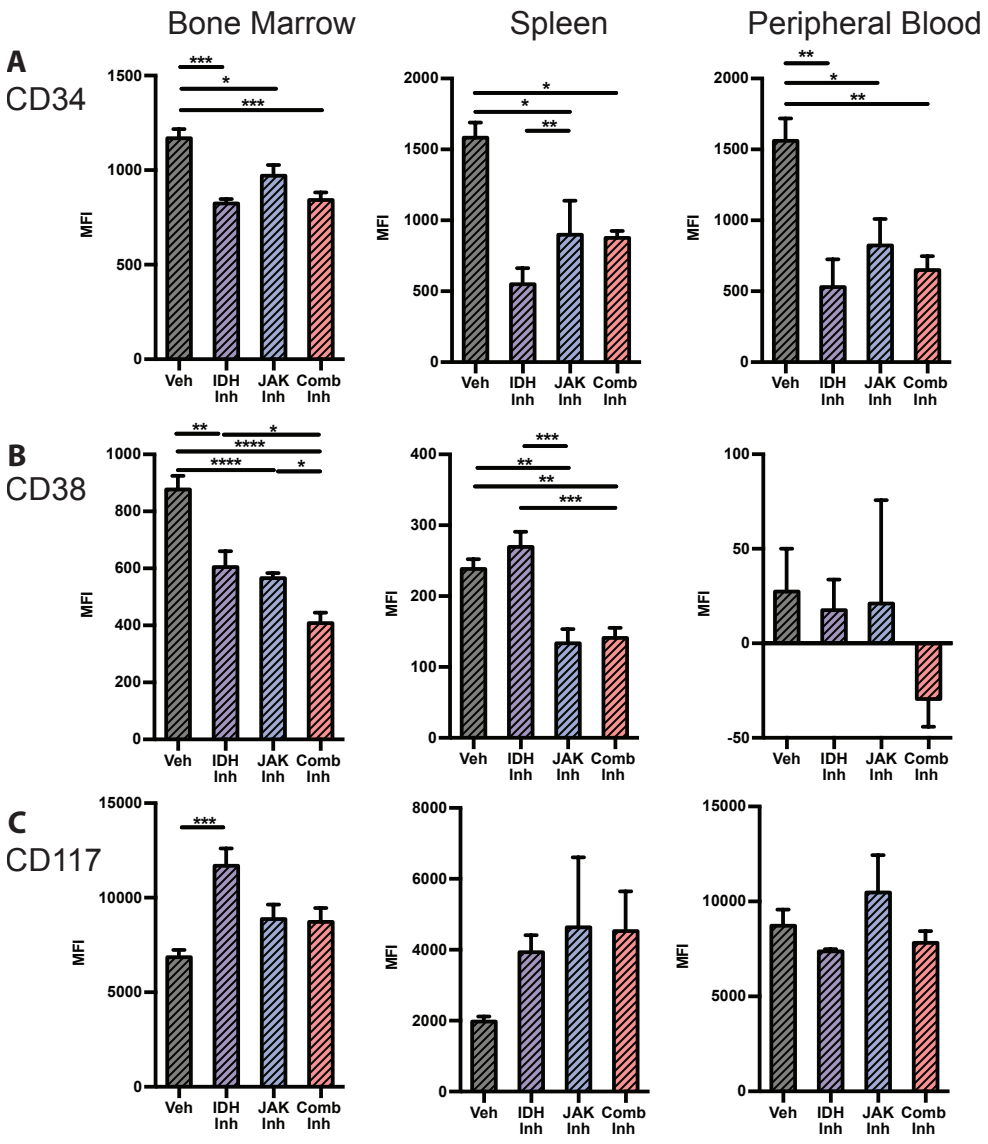

Figure 3.13: IDH1 mutant JAK2 mutant xenograft treatment with IDH1 inhbitor results in downregulation of canonical immature markers

(A-C) FACS quantification of mean fluorescence intensity of human $CD45^{+}$ cells extracted from corresponding tissues of treated xenograft mice at sacrifice: (A) CD34, (B) CD38, (C) CD117.

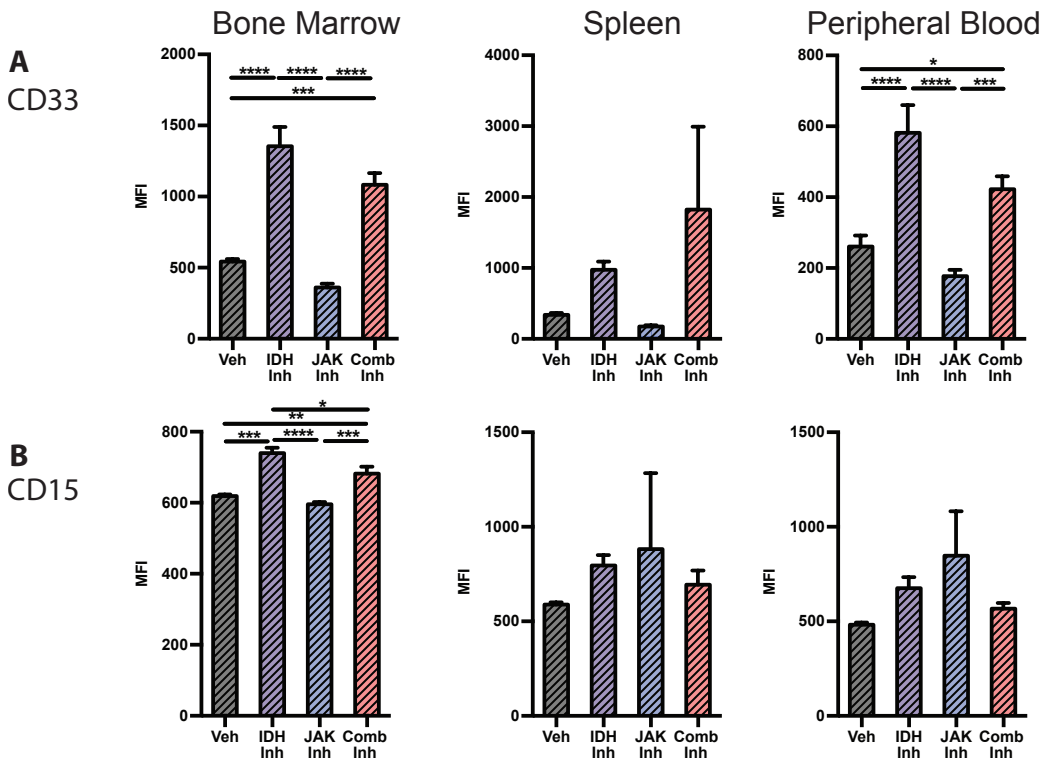

Figure 3.14: IDH1 mutant JAK2 mutant xenograft treated with AGI-5198 upregulates myeloid differentiation surface markers

(A-C) FACS quantification of mean fluorescence intensity of human $CD45^{+}$ cells extracted from corresponding tissues of treated xenograft mice at sacrifice: (A) CD33, (B) CD15.

DISCUSSION

This data shows a clear effect of IDH inhibitor therapy on mutant mouse and human cells. In mouse models, monotherapy results in resolution of all phenotypic measures of MPN, contraction of LSK and myeloprogenitor compartments, resolution of histological signs of preleukemic disease, and reduction of aberrant RNA expression in LSK stem cells. All of these measures were further improved with the addition of JAK2 inhibitor, often to the point of normalization of counts and phenotype to that of a wild type mouse. These effects appeared to be specific to mutant cells, as intermixed wild type cells did not appear to be affected. Although not all progenitor populations returned to normal proportions with combined therapy, most populations were reduced in size. In the context of our understanding of IDH mutation, this is consistent with increased differentiation has exhausted the early species that had accumulated in the presence of IDH mutation. This displays the potential efficacy of combined therapeutic regimen in combined mutant MPNs.

These *ex vivo* and PDX human samples showed clear evidence of differentiation as measured by cell surface antigens that label stem cells, maturing erythrocytes, and maturing granulocytes. All samples showed reductions in immature markers, indicating progressive maturity of these cells with treatment. In most of these patient samples, more mature markers of differentiation in the erythrocytic or granulocytic lineages were also upregulated, indicating at least one direction for this expansion of cells with treatment. Since this experimental system generally induces differentiation in erythrocytic and granulocytic lineages, further investigation is needed to determine if the samples would differentiate into other myeloid lineages (i.e.: megakaryocytes.)

Disease burden is an important issue in the therapy of MPNs, as previous therapies have not shown efficacy in reducing or eliminating the disease-initiating clone. In combined mutant mouse cells, there is a specific reduction in donor chimerism with monotherapy, which is further enhanced by combination with ruxolitinib. One prominent variation between the response of human cells and mouse cells is that, in human cells, the number of mutant cells increases with therapy. This is actually consistent with experiences in clinical trials, which show an expansion of differentiated granulocytes with short term treatment. However, with prolonged treatment, these patients are capable of achieving complete remission.[153-155]) Further experimentation is necessary to see if extending the length of treatment regimens in human samples (or looking at very short timescales in mice) will resolve this issue. One reason this timescale for disease recession may be so discrepant between mice and humans could be the much higher physiologic baseline serum 2-HG found in mice in comparison to humans.

Interestingly, there does appear to be a minor but significant effect of JAK2 inhibitor therapy on physiologic 2-HG which, consistent with our observations in primary mice, does not completely correlate with simple reduction in tumor burden as measured through bone marrow chimerism or spleen weight (data not shown.) This observation opens the question about potential effects of inhibition of JAK2 signaling on the activity of mutant (or native) IDH activity. Further experimentation is necessary to explore interaction of inhibition of these two pathways.

BIBLIOGRAPHY

1 James, C. *et al.* A unique clonal JAK2 mutation leading to constitutive signalling causes polycythaemia vera. *Nature* **434**, 1144-1148, doi:10.1038/nature03546 (2005).

2 Lu, X. *et al.* Expression of a homodimeric type I cytokine receptor is required for JAK2V617F-mediated transformation. *Proceedings of the National Academy of Sciences of the United States of America* **102**, 18962-18967, doi:10.1073/pnas.0509714102 (2005).

3 Levine, R. L., Pardanani, A., Tefferi, A. & Gilliland, D. G. Role of JAK2 in the pathogenesis and therapy of myeloproliferative disorders. *Nature Reviews Cancer* **7**, 673-683, doi:10.1038/nrc2210 (2007).

4 Levine, R. L. *et al.* X-inactivation-based clonality analysis and quantitative JAK2V617F assessment reveal a strong association between clonality and JAK2V617F in PV but not ET/MMM, and identifies a subset of JAK2V617F-negative ET and MMM patients with clonal hematopoiesis. *Blood* **107**, 4139-4141, doi:10.1182/blood-2005-09-3900 (2006).

5 Scott, L. M. *et al.* JAK2 exon 12 mutations in polycythemia vera and idiopathic erythrocytosis. *New England Journal of Medicine* **356**, 459-468, doi:10.1056/NEJMoa065202 (2007).

6 Pikman, Y. *et al.* MPLW515L is a novel somatic activating mutation in myelofibrosis with myeloid metaplasia. *PLoS medicine* **3**, e270, doi:10.1371/journal.pmed.0030270 (2006).

7 Pardanani, A. D. *et al.* MPL515 mutations in myeloproliferative and other myeloid disorders: a study of 1182 patients. *Blood* **108**, 3472-3476, doi:10.1182/blood-2006-04-018879 (2006).

8 Beer, P. A. *et al.* MPL mutations in myeloproliferative disorders: analysis of the PT-1 cohort. *Blood* **112**, 141-149, doi:10.1182/blood-2008-01-131664 (2008).

9 Vannucchi, A. M. *et al.* Characteristics and clinical correlates of MPL 515W>L/K mutation in essential thrombocythemia. *Blood* **112**, 844-847, doi:10.1182/blood-2008-01-135897 (2008).

10 Nangalia, J. *et al.* Somatic CALR mutations in myeloproliferative neoplasms with nonmutated JAK2. *New England Journal of Medicine* **369**, 2391-2405, doi:10.1056/NEJMoa1312542 (2013).

11 Klampfl, T. *et al.* Somatic mutations of calreticulin in myeloproliferative neoplasms. *New England Journal of Medicine* **369**, 2379-2390, doi:10.1056/NEJMoa1311347 (2013).

12 Mesa, R. A. *et al.* Leukemic transformation in myelofibrosis with myeloid metaplasia: a single-institution experience with 91 cases. *Blood* **105**, 973-977, doi:10.1182/blood-2004-07-2864 (2005).

13 Passamonti, F. *et al.* Leukemic transformation of polycythemia vera: a single center study of 23 patients. *Cancer* **104**, 1032-1036, doi:10.1002/cncr.21297 (2005).

14 Gangat, N. *et al.* Risk stratification for survival and leukemic transformation in essential thrombocythemia: a single institutional study of 605 patients. *Leukemia* **21**, 270-276, doi:10.1038/sj.leu.2404500 (2007).

15 Abdulkarim, K. *et al.* AML transformation in 56 patients with Ph− MPD in two well defined populations. *European Journal of Haematology* **82**, 106-111, doi:10.1111/j.1600-0609.2008.01163.x (2009).
16 Barosi, G. *et al.* JAK2 V617F mutational status predicts progression to large splenomegaly and leukemic transformation in primary myelofibrosis. *Blood* **110**, 4030-4036, doi:10.1182/blood-2007-07-099184 (2007).
17 Gangat, N. *et al.* Leucocytosis in polycythaemia vera predicts both inferior survival and leukaemic transformation. *British Journal of Haematology* **138**, 354-358, doi:10.1111/j.1365-2141.2007.06674.x (2007).
18 Huang, J. *et al.* Risk factors for leukemic transformation in patients with primary myelofibrosis. *Cancer* **112**, 2726-2732, doi:10.1002/cncr.23505 (2008).
19 Passamonti, F. *et al.* Prognostic factors for thrombosis, myelofibrosis, and leukemia in essential thrombocythemia: a study of 605 patients. *Haematologica* **93**, 1645-1651, doi:10.3324/haematol.13346 (2008).
20 Tefferi, A. *et al.* Low JAK2V617F allele burden in primary myelofibrosis, compared to either a higher allele burden or unmutated status, is associated with inferior overall and leukemia-free survival. *Leukemia* **22**, 756-761, doi:10.1038/sj.leu.2405097 (2008).
21 Tefferi, A. *et al.* 20+ yr without leukemic or fibrotic transformation in essential thrombocythemia or polycythemia vera: predictors at diagnosis. *European Journal of Haematology* **80**, 386-390, doi:10.1111/j.1600-0609.2008.01038.x (2008).
22 Passamonti, F. *et al.* A prospective study of 338 patients with polycythemia vera: the impact of JAK2 (V617F) allele burden and leukocytosis on fibrotic or leukemic disease transformation and vascular complications. *Leukemia* **24**, 1574-1579, doi:10.1038/leu.2010.148 (2010).
23 Björkholm, M. *et al.* Treatment-related risk factors for transformation to acute myeloid leukemia and myelodysplastic syndromes in myeloproliferative neoplasms. *Journal of Clinical Oncology* **29**, 2410-2415, doi:10.1200/JCO.2011.34.7542 (2011).
24 Theocharides, A. *et al.* Leukemic blasts in transformed JAK2-V617F-positive myeloproliferative disorders are frequently negative for the JAK2-V617F mutation. *Blood* **110**, 375-379, doi:10.1182/blood-2006-12-062125 (2007).
25 Zhang, S. J. *et al.* Genetic analysis of patients with leukemic transformation of myeloproliferative neoplasms shows recurrent SRSF2 mutations that are associated with adverse outcome. *Blood* **119**, 4480-4485, doi:10.1182/blood-2011-11-390252 (2012).
26 Patel, J. P. *et al.* Prognostic Relevance of Integrated Genetic Profiling in Acute Myeloid Leukemia. *New England Journal of Medicine* **366**, 1079-1089, doi:10.1056/NEJMoa1112304 (2012).
27 Jelinek, J. *et al.* JAK2 mutation 1849G>T is rare in acute leukemias but can be found in CMML, Philadelphia chromosome-negative CML, and megakaryocytic leukemia. *Blood* **106**, 3370-3373, doi:10.1182/blood-2005-05-1800 (2005).

28 Fröhling, S. *et al.* Rare occurrence of the JAK2 V617F mutation in AML subtypes M5, M6, and M7. *Blood* **107**, 1242-1243, doi:10.1182/blood-2005-09-3644 (2006).
29 Levine, R. L. The JAK2V617F activating mutation occurs in chronic myelomonocytic leukemia and acute myeloid leukemia, but not in acute lymphoblastic leukemia or chronic lymphocytic leukemia. *Blood* **106**, 3377-3379, doi:10.1182/blood-2005-05-1898 (2005).
30 Abdel-Wahab, O. *et al.* Genetic Analysis of Transforming Events That Convert Chronic Myeloproliferative Neoplasms to Leukemias. *Cancer Research* **70**, 447-452, doi:10.1158/0008-5472.CAN-09-3783 (2010).
31 Tefferi, A. *et al.* IDH mutations in primary myelofibrosis predict leukemic transformation and shortened survival: clinical evidence for leukemogenic collaboration with JAK2V617F. *Leukemia* **26**, 475-480, doi:10.1038/leu.2011.253 (2011).
32 Ding, Y., Harada, Y., Imagawa, J., Kimura, A. & Harada, H. AML1/RUNX1 point mutation possibly promotes leukemic transformation in myeloproliferative neoplasms. *Blood* **114**, 5201-5205, doi:10.1182/blood-2009-06-223982 (2009).
33 Zhang, S.-J. & Abdel-Wahab, O. Disordered Epigenetic Regulation in the Pathophysiology of Myeloproliferative Neoplasms. *Current Hematologic Malignancy Reports* **7**, 34-42, doi:10.1007/s11899-011-0105-y (2011).
34 Harutyunyan, A., Klampfl, T., Cazzola, M. & Kralovics, R. p53 lesions in leukemic transformation. *New England Journal of Medicine* **364**, 488-490, doi:10.1056/NEJMc1012718 (2011).
35 Pardanani, A. *et al.* LNK mutation studies in blast-phase myeloproliferative neoplasms, and in chronic-phase disease with TET2, IDH, JAK2 or MPL mutations. *Leukemia* **24**, 1713-1718, doi:10.1038/leu.2010.163 (2010).
36 Beer, P. A. *et al.* Two routes to leukemic transformation after a JAK2 mutation-positive myeloproliferative neoplasm. *Blood* **115**, 2891-2900, doi:10.1182/blood-2009-08-236596 (2010).
37 Jäger, R. *et al.* Deletions of the transcription factor Ikaros in myeloproliferative neoplasms. *Leukemia* **24**, 1290-1298, doi:10.1038/leu.2010.99 (2010).
38 Swolin, B., Rödjer, S. & Westin, J. Therapy-related patterns of cytogenetic abnormalities in acute myeloid leukemia and myelodysplastic syndrome post polycythemia vera: single center experience and review of literature. *Annals of hematology* **87**, 467-474, doi:10.1007/s00277-008-0461-4 (2008).
39 Thoennissen, N. H. *et al.* Prevalence and prognostic impact of allelic imbalances associated with leukemic transformation of Philadelphia chromosome-negative myeloproliferative neoplasms. *Blood* **115**, 2882-2890, doi:10.1182/blood-2009-07-235119 (2010).
40 Green, A. & Beer, P. Somatic mutations of IDH1 and IDH2 in the leukemic transformation of myeloproliferative neoplasms. *New England Journal of Medicine* **362**, 369-370, doi:10.1056/NEJMc0910063 (2010).
41 Zhang, Y. *et al.* Mutation analysis of isocitrate dehydrogenase in acute lymphoblastic leukemia. *Genetic testing and molecular biomarkers* **16**, 991-995, doi:10.1089/gtmb.2011.0323 (2012).

42 Reitman, Z. J. & Yan, H. Isocitrate Dehydrogenase 1 and 2 Mutations in Cancer: Alterations at a Crossroads of Cellular Metabolism. *JNCI Journal of the National Cancer Institute* **102**, 932-941, doi:10.1093/jnci/djq187 (2010).
43 Yen, K. E., Bittinger, M. A., Su, S. M. & Fantin, V. R. Cancer-associated IDH mutations: biomarker and therapeutic opportunities. *Oncogene* **29**, 6409-6417, doi:10.1038/onc.2010.444 (2010).
44 Sjoblom, T. *et al.* The Consensus Coding Sequences of Human Breast and Colorectal Cancers. *Science* **314**, 268-274, doi:10.1126/science.1133427 (2006).
45 Parsons, D. W. *et al.* An Integrated Genomic Analysis of Human Glioblastoma Multiforme. *Science* **321**, 1807-1812, doi:10.1126/science.1164382 (2008).
46 Mardis, E. R. *et al.* Recurring Mutations Found by Sequencing an Acute Myeloid Leukemia Genome. *New England Journal of Medicine* **361**, 1058-1066, doi:10.1056/NEJMoa0903840 (2009).
47 Cairns, R. A. *et al.* IDH2 mutations are frequent in angioimmunoblastic T-cell lymphoma. *Blood* **119**, 1901-1903, doi:10.1182/blood-2011-11-391748 (2012).
48 Borger, D. R. *et al.* Frequent mutation of isocitrate dehydrogenase (IDH)1 and IDH2 in cholangiocarcinoma identified through broad-based tumor genotyping. *The oncologist* **17**, 72-79, doi:10.1634/theoncologist.2011-0386 (2012).
49 Amary, M. F. *et al.* IDH1 and IDH2 mutations are frequent events in central chondrosarcoma and central and periosteal chondromas but not in other mesenchymal tumours. *The Journal of pathology* **224**, 334-343, doi:10.1002/path.2913 (2011).
50 Prensner, J. R. & Chinnaiyan, A. M. Metabolism unhinged: IDH mutations in cancer. *Nature Publishing Group* **17**, 291-293, doi:10.1038/nm0311-291 (2011).
51 Koszarska, M. *et al.* Type and location of isocitrate dehydrogenase mutations influence clinical characteristics and disease outcome of acute myeloid leukemia. *Leukemia & Lymphoma*, doi:10.3109/10428194.2012.736981 (2012).
52 Boissel, N. *et al.* Prognostic impact of isocitrate dehydrogenase enzyme isoforms 1 and 2 mutations in acute myeloid leukemia: a study by the Acute Leukemia French Association group. *Journal of Clinical Oncology* **28**, 3717-3723, doi:10.1200/JCO.2010.28.2285 (2010).
53 Marcucci, G. *et al.* IDH1 and IDH2 Gene Mutations Identify Novel Molecular Subsets Within De Novo Cytogenetically Normal Acute Myeloid Leukemia: A Cancer and Leukemia Group B Study. *Journal of Clinical Oncology* **28**, 2348-2355, doi:10.1200/JCO.2009.27.3730 (2010).
54 Green, C. L. *et al.* The prognostic significance of IDH2 mutations in AML depends on the location of the mutation. *Blood* **118**, 409-412, doi:10.1182/blood-2010-12-322479 (2011).
55 Chotirat, S., Thongnoppakhun, W., Promsuwicha, O., Boonthimat, C. & Auewarakul, C. U. Molecular alterations of isocitrate dehydrogenase 1 and 2 (IDH1 and IDH2) metabolic genes and additional genetic mutations in newly diagnosed acute myeloid leukemia patients. *Journal of hematology & oncology* **5**, 5, doi:10.1186/1756-8722-5-5 (2012).
56 Thol, F. *et al.* Prognostic impact of IDH2 mutations in cytogenetically normal acute myeloid leukemia. *Blood* **116**, 614-616, doi:10.1182/blood-2010-03-272146 (2010).

57 Chou, W. C. *et al.* Distinct clinical and biologic characteristics in adult acute myeloid leukemia bearing the isocitrate dehydrogenase 1 mutation. *Blood* **115**, 2749-2754, doi:10.1182/blood-2009-11-253070 (2010).
58 Damm, F. *et al.* Prevalence and prognostic value of IDH1 and IDH2 mutations in childhood AML: a study of the AML-BFM and DCOG study groups. *Leukemia* **25**, 1704-1710, doi:10.1038/leu.2011.142 (2011).
59 McKenney, A. S. & Levine, R. L. Isocitrate dehydrogenase mutations in leukemia. *The Journal of clinical investigation* **123**, 3672-3677, doi:10.1172/JCI67266 (2013).
60 Alam, N. A. Genetic and functional analyses of FH mutations in multiple cutaneous and uterine leiomyomatosis, hereditary leiomyomatosis and renal cancer, and fumarate hydratase deficiency. *Human Molecular Genetics* **12**, 1241-1252, doi:10.1093/hmg/ddg148 (2003).
61 Toro, J. R. *et al.* Mutations in the fumarate hydratase gene cause hereditary leiomyomatosis and renal cell cancer in families in North America. *American journal of human genetics* **73**, 95-106, doi:10.1086/376435 (2003).
62 Baysal, B. E. Mutations in SDHD, a Mitochondrial Complex II Gene, in Hereditary Paraganglioma. *Science* **287**, 848-851, doi:10.1126/science.287.5454.848 (2000).
63 Kaelin Jr, W. G. SDH5 Mutations and Familial Paraganglioma: Somewhere Warburg is Smiling. *Cancer Cell* **16**, 180-182, doi:10.1016/j.ccr.2009.08.013 (2009).
64 Pollard, P., Wortham, N. & Tomlinson, I. The TCA cycle and tumorigenesis: the examples of fumarate hydratase and succinate dehydrogenase. *Annals of Medicine* **35**, 634-635, doi:10.1080/07853890310018458 (2003).
65 Dang, L. *et al.* Cancer-associated IDH1 mutations produce 2-hydroxyglutarate. *Nature* **462**, 739-744, doi:10.1038/nature08617 (2009).
66 Gross, S. *et al.* Cancer-associated metabolite 2-hydroxyglutarate accumulates in acute myelogenous leukemia with isocitrate dehydrogenase 1 and 2 mutations. *Journal of Experimental Medicine* **207**, 339-344, doi:10.1084/jem.20092506 (2010).
67 Losman, J.-A. *et al.* (R)-2-Hydroxyglutarate Is Sufficient to Promote Leukemogenesis and Its Effects Are Reversible. *Science*, doi:10.1126/science.1231677 (2013).
68 Lu, C. *et al.* IDH mutation impairs histone demethylation and results in a block to cell differentiation. *Nature* **483**, 474-478, doi:10.1038/nature10860 (2012).
69 Saha, S. K. *et al.* Mutant IDH inhibits HNF-4α to block hepatocyte differentiation and promote biliary cancer. *Nature*, 1-18, doi:10.1038/nature13441 (2014).
70 Abdel-Wahab, O. *et al.* Genetic characterization of TET1, TET2, and TET3 alterations in myeloid malignancies. *Blood* **114**, 144-147, doi:10.1182/blood-2009-03-210039 (2009).
71 Delhommeau, F. *et al.* Mutation in TET2 in myeloid cancers. *New England Journal of Medicine* **360**, 2289-2301, doi:10.1056/NEJMoa0810069 (2009).

72 Jankowska, A. M. *et al.* Loss of heterozygosity 4q24 and TET2 mutations associated with myelodysplastic/myeloproliferative neoplasms. *Blood* **113**, 6403-6410, doi:10.1182/blood-2009-02-205690 (2009).
73 Langemeijer, S. M. C. *et al.* Acquired mutations in TET2 are common in myelodysplastic syndromes. *Nature Publishing Group* **41**, 838-842, doi:10.1038/ng.391 (2009).
74 Ko, M. *et al.* Impaired hydroxylation of 5-methylcytosine in myeloid cancers with mutant TET2. *Nature* **468**, 839-843, doi:10.1038/nature09586 (2010).
75 Lorsbach, R. B. *et al.* TET1, a member of a novel protein family, is fused to MLL in acute myeloid leukemia containing the t(10;11)(q22;q23). *Leukemia* **17**, 637-641, doi:10.1038/sj.leu.2402834 (2003).
76 Ono, R. *et al.* LCX, leukemia-associated protein with a CXXC domain, is fused to MLL in acute myeloid leukemia with trilineage dysplasia having t(10;11)(q22;q23). *Cancer Research* **62**, 4075-4080 (2002).
77 Tahiliani, M. *et al.* Conversion of 5-Methylcytosine to 5-Hydroxymethylcytosine in Mammalian DNA by MLL Partner TET1. *Science* **324**, 930-935, doi:10.1126/science.1170116 (2009).
78 Cimmino, L., Abdel-Wahab, O., Levine, R. L. & Aifantis, I. TET family proteins and their role in stem cell differentiation and transformation. *Cell Stem Cell* **9**, 193-204, doi:10.1016/j.stem.2011.08.007 (2011).
79 Ficz, G. *et al.* Dynamic regulation of 5-hydroxymethylcytosine in mouse ES cells and during differentiation. *Nature* **473**, 398-402, doi:10.1038/nature10008 (2011).
80 Guo, J. U., Su, Y., Zhong, C., Ming, G.-l. & Song, H. Hydroxylation of 5-Methylcytosine by TET1 Promotes Active DNA Demethylation in the Adult Brain. *Cell* **145**, 423-434, doi:10.1016/j.cell.2011.03.022 (2011).
81 Ito, T. *et al.* Regulation of myeloid leukaemia by the cell-fate determinant Musashi. *Nature* **466**, 765-768, doi:10.1038/nature09171 (2010).
82 Williams, K. *et al.* TET1 and hydroxymethylcytosine in transcription and DNA methylation fidelity. *Nature* **473**, 343-348, doi:10.1038/nature10066 (2011).
83 Wu, H. *et al.* Dual functions of Tet1 in transcriptional regulation in mouse embryonic stem cells. *Nature* **473**, 389-393, doi:10.1038/nature09934 (2011).
84 Xu, Y. *et al.* Genome-wide Regulation of 5hmC, 5mC, and Gene Expression by Tet1 Hydroxylase in Mouse Embryonic Stem Cells. *Molecular Cell* **42**, 451-464, doi:10.1016/j.molcel.2011.04.005 (2011).
85 He, Y. F. *et al.* Tet-Mediated Formation of 5-Carboxylcytosine and Its Excision by TDG in Mammalian DNA. *Science* **333**, 1303-1307, doi:10.1126/science.1210944 (2011).
86 Ito, S. *et al.* Tet Proteins Can Convert 5-Methylcytosine to 5-Formylcytosine and 5-Carboxylcytosine. *Science* **333**, 1300-1303, doi:10.1126/science.1210597 (2011).
87 Kranendijk, M. *et al.* IDH2 mutations in patients with D-2-hydroxyglutaric aciduria. *Science* **330**, 336, doi:10.1126/science.1192632 (2010).
88 Struys, E. A. *et al.* Mutations in the D-2-hydroxyglutarate dehydrogenase gene cause D-2-hydroxyglutaric aciduria. *American journal of human genetics* **76**, 358-360, doi:10.1086/427890 (2005).

89 Fathi, A. T. *et al.* Prospective serial evaluation of 2-hydroxyglutarate, during treatment of newly diagnosed acute myeloid leukemia, to assess disease activity and therapeutic response. *Blood* **120**, 4649-4652, doi:10.1182/blood-2012-06-438267 (2012).

90 Figueroa, M. E. *et al.* Leukemic IDH1 and IDH2 Mutations Result in a Hypermethylation Phenotype, Disrupt TET2 Function, and Impair Hematopoietic Differentiation. *Cancer Cell* **18**, 553-567, doi:10.1016/j.ccr.2010.11.015 (2010).

91 Shen, Y. *et al.* Gene mutation patterns and their prognostic impact in a cohort of 1185 patients with acute myeloid leukemia. *Blood* **118**, 5593-5603, doi:10.1182/blood-2011-03-343988 (2011).

92 Xu, W. *et al.* Oncometabolite 2-Hydroxyglutarate Is a Competitive Inhibitor of α-Ketoglutarate-Dependent Dioxygenases. *Cancer Cell* **19**, 17-30, doi:10.1016/j.ccr.2010.12.014 (2011).

93 Couture, J.-F., Collazo, E., Ortiz-Tello, P. A., Brunzelle, J. S. & Trievel, R. C. Specificity and mechanism of JMJD2A, a trimethyllysine-specific histone demethylase. *Nature Structural & Molecular Biology* **14**, 689-695, doi:10.1038/nsmb1273 (2007).

94 Hou, H. & Yu, H. Structural insights into histone lysine demethylation. *Current Opinion in Structural Biology* **20**, 739-748, doi:10.1016/j.sbi.2010.09.006 (2010).

95 Klose, R. J., Kallin, E. M. & Zhang, Y. JmjC-domain-containing proteins and histone demethylation. *Nature reviews. Genetics* **7**, 715-727, doi:10.1038/nrg1945 (2006).

96 Tsukada, Y.-i. *et al.* Histone demethylation by a family of JmjC domain-containing proteins. *Nature Cell Biology* **439**, 811-816, doi:10.1038/nature04433 (2005).

97 Chowdhury, R. *et al.* The oncometabolite 2-hydroxyglutarate inhibits histone lysine demethylases. *Nature Publishing Group* **12**, 463-469, doi:10.1038/embor.2011.43 (2011).

98 Xiao, M. *et al.* Inhibition of -KG-dependent histone and DNA demethylases by fumarate and succinate that are accumulated in mutations of FH and SDH tumor suppressors. *Genes & Development* **26**, 1326-1338, doi:10.1101/gad.191056.112 (2012).

99 Zhao, S. *et al.* Glioma-derived mutations in IDH1 dominantly inhibit IDH1 catalytic activity and induce HIF-1alpha. *Science* **324**, 261-265, doi:10.1126/science.1170944 (2009).

100 Sasaki, M. *et al.* D-2-hydroxyglutarate produced by mutant IDH1 perturbs collagen maturation and basement membrane function. *Genes & Development* **26**, 2038-2049, doi:10.1101/gad.198200.112 (2012).

101 Pollard, P. J. Accumulation of Krebs cycle intermediates and over-expression of HIF1 in tumours which result from germline FH and SDH mutations. *Human Molecular Genetics* **14**, 2231-2239, doi:10.1093/hmg/ddi227 (2005).

102 Selak, M. A. *et al.* Succinate links TCA cycle dysfunction to oncogenesis by inhibiting HIF-α prolyl hydroxylase. *Cancer Cell* **7**, 77-85, doi:10.1016/j.ccr.2004.11.022 (2005).

103 Koivunen, P. *et al.* Transformation by the (R)-enantiomer of 2-hydroxyglutarate linked to EGLN activation. *Nature* **483**, 484-488, doi:10.1038/nature10898 (2012).
104 Rane, S. G. & Reddy, E. P. Janus kinases: components of multiple signaling pathways. *Oncogene* **19**, 5662-5679, doi:10.1038/sj.onc.1203925 (2000).
105 Velazquez, L., Fellous, M., Stark, G. R. & Pellegrini, S. A protein tyrosine kinase in the interferon alpha/beta signaling pathway. *Cell* **70**, 313-322 (1992).
106 Ihle, J. N. Cytokine receptor signalling. *Nature* **377**, 591-594, doi:10.1038/377591a0 (1995).
107 Bromberg, J. Stat proteins and oncogenesis. *Journal of Clinical Investigation* **109**, 1139-1142, doi:10.1172/JCI200215617 (2002).
108 Kile, B. T. & Alexander, W. S. The suppressors of cytokine signalling (SOCS). *Cellular and Molecular Life Sciences* **58**, 1627-1635 (2001).
109 Yoshimura, A., Naka, T. & Kubo, M. SOCS proteins, cytokine signalling and immune regulation. *Nature reviews. Immunology* **7**, 454-465, doi:10.1038/nri2093 (2007).
110 Howard, J. K. & Flier, J. S. Attenuation of leptin and insulin signaling by SOCS proteins. *Trends in Endocrinology & Metabolism* **17**, 365-371, doi:10.1016/j.tem.2006.09.007 (2006).
111 Kawazoe, Y. *et al.* Signal transducer and activator of transcription (STAT)-induced STAT inhibitor 1 (SSI-1)/suppressor of cytokine signaling 1 (SOCS1) inhibits insulin signal transduction pathway through modulating insulin receptor substrate 1 (IRS-1) phosphorylation. *The Journal of experimental medicine* **193**, 263-269 (2001).
112 Thirone, A. C. P., JeBailey, L., Bilan, P. J. & Klip, A. Opposite effect of JAK2 on insulin-dependent activation of mitogen-activated protein kinases and Akt in muscle cells: possible target to ameliorate insulin resistance. *Diabetes* **55**, 942-951 (2006).
113 Neubauer, H. *et al.* Jak2 deficiency defines an essential developmental checkpoint in definitive hematopoiesis. *Cell* **93**, 397-409 (1998).
114 Parganas, E. *et al.* Jak2 is essential for signaling through a variety of cytokine receptors. *Cell* **93**, 385-395 (1998).
115 Verstovsek, S. *et al.* Safety and efficacy of INCB018424, a JAK1 and JAK2 inhibitor, in myelofibrosis. *New England Journal of Medicine* **363**, 1117-1127, doi:10.1056/NEJMoa1002028 (2010).
116 Verstovsek, S. *et al.* A double-blind, placebo-controlled trial of ruxolitinib for myelofibrosis. *New England Journal of Medicine* **366**, 799-807, doi:10.1056/NEJMoa1110557 (2012).
117 Dawson, M. A. *et al.* JAK2 phosphorylates histone H3Y41 and excludes HP1α from chromatin. *Nature* **461**, 819-822, doi:10.1038/nature08448 (2009).
118 Liu, F. *et al.* JAK2V617F-Mediated Phosphorylation of PRMT5 Downregulates Its Methyltransferase Activity and Promotes Myeloproliferation. *Cancer Cell* **19**, 283-294, doi:10.1016/j.ccr.2010.12.020 (2011).
119 Qian, C.-J., Yao, J. & Si, J.-M. Nuclear JAK2: Form and Function in Cancer. *The Anatomical Record: Advances in Integrative Anatomy and Evolutionary Biology* **294**, 1446-1459, doi:10.1002/ar.21443 (2011).

120 Rinaldi, C. R. *et al.* Preferential nuclear accumulation of JAK2V617F in CD34+ but not in granulocytic, megakaryocytic, or erythroid cells of patients with Philadelphia-negative myeloproliferative neoplasia. *Blood* **116**, 6023-6026, doi:10.1182/blood-2010-08-302265 (2010).
121 Wernig, G. *et al.* Expression of Jak2V617F causes a polycythemia vera-like disease with associated myelofibrosis in a murine bone marrow transplant model. *Blood* **107**, 4274-4281, doi:10.1182/blood-2005-12-4824 (2006).
122 Lacout, C. *et al.* JAK2V617F expression in murine hematopoietic cells leads to MPD mimicking human PV with secondary myelofibrosis. *Blood* **108**, 1652-1660, doi:10.1182/blood-2006-02-002030 (2006).
123 Bumm, T. G. P. *et al.* Characterization of murine JAK2V617F-positive myeloproliferative disease. *Cancer Research* **66**, 11156-11165, doi:10.1158/0008-5472.CAN-06-2210 (2006).
124 Zaleskas, V. M. *et al.* Molecular pathogenesis and therapy of polycythemia induced in mice by JAK2 V617F. *PLoS ONE* **1**, e18, doi:10.1371/journal.pone.0000018 (2006).
125 Mullally, A. *et al.* Physiological Jak2V617F expression causes a lethal myeloproliferative neoplasm with differential effects on hematopoietic stem and progenitor cells. *Cancer Cell* **17**, 584-596, doi:10.1016/j.ccr.2010.05.015 (2010).
126 Akada, H. *et al.* Conditional expression of heterozygous or homozygous Jak2V617F from its endogenous promoter induces a polycythemia vera-like disease. *Blood* **115**, 3589-3597, doi:10.1182/blood-2009-04-215848 (2010).
127 Moran-Crusio, K. *et al.* Tet2 Loss Leads to Increased Hematopoietic Stem Cell Self-Renewal and Myeloid Transformation. *Cancer Cell*, 1-14, doi:10.1016/j.ccr.2011.06.001 (2011).
128 Ko, M. *et al.* Ten-Eleven-Translocation 2 (TET2) negatively regulates homeostasis and differentiation of hematopoietic stem cells in mice. *Proceedings of the National Academy of Sciences of the United States of America* **108**, 14566-14571, doi:10.1073/pnas.1112317108 (2011).
129 Li, Z. *et al.* Deletion of Tet2 in mice leads to dysregulated hematopoietic stem cells and subsequent development of myeloid malignancies. *Blood* **118**, 4509-4518, doi:10.1182/blood-2010-12-325241 (2011).
130 Quivoron, C. *et al.* TET2 inactivation results in pleiotropic hematopoietic abnormalities in mouse and is a recurrent event during human lymphomagenesis. *Cancer Cell* **20**, 25-38, doi:10.1016/j.ccr.2011.06.003 (2011).
131 Sasaki, M. *et al.* IDH1(R132H) mutation increases murine haematopoietic progenitors and alters epigenetics. *Nature*, 1-7, doi:10.1038/nature11323 (2012).
132 Akbay, E. A. *et al.* D-2-hydroxyglutarate produced by mutant IDH2 causes cardiomyopathy and neurodegeneration in mice. *Genes & Development* **28**, 479-490, doi:10.1101/gad.231233.113 (2014).
133 Shih, A. H. *et al.* Mutational cooperativity linked to combinatorial epigenetic gain of function in acute myeloid leukemia. *Cancer Cell* **27**, 502-515, doi:10.1016/j.ccell.2015.03.009 (2015).
134 Kats, L. M. *et al.* Proto-oncogenic role of mutant IDH2 in leukemia initiation and maintenance. *Cell Stem Cell* **14**, 329-341, doi:10.1016/j.stem.2013.12.016 (2014).

135 Chen, E. *et al.* Distinct effects of concomitant Jak2V617F expression and Tet2 loss in mice promote disease progression in myeloproliferative neoplasms. *Blood* **125**, 327-335, doi:10.1182/blood-2014-04-567024 (2014).
136 Koppikar, P. *et al.* Efficacy of the JAK2 inhibitor INCB16562 in a murine model of MPLW515L-induced thrombocytosis and myelofibrosis. *Blood* **115**, 2919-2927, doi:10.1182/blood-2009-04-218842 (2010).
137 Pronk, C. J. H. *et al.* Elucidation of the Phenotypic, Functional, and Molecular Topography of a Myeloerythroid Progenitor Cell Hierarchy. *Cell Stem Cell* **1**, 428-442, doi:10.1016/j.stem.2007.07.005 (2007).
138 Lu, W., Kimball, E. & Rabinowitz, J. D. A high-performance liquid chromatography-tandem mass spectrometry method for quantitation of nitrogen-containing intracellular metabolites. *Journal of the American Society for Mass Spectrometry* **17**, 37-50, doi:10.1016/j.jasms.2005.09.001 (2006).
139 Rampal, R. *et al.* DNA hydroxymethylation profiling reveals that WT1 mutations result in loss of TET2 function in acute myeloid leukemia. *CellReports* **9**, 1841-1855, doi:10.1016/j.celrep.2014.11.004 (2014).
140 Druker, B. J. *et al.* Efficacy and safety of a specific inhibitor of the BCR-ABL tyrosine kinase in chronic myeloid leukemia. *New England Journal of Medicine* **344**, 1031-1037, doi:10.1056/NEJM200104053441401 (2001).
141 Hexner, E. O. *et al.* Lestaurtinib (CEP701) is a JAK2 inhibitor that suppresses JAK2/STAT5 signaling and the proliferation of primary erythroid cells from patients with myeloproliferative disorders. *Blood* **111**, 5663-5671, doi:10.1182/blood-2007-04-083402 (2008).
142 Pardanani, A. *et al.* TG101209, a small molecule JAK2-selective kinase inhibitor potently inhibits myeloproliferative disorder-associated JAK2V617F and MPLW515L/K mutations. *Leukemia* **21**, 1658-1668, doi:10.1038/sj.leu.2404750 (2007).
143 Wernig, G. *et al.* Efficacy of TG101348, a selective JAK2 inhibitor, in treatment of a murine model of JAK2V617F-induced polycythemia vera. *Cancer Cell* **13**, 311-320, doi:10.1016/j.ccr.2008.02.009 (2008).
144 LaFave, L. M. & Levine, R. L. JAK2 the future: therapeutic strategies for JAK-dependent malignancies. *Trends in Pharmacological Sciences* **33**, 574-582, doi:10.1016/j.tips.2012.08.005 (2012).
145 Cervantes, F. *et al.* Three-year efficacy, safety, and survival findings from COMFORT-II, a phase 3 study comparing ruxolitinib with best available therapy for myelofibrosis. *Blood* **122**, 4047-4053, doi:10.1182/blood-2013-02-485888 (2013).
146 Marubayashi, S. *et al.* HSP90 is a therapeutic target in JAK2-dependent myeloproliferative neoplasms in mice and humans. *Journal of Clinical Investigation* **120**, 3578-3593, doi:10.1172/JCI42442DS1 (2010).
147 Bali, P. *et al.* Inhibition of histone deacetylase 6 acetylates and disrupts the chaperone function of heat shock protein 90: a novel basis for antileukemia activity of histone deacetylase inhibitors. *The Journal of biological chemistry* **280**, 26729-26734, doi:10.1074/jbc.C500186200 (2005).

148 Koppikar, P. *et al.* Heterodimeric JAK-STAT activation as a mechanism of persistence to JAK2 inhibitor therapy. *Nature* **489**, 155-159, doi:10.1038/nature11303 (2012).
149 Eghtedar, A. *et al.* Phase 2 study of the JAK kinase inhibitor ruxolitinib in patients with refractory leukemias, including postmyeloproliferative neoplasm acute myeloid leukemia. *Blood* **119**, 4614-4618, doi:10.1182/blood-2011-12-400051 (2012).
150 Popovici-Muller, J. *et al.* Discovery of the First Potent Inhibitors of Mutant IDH1 That Lower Tumor 2 ‐ HG in Vivo. *ACS Medicinal Chemistry Letters* **3**, 850-855, doi:10.1021/ml300225h (2012).
151 Rohle, D. *et al.* An inhibitor of mutant IDH1 delays growth and promotes differentiation of glioma cells. *Science* **340**, 626-630, doi:10.1126/science.1236062 (2013).
152 Wang, F. *et al.* Targeted Inhibition of Mutant IDH2 in Leukemia Cells Induces Cellular Differentiation. *Science*, 1-7, doi:10.1126/science.1234769 (2013).
153 C, D. *et al.* in *Proceedings of the th Congress of the European Hematology Association* (2015 Jun 11–14, 2015).
154 Stein, E. M. IDH2 inhibition in AML: Finally progress? *Best Practice and Research: Clinical Haematology* **28**, 112-115, doi:10.1016/j.beha.2015.10.016 (2015).
155 Stein, E. M., DiNardo, C., Altman, J. K. & Collins, R. Safety and efficacy of AG-221, a potent inhibitor of mutant IDH2 that promotes differentiation of myeloid cells in patients with advanced hematologic …. *Blood* (2015).